Harpin-mediated cell death: Studies on events of cell death and bio-physical features of harpin$_{Pss}$

Thesis submitted for the award of

Doctor of Philosophy

by

Vedantam Lakshmi Vasudev

(Regd. No. 05LPPH05)

Department of Plant Sciences
School of Life Sciences
University of Hyderabad
Hyderabad- 500 046
India

July 2009

University of Hyderabad
(A Central University established in 1974 by act of parliament)
HYDERABAD – 500 046, INDIA

CERTIFICATE

This is to certify that Mr. V.L.VASUDEV has carried out the research work embodied in the present thesis under my supervision and guidance for a full period prescribed under the Ph.D ordinance of this University. We recommend his thesis ***"Harpin-mediated cell death: Studies on events of cell death and bio-physical features of harpin$_{Pss}$"*** for submission for the degree of Doctor of Philosophy of the University.

Prof. Appa Rao Podile
(Research Supervisor)

Head,
Department of Plant Sciences

Dean,
School of Life Sciences

University of Hyderabad
(A Central University established in 1974 by act of parliament)
HYDERABAD – 500 046, INDIA

DECLARATION

I hereby declare that the work embodied in this thesis entitled ***"Harpin-mediated cell death: Studies on events of cell death and bio-physical features of harpin$_{Pss}$"*** has been carried out by me under the supervision of Prof. Appa Rao Podile and this has not been submitted for any degree or diploma in any other University earlier.

V.L. VASUDEV

Prof. Appa Rao Podile
(Research Supervisor)

Acknowledgements

I would like to extend my sincere gratitude to my supervisor Prof. Appa Rao Podile, for his constant encouragement, moral support and guidance throughout my doctoral research without whom this endeavor would not have been possible. I am also grateful to him for his suggestions and critical examination of my thesis.

I thank the Dean, school of Life Sciences, Prof. A. S. Raghavendra and the present and former Heads, Department of Plant Sciences Prof. A. R. Reddy, Prof. P. B. Kirti and Prof. Appa Rao Podile for allowing me to use the facilities of the school and the Department.

I thank the former and the present Heads, Dept of Animal sciences, Prof. Aparna Dutta Gupta and Prof. S. Dayananda for giving me the FACS facility and other instruments.

My heartful thanks to Prof. M. J. Swamy and his student Mr. Pradip Tarafdar for helping us in carrying out the biophysical studies.

I specially thank Prof. P. Prakash Babu for allowing me to use his cell culture facility.

I thank Dr. R. Sankarnarayanan, Dr. Biswajit Pal and Sambhavi, CCMB for helping us to carry out the Crystallization of our protein.

I thank Prof. M. Ramanadham, Prof. O.H. Shetty, Prof. Abani Bhuyan and Dr. Naresh Sepuri for their help and suggestions in my work. Thanks are also due for all the faculty members of the School of Life Sciences.

My special thanks to Prof. P. Reddanna and his students especially Dr. Roy, Dr. Anil, Dr. Smitha and Dr. G V Reddy for their help and cooperation.

I thank all the research scholars of the School of Life Sciences for their cooperation.

The help and cooperation of Mr. Mohan Rao, Sudarshanam, Ramesh and other non-teaching staff is acknowledged

I would like to acknowledge the infrastructural support provided by UGC-SAP and DST-FIST to the Dept. of Plant Sciences

I thank DST & ICMR for the research fellowship. My thanks to UPE program, University of Hyderabad for funding my travel to USA for attending the international conference on "Yeast Apoptosis".

I wish to thank my seniors Dr. N. C. Shreeram, Dr. P. Sripriya, Dr. C. Tripura, Dr. B. Madhuri and Dr. B. Sashidhar for their suggestions and help.

I thank all my labmates Anil, Neeraja, Debashish, Purushotham, Suma, Sippy, Uma, Swaroopa, Sharma, Nandu, Das, Suprava, Dr. Swarnalee, Srinu, Mahesh, Madhu for their cooperation.

I also thank our lab assistants Satyanarayana, Madhu, Narasimha and Srinivas.

I thank my friends Ranjit, Rajini, Chaitanya, Dinakar, Sunil, Gopi, Rajkumar, Purushotham for their support and help during my stay here.

Ultimately I thank my parents and sister for their love and patience. Without their blessings I would not have been successful in completing this research work.

CONTENTS

ABBREVIATIONS

μg	:	microgram
μM	:	micro molar
^{0}C	:	degree Celsius
Abs	:	absorption
AFM	:	atomic force microscope
ALP	:	alkaline phosphatase
ATP	:	adenosine tri phosphate
BCIP	:	5-bromo-4-chloro-3-indolyl phosphate
bp	:	base pair
BSA	:	bovine serum albumin
CD	:	circular dichroism
CR	:	congo red
C-terminal	:	carboxy terminal
Cyt C	:	cytochrome C
DLS	:	dynamic light scattering
DMSO	:	dimethyl sulfoxide
DNA	:	deoxy ribonucleic acid
DSC	:	differential scanning calorimeter
DTT	:	dithiothreitol
Ea	:	*Erwinia amylovora*
EDTA	:	ethylene diamine tetra acetic acid
ELISA	:	enzyme linked immuno sorbant assay
FACS	:	Fluorescence activated cell sorting
FITC	:	fluorescein iso thio cyanate.
FBS	:	fetal bovine serum
g	:	gram
GSH	:	glutathione reduced
GSSG	:	glutathione oxidised
H_2DCFDA	:	2'7' Dichloro dihydro fluorescein diacetate
h	:	hour(s)

HR	:	hypersensitive response
hrp	:	hypersensitive response pathogenicity
hrpZ	:	gene encoding harpin$_{Pss}$
IPTG	:	isopropyl β-D-thiogalactoside
kb	:	kilobase pair
kDa	:	kilodaltons
KI	:	potassium iodide
l	:	litre
LB	:	Luria-Bertani
MALDI	:	matrix assisted laser desorption ionization
MPTP	:	mitochondrial permeability transition pore
MTT	:	3-(4,5-dimethyl thiazol-2yl)-2,5 diphenyl tetrazolium bromide
mg	:	milligram
min	:	minute
ml	:	milliliter
mM	:	millimolar
NAD	:	nicotinamide adenine dinucleotide
NBT	:	nitroblue tetrozolium
Ni-NTA	:	nickel-nitroacetic acid agarose
nm	:	nanometers
N-terminal	:	amino terminal
OD	:	optical density
ORF	:	open reading frame
PAGE	:	polyacrylamide gel electrophoresis
PBS	:	phosphate buffered saline
PCR	:	polymerase chain reaction
PCD	:	Programmed cell death
PEG	:	polyethylene glycol
PI	:	propidium iodide
pmole	:	picomole

PMSF	:	phenyl methyl sulfonylfluoride
Pss	:	*Pseudomonas syringae* pv. *syringae*
Psph	:	*Pseudomonas syringae* pv. *phaseolicola*
Pst	:	*Pseudomonas syringae* pv. *tomato*
Rh-123	:	Rhodamine-123
R_h	:	hydrodynamic radius
ROS	:	reactive oxygen species
RPMI	:	rosewell park memorial institute
rpm	:	revolutions per minute
SAR	:	systemic acquired resistance
SD		synthetic drop out media
SDS	:	sodium dodecyl sulphate
ssDNA	:	single stranded DNA
TE	:	TRIS-EDTA
TEMED	:	N,N,N',N'-tetramethylene diamine
TMV	:	tobacco mosaic virus
TNF	:	tumor necrosis factor
TOF	:	time of flight
TTC	:	2,3,5-triphenyl tetrazolium chloride
TTSS	:	type III secretion system
Tris	:	tris-(hydroxymethyl) aminoethane
UV	:	ultraviolet
V	:	volts
VPE	:	vacuolar processing enzyme
YCD	:	yeast cell death
YMM	:	yeast minimal media

LIST OF FIGURES

LIST OF TABLES

Dedicated
to
Almighty
&
Beloved Parents

1. Hypersensitive response (HR) is a strong resistance reaction of plants against pathogens

The plant 'hypersensitive response' (HR), a defense mechanism, involves interaction between products of an '*avr'* gene of the pathogen and a matching '*R*' gene of the plant (Dodds *et al.,* 2006). Plant HR is the result of an 'incompatible reaction', in which the '*R*' gene of the non-host plant corresponds to the '*avr*' gene of the pathogen, where as in a 'compatible reaction' the '*R*' gene of the host plant does not match with the '*avr*' gene of the pathogen resulting in the spread of pathogen through out the plant and disease occurs. The HR is one kind of programmed cell death (PCD) associated with the death of a small number of cells at and around the site of infection (Fig 1.1). HR serves to inhibit the growth of the invading pathogen by killing infected and uninfected cells, producing a physical barrier composed of dead cells. During HR, the dying plant cells strengthen their cell walls and accumulate certain toxic compounds like phenols and phytoalexins (Dangl *et al*., 1996) (Fig 1.2). An HR also occurs when pathogen-derived molecules or unique proteinaceous bacterial elicitors like 'harpin' interact with non-host plants (Fig 1.3). Membrane damage, necrosis, and collapse of challenged cells are the common features in a highly orchestrated form of genetically-regulated PCD in plants (Greenberg *et al.,* 1994), which is similar to 'apoptosis' in response to viruses or pathogenic bacteria in animal cells. The mechanism of cell death activation seems to be common in all living beings, while the precursors and the processes involved might have little variations.

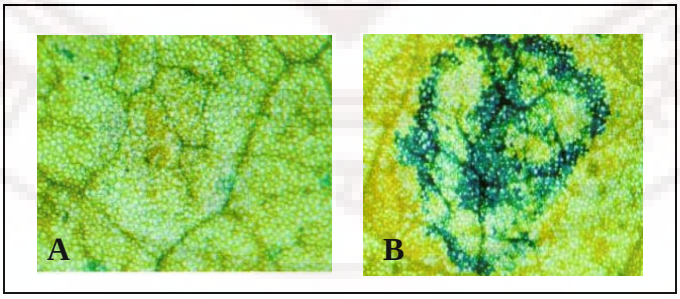

Fig 1.1 Hypersensitive response on a tobacco leaf during pathogen infection

Hypersensitive response (HR) manifested with the development of necrotic lesions (stained with Evans blue) followed by localized desiccation and browning of the affected cells. A) initial hours of infection and B) late hours of infection (adapted from Wright *et al*., 2000).

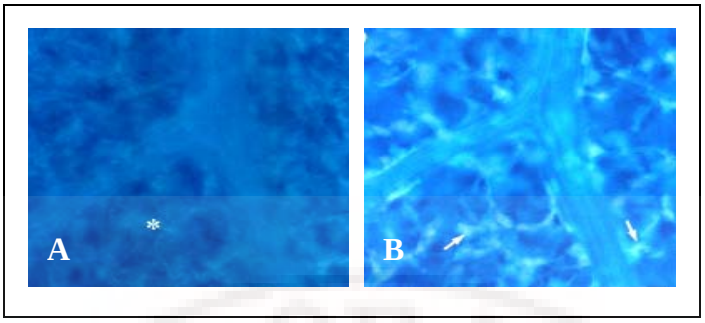

Fig 1.2 Accumulation of phenolic compounds during HR

Autofluorescence of phenolic compounds and cell wall thickenings in plant tissues during HR, observed under UV light. A) initial hours of pathogen infection (absence of phenols shown with asterix) and B) late hours of infection (phenol compounds shown with arrows) (adapted from Soylu, 2006).

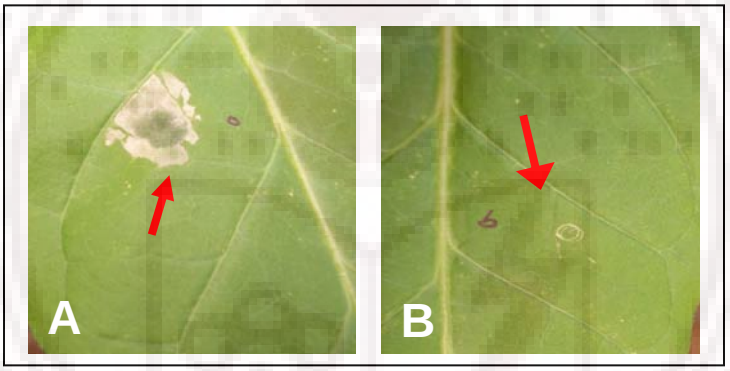

Fig 1.3 Harpin$_{Pss}$ infiltration induces HR on tobacco leaves

Reaction of tobacco leaves with (A) harpin$_{Pss}$ and (B) control leaf (buffer alone).

A variety of bacterial or fungal products elicit defensive plant responses in both host and non-host plants and these non-specific elicitors are the prime inducers of defense responses in non-host plant-pathogen interactions. An example of non-specific elicitors from bacteria are the 'harpins', which are heat stable proteins and encoded by members of '*hrp*' (hypersensitive response pathogenicity) gene cluster of some Gram-negative phytopathogenic bacteria (Collmer *et al*., 2000). Generally phytopathogenic bacteria have limited host ranges, often confined to members of a single plant species or genus. Most of the phytopathogenic bacteria are specialized in colonizing the apoplast and trigger diseases in plants causing rots, spots, vasucular wilts, cankers and blights (Alfano and

Collmer, 1996). The majority of these pathogens are Gram-negative rod shaped bacteria from the genera *Erwinia*, *Pseudomonas*, *Xanthomonas* and *Ralstonia*. These bacteria reside within the intercellular spaces of various plant organs or in the xylem, causing plant tissue damage by secreting toxins, extracellular polysaccharides or cell wall degrading enzymes at some stage during pathogenesis. Several bacterial genes referred to as the *hrp* cluster are required for bacterial pathogenesis. These *hrp* genes are similar to genes of pathogenic bacteria from animals suggesting that, distinct pathogens have similar virulence strategies, emphasizing the conserved mechanisms during the process of evolution (Alfano *et al*., 2000; Cao *et al*., 2001).

1.1 Plants operate programmed cell death during development and defense

Programmed cell death (PCD) plays an important role in development of the organism, in defense against pathogens and environmental stresses. The molecular details of the signaling pathways underlying PCD, in particular, have been well studied in animals. Cells undergo apoptosis through two major pathways controlled by complex regulatory networks: the extrinsic pathway (death receptor pathway) or the intrinsic pathway (mitochondrial pathway). Caspases are the key executioners of apoptosis in animals. In the past few years, the understanding of PCD mechanisms in plants has greatly increased.

In plants, PCD plays an important role in development, response to various pathogens and abiotic stress but the key proteases involved in the execution of PCD in plants still remains unanswered. The PCD in plants plays normal physiological roles in a variety of processes including, deletion of cells with temporary functions such as the aleurone cells in seeds and the suspensor cells in embryos; removal of unwanted cells, such as the root cap cells found in the tips of elongating plant roots and the stamen primordia cells in unisexual flowers; deletion of cells during sculpting of the plant body and formation of leaf lobes and perforations; death of cells during plant specialization, leaf senescence; and responses to plant pathogens and abiotic stresses (Pennell and Lamb 1997; Danon *et al*., 2004; Kuriyama and Fukuda 2002). PCD in plants is an active suicidal process that removes unwanted or severely damaged cells (Dangl and Jones 2001; Kuriyama and Fukuda 2002), that resembles type II or autophagic cell death in animals (Liu *et al*.,

2005). Some common features of type I cell death or apoptosis are conserved in both plants and metazoa (Danon and Gallois 1998; Yao *et al*., 2004) which include cytoplasm shrinkage, cytochrome c leakage out of mitochondria, chromatin condensation, altered nuclear morphology and DNA laddering.

PCD can be induced in plants by elicitors or toxins produced by a number of pathogens that include 'harpins' from *Pseudomonas syringae, Erwinia amylovora*, *Xanthomonas campestris*, the fungal toxin victorin, xylanase from *Trichoderma viridae* (He, 1996; Grant and Mansfield, 1999; Lam *et al*., 1999), *Alternaria alternata* AAL toxin, the fungal toxin Fumonisin B1 (FUM) from *Fusarium moniliforme* (Wang *et al*., 1996), fungal toxin cryptogein from *Phytophthora cryptogea* (Hirasawa *et al*., 2005). Also, plant viruses such as tobacco mosaic virus (TMV) are reported to elicit PCD (Del Pozo and Lam, 2003). While the signalling events and cell death cascades have been well studied in animals, little is known about the regulation and execution of PCD in plants (Hoeberichts and Woltering 2003). However, animal Bcl-2 members have been found to modify cell death processes in plants (Lam *et al*., 1999; Baek *et al*., 2004), indicating a possible identical apoptotic machinery in plants. Caspase-like activities have been measured in plant extracts and implicated in PCD processes, even though no sequence homologues have been found at the molecular level. Identification of such caspase-like proteases is essential to reveal the molecular mechanism that operates in plant PCD and to provide some insights into differences between plant and animal PCD. The identification, in plants, of a class of putative proteases related to animal caspases and termed metacaspases (Uren *et al*., 2000) has stimulated research in this protein family. New types of substilisin-like proteases (named saspases-A and -B) from oats and a vacuolar processing enzyme (VPE) from tobacco may play important roles as caspase-like proteases in the execution of PCD in plants (Coffeen and Wolpert 2004; Hatsugai *et al*. 2004).

1.2 HR is a form of PCD

Plant defense responses are frequently expressed in part as the so-called hypersensitive response (HR), which is characterized by necrosis at the sites of infection (resembling

animal PCD) and restriction of pathogen growth and spread. The HR is associated with the induction of defense-related genes which play important roles in containing pathogen growth either indirectly by helping to reinforce the plant cell walls, or directly by providing antimicrobial enzymes and phytoalexins (Dangl and Jones, 2001; Scheel, 1998). HR in plants is characterized by an increase of reactive oxygen species (ROS) such as hydrogen peroxide (H_2O_2) and nitric oxide (NO) and is often followed by a systemic response called systemic acquired resistance (SAR) (Strobel *et al*., 1996; Baker *et al*., 1993). The most persuasive evidence that the HR is a PCD process is the existence of mutants that spontaneously activate the HR in the absence of a pathogen (Dangl *et al*., 1996). These mutants referred to as "disease lesion mimics", were isolated from maize, rice, barley & Arabidopsis. The mutations that cause the appearance of HR lesions in the absence of a pathogen are thought to occur in plant genes that control PCD, thus presenting a powerful tool for the study of HR in plants.

Molecular and biochemical studies support the hypothesis that caspase-like enzymes are involved in the HR. These include the suppression of HR by synthetic peptide caspase inhibitors and the observed increase of caspase-like protease activity in plant cells undergoing HR (Lam *et al*., 2001). Additional players that may be similar to some of those controlling PCD in animals are small GTP-binding proteins of the 'Ras' family and cysteine-sensitive proteases. Hatsugai *et al*., (2004) showed that VPE and the cellular vacuole control the cellular suicide that is essential for HR in response to TMV. Major players involved in the activation of the HR are ROS, NO, calcium and proton pumps, mitogen-activated protein kinases (MAPKs), and salicylic acid (SA). The initial recognition of the pathogen by a plant receptor (gene-for-gene response) activates a signal transduction pathway that involves the translocation of Ca2+ and protons across the plasma membrane into the cytosol, protein phosphorylation/dephosphorylation, activation of enzymes that generate ROS such as NADPH-oxidase and peroxidases, and accumulation of NO and SA. Specific diffusible molecules known as stress phytohormones (salicylic acid, jasmonic acid and ethylene) from challenged HR developing cells, play an important signalling function in establishing resistance both

locally (local acquired resistance, LAR) and systemically (systemic acquired resistance, SAR).

1.3 Type III secretion system (TTSS) delivers bacterial proteins into host milieu

Several Gram-negative pathogens of both plant and animals (Hueck, 1998; Galan and Collmer, 1999; Cornelis and Gijsegem, 2000) use type III protein secretion systems (TTSS). These secretion systems are particularly noteworthy because they can translocate effector proteins directly into eukaryotic cells (Cornelis and Wolf-Watz, 1997). In bacterial plant pathogens belonging to the genera *Erwinia*, *Pseudomonas*, *Ralstonia* and *Xanthomonas*, TTSS (also referred to as Hrp systems) are encoded by *hrp*/*hrc* genes (Lindgren, 1997; He, 1998). *Pseudomonas syringae* uses a TTSS system encoded by the Hrp pathogenicity island (Pai) to translocate effector proteins into plant cells (Alfano *et al.,* 2000). A small open reading frame (ORF), named shcA, precedes the *hopPsyA* gene in the Hrp Pai of *P. s*. pv. *syringae* 61. The HopPsyA protein is secreted in culture by *P. syringae* and, when expressed transiently in tobacco, it elicits an HR, indicating that its site of action is inside plant cells (Alfano *et al.,* 1997; van Dijk *et al.,* 1999; Collmer *et al.,* 2000). The predicted product of ORF shares several of the general characteristics of chaperones used in the TTSS of animal pathogens (Wattiau *et al.,* 1996; Cornelis *et al.,* 1998).

Successful parasitism appears to require multiple TTSS effectors. Genomic searches for TTSS effector genes in *P. syringae* pv. *tomato* DC 3000 revealed 33 confirmed effectors and several effector candidates (Buell *et al.,* 2003; Collmer *et al*., 2002; Guttman *et al.,* 2002). A few of the type III effectors from *Pseudomonas syringae* pv. *tomato* were also shown to inhibit growth in yeast and cause cell death during ectopic expression (Munkvold *et al*., 2008). Indeed, several *P. syringae* effectors were shown to suppress plant defenses (Abramovitch *et al*., 2003; Bretz *et al*., 2003). Several of the effectors that suppress the HR can also suppress Bax-triggered PCD in yeast and plants. $AcrPphE_{pto}$, $AvrPpiBl_{pto}$, AvtPtoB, HopPtoF and HopPtoG effectors were found to possess such suppressor activity (Jamir *et al*., 2004).

1.4 Harpins are the most studied type III effectors of phytopathogenic bacteria

Harpins are effector proteins secreted by TTSS of bacterial pathogens. Although harpins were originally defined as elicitors of HR, some other biological activity e.g. induction of disease resistance has been reported (Dong *et al.,* 1999). Beside the important biological activities, harpins also attract considerable interest due to their potential application as pesticides. Harpins elicit a protective response in the plant which imparts resistance to it from wide range of fungal, bacterial, and viral infections. Since harpins do not directly interact with the disease-causing organisms, pathogens are not expected to develop resistance to harpins. As harpins are biodegradable and have no adverse effects on human health, use of harpins can substantially reduce use of more toxic chemical pesticides. The correlation of structure with activity in harpin may lead to the development of improved, engineered pesticides.

Pseudomonas syringae pv. *syringae* 61 *hrpZ* gene encodes harpin$_{Pss}$, a 34.7 kDa extracellular protein, which elicits HR in several plants, including tobacco (He *et al.,* 1993). *HrpN* of *Erwinia amylovora* was the first harpin protein shown to elicit HR in tobacco (Wei *et al*., 1992), secreted *via* the TTSS system. Harpins are hydrophilic in nature, rich in leucine & glycine, heat stable and elicit HR when infiltrated into the apoplast of certain plants (Bauer *et al*., 1995). Harpin proteins, isolated from a variety of Gram–ve phytopathogenic bacteria such as *P. syringae* pv. *syringae (hrpZ)*, *Xanthomonas axonopodis*, *E. chrysanthemi (hrpN)*, *E. carotovora (hrpN)*, have been characterized (He *et al.,*1993; Kim *et al.,* 2003; Bauer *et al.,*1995; Mukherjee *et al.,* 1997). In *Ralstonia solanacearum*, a harpin-like protein, PopA, has been shown to induce HR in non host tobacco plants (Arlat *et al.,* 1994).

1.5 Harpins possess unique biochemical features and activate host cell machinery

Harpin$_{Pss}$ exists as a polydispersed protein in nature, the multimeric forms include, but are probably not restricted to – dimer, trimer, tetramer and octamer (Chen *et al.,* 1998). Partial deletion mutation revealed that several truncated peptides e.g., *N*-terminal 153

amino acids, *C*-terminal 216 amino acids can also elicit a strong HR (Alfano *et al.,*1996). Like other harpins the mechanism of HR elicitation by $harpin_{Pss}$ and its truncated peptides is not clear. Exploiting the high thermal stability of this protein He *et al*., (1993) developed a simple method to purify it from a mixture of mesophilic proteins. Biochemical mechanism of harpin-elicited HR in non-host plants is far from being completely understood. $Harpin_{Ea}$-induced responses in tobacco suspension cells such as oxidative burst (Baker *et al.,* 1993), pH change, K^+ efflux, extracellular alkalinization and membrane depolarization are blocked by lanthanum chloride, a Ca^{2+} channel blocker and K252a, a protein kinase inhibitor (Baker *et al.,* 1993, He *et al.,* 1993, Popham *et al.,* 1995). Though structurally different, $harpin_{Pss}$ and $harpin_{Ea}$, both cause immediate K^+ efflux and extracellular alkalinization in tobacco suspension-cultured cells (Wei *et al.,* 1992; He *et al.,* 1993; Popham *et al.,* 1995) which suggest that $harpin_{Pss}$ triggers a signal transduction pathway that involves active oxygen species production, protein phosphorylation, and Ca^{2+} influx. Alkalinization was induced immediately after addition of different concentrations of full-length $harpin_{Pss}$. The pH change caused by the same concentrations of truncated $harpin_{Pss}$ is similar in magnitude to the changes caused by the full-length protein. At the same protein concentration, truncated protein and protease inactivated $harpin_{Pss}$ caused similar but smaller alkalinization that $harpin_{Pss}$ contribute to the residual pH changes in the protoplast medium and suggest that the cell wall is important for the pH change induced by either $harpin_{Pss}$ or *P. syringae* pv. *syringae* (Hoyos *et al.,* 1996). A wall-associated kinase (Wak 1) that could function in cell wall-to-membrane signal transduction has been reported and the crucial role of plant cell wall in $harpin_{Pss}$-mediated plant HR has been established (Hoyos *et al.,* 1996). Mitochondria play a central role in apoptosis, and as well, $harpin_{Ea}$ treatment in tobacco suspension cells lead to altered mitochondrial functions (Xie and Chen, 2000).

Harpins do not have structural homology with known proteins or among themselves. Absence of homology makes it hard to establish structure-activity relationship for this class of proteins. In spite of the absence of structural homology in harpins, they share some common properties i.e. they contain a high proportion of glycine, they lack cysteine, and are thermally stable. A large number of harpins act on plant cell walls and

form amyloid fibrils in apoplastic fluid (Oh *et al.,* 2007). $Harpin_{Psph}$ from *P. syringae* pv. *phaseolicola* associates with liposomes and synthetic bilayer membranes and mediates the formation of an ion-conducting pore (Lee *et al.,* 2001). Immunolocalisation revealed Ca^{+2}-dependent association of *P. syringae* pv. *syringae* harpin with plant cell walls (Hoyos *et al.,*1996). Additionally, HrpN from *E. amylovora* and *Pantoea stewartii* subsp. *stewartii* was reported to depolarize plant cell membranes (Pike *et al.,*1998; Ahmad *et al.,* 2001), and PopA from *R. solanacearum* exhibits pore-forming activity and integrates into liposomes and membranes of *Xenopus laevis* (Recape *et al.,* 2005). As the unusual membrane permeability was proposed to cause cellular dysfunction and death, it may be possible that destabilization of membranes induces HR in plants. A molecular level understanding about how harpins destabilize membranes to cause HR still remains unclear.

1.6 PCD in animal cells has been widely studied

Cell death is divided in animal species into PCD and necrosis. PCD is an important process for multicellular organisms. As it removes superfluous, damaged or infected cells in an organized manner, PCD plays an important role in development, in tissue homeostasis, in the immune responses and to cope with adverse environmental stresses (Steller, 1995; Meier *et al*., 2000; Lawen, 2003; Jin and El-Deiry, 2005). PCD was held synonymous with apoptosis. The term apoptosis is derived from the Greek word for the process of leaves falling from trees or petals falling from flowers. It was introduced in the 1970s to differentiate a morphologically distinctive form of cell death associated with normal physiology (Kerr *et al*., 1972). Apoptosis is associated with activation of caspases, executioners of cell destruction. Four mechanistic classes of proteases, recognized by the International Union of Biochemistry and Molecular Biology in 1984, including serine, cysteine, aspartic and metallo proteases. Caspases belong to an evolutionarily conserved family of cysteine proteases (Kroemer and Martin, 2005). Necrosis is associated with acute injury to cells, leading to loss of membrane integrity, swelling and disruption of the cells. During necrosis, cellular contents are released uncontrolled into the cell's environment which results in damage of surrounding cells and a strong inflammatory response in the corresponding tissue (Leist and Jaatela, 2001).

Since, other types of PCD have been proposed, for which cell death was found to occur in a programmed fashion, but in complete absence and independent of caspase activation. PCD has been classified into three main types according to Clarke's classification based on lysosomal involvement (Clarke, 1990; Chipuk and Green, 2004; Kim, 2005) - apoptosis (or type I cell death), autophagic cell death (also known as cytoplasmic, or type II cell death) and necrosis-like cell death (also known as type III or non-lysosomal cell death).

Type I cell death, apoptosis, is a form of PCD morphologically defined by condensation of the nucleus and cytoplasm, association of chromatin with the nuclear periphery, DNA fragmentation, membrane blebbing, and engulfment and lysosomal degradation of the dying cell by a phagocyte (Kerr *et al*., 1972). Biochemical evidence has indicated the caspase family of cysteine protease as well as certain proteins of the mitochondria to be mediators of type I PCD. Type II, autophagic cell death, is characterized by sequestration of bulk cytoplasm and organelles in double or multi-membrane autophagic vesicles and their delivery to and subsequent degradation by the cell's own lysosomal system before the nucleus is destroyed (Bursch *et al*., 2000; Levine and Klionsky, 2004). The sequestered cytoplasmic components may be degraded prior to heterophagocytosis of cellular remains. Type III, non-lysosomal or necrosis-like cell death, is characterized by breakdown of the plasma membrane, swelling of organelles, lysosome-independent formation of 'empty spaces' in the cytoplasm and disintegration of the cytoplasm (Gozuacik and Kimchi, 2004).

Types I and II cell death have been observed in many animal species during development, whereas type III cell death is common in pathological conditions. Types II and III cell death are genetically regulated and often have morphological features resembling necrosis, yet their underlying molecular mechanisms are unclear. The various types of PCD have in common that they are executed by active cellular processes that can be intercepted by interfering with intracellular signaling. Those types cannot be categorized because they might overlap since they share the same activation intermediaries or they can be activating each other (Lockshin and Zakeri, 2004). The

cellular components are safely isolated by membranes, and then consumed by adjacent cells and/or resident phagocytes without inflammation. The elimination of PCD debris may remain virtually unnoticed by the body which distinguishes them from "accidental" necrosis. The caspase-independent cell death pathways - type II and type III cell death - are important safeguard mechanisms to protect the organism against unwanted and potential harmful cells when caspase-mediated routes fail but can also be triggered in response to cytotoxic agents or other death stimuli. In the case of accidental necrosis, cytosolic constituents spill into extracellular space through damaged plasma membrane and provoke an inflammatory response. The necrotic cell removal induces and amplifies pathological processes.

1.7 Key elements involved in regulation of cell death

Mitochondria play not only a key role in cellular metabolism and in signal transduction cascades but also an important role in the regulation of PCD (Ferri and Kroemer, 2001). Mitochondrial alterations – following release of sequestered apoptogenic proteins, loss of transmembrane potential, production of ROS, disruption of electron transport chain, and decreases in ATP synthesis - have been shown to be responsible for the different types of cell death (Bras *et al*., 2005). Thus, the mitochondria can be viewed as a central regulator of the decision between cellular survival and cell death.

During cell death, the ATP levels are determinant in directing toward PCD or necrosis (Leist *et al*., 1997; Nicotera *et al*., 1998; Formigli *et al*., 2000). The disruption of the mitochondrial electron transport chain would result in diminished ATP production and consequently in a striking perturbation of the bioenergetic state of the cell. The inhibition of ATP production has been observed in both type I and type III cell death. However, this phenomenon occurs relatively late in type I cell death, as the complete apoptotic program involves the energy-dependent formation of the apoptosome (cytochrome c/ Apaf-1 / dATP complex) and hydrolysis of macromolecules. By contrast, type III cell death is characterized by an early loss of ATP synthesis and seems to proceed in conditions of low cytosolic ATP levels (Kim *et al.,* 2003). ATP dependency has been observed for the autophagic type II pathway, apparently at the lysosomal level (Plomp *et al*., 1989).

Moreover, intracellular nucleotides can regulate apoptosis, they can directly block the cytochrome c initiated apoptosome formation and the caspase activation by interfering with Apaf-1 (Chandra *et al*., 2006).

Calcium is a key regulator of mitochondrial function and acts at several levels within the organelle to stimulate ATP synthesis. Mitochondrial matrix Ca^{2+} overload can lead to enhanced generation of ROS. The ROS triggers the opening of the mitochondrial permeability transition pore (MPTP). If the pore remains open, cells do not maintain their ATP levels and this leads to cell death by necrosis. When cells experience a less severe insult, the MPTP may open transiently. The resulting mitochondrial swelling may be sufficient to cause release of cytochrome c and activation of the apoptotic pathway rather than necrosis (Green and Kroemer 2004).

The efflux of cytochrome c from mitochondria is also a pivotal event in apoptosis, as it drives the assembly of the apoptosome in the cytoplasm, the activation of a proteolytic cascade involving caspase proteases is an irreversible step (Abraham and Shaham, 2004). Caspases cleave a variety of proteins after specific aspartate residues, ultimately leading to cell death. The contents of dead cells are packaged into apoptotic bodies, which are recognized by neighboring cells or macrophages and cleared by phagocytes. De-regulation of apoptosis may lead to pathological disorders such as developmental defects, autoimmune diseases, neurodegeneration or cancer.

1.8 Apoptotic pathways

The apoptotic cascade can be initiated *via* two major pathways (Fig 1.4). These pathways involve either the activation of death receptors in response to ligand binding (death receptor pathway), or the release of cytochrome c from the mitochondria (mitochondrial pathway) (Ashkenazi and Dixit 1998; Hengartner, 2000). Both pathways involve a specific family of cysteine proteases, the caspases, that are activated to execute PCD. The execution of PCD results in the typical morphologic changes (Degterev *et al*., 2003). In mammals, the cell surface death receptor-mediated pathway involves cell surface death receptors such as Fas, Tumor Necrosis Factor (TNF), or TRAIL receptors (Ashkenazi and

Dixit 1998). Death ligand stimulation, *via* a series of protein-protein interactions, results in oligomerization of the receptors and recruitment of an adaptor protein and caspase-8 or -10, forming a death-inducing signalling complex (DISC). Autoactivation of caspase-8 at the DISC is followed by activation of other caspases, including caspase 3, 6 and 7. These activated caspases function as downstream effectors of the cell death program.

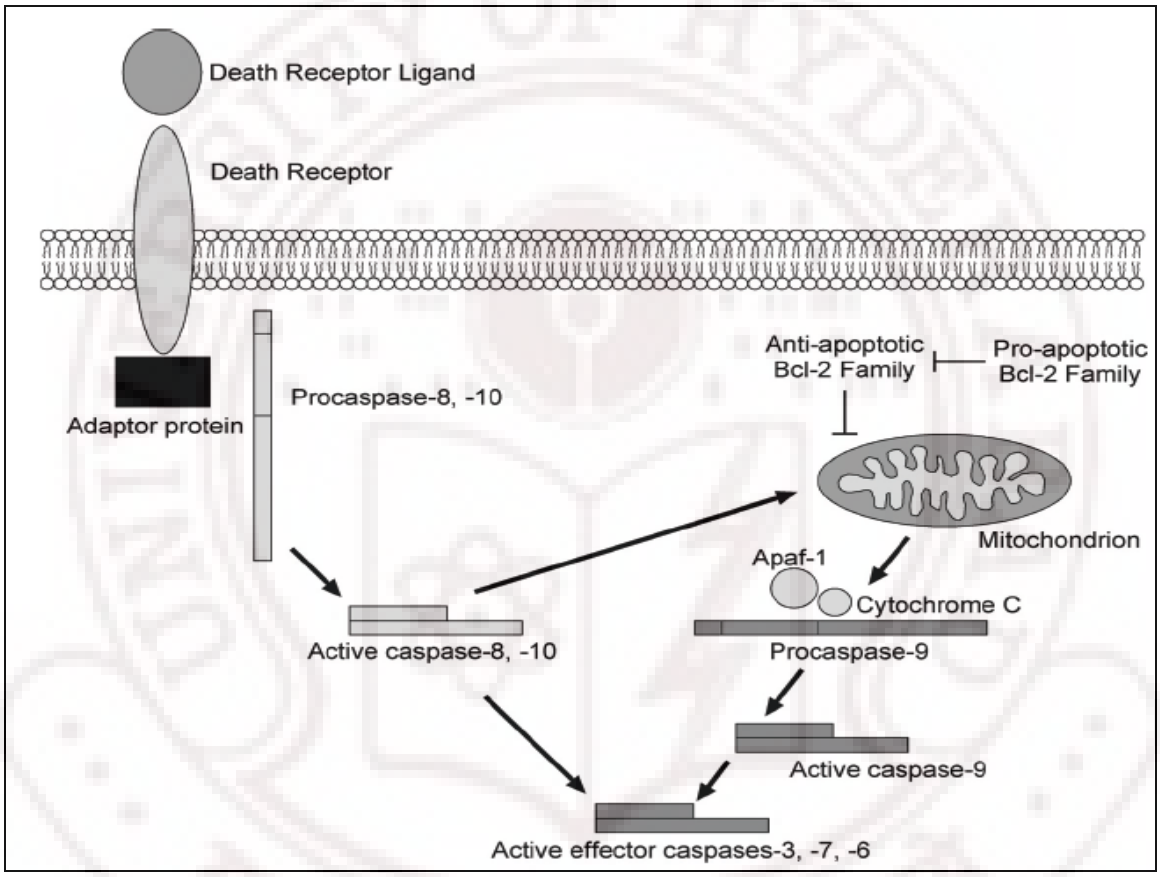

Fig. 1.4 Apoptotic pathways in mammalian cell death.

The extrinsic apoptotic pathway (left) is induced by a death receptor ligand (TNF, TRAIL, FasL etc) which results in the recruitment and formation of a multiprotein complex DISC that includes the death receptor, intracellular adaptor proteins (TRADD, FADD, RAIDD) and initiator caspases (procaspase-8 or -10). The complex leads to autocatalytic processing and activation of the initiator caspase. The intrinsic pathway (right) is initiated by the majority of apoptotic stimuli, including irradiation, cytotoxic drugs, DNA damage etc. Loss of mitochondrial membrane potential and release of pro-apoptotic cell death proteins results in the formation of another multiprotein complex, the apoptosome, that includes Apaf-1, cytochrome c, ATP/dATP and the initiator caspase, procaspase 9. That complex leads to autocatalytic activation of caspase-9 and subsequent effector caspases. Pro- and anti-apoptotic bcl-2 homologues regulate the release of pro-cell death mitochondrial proteins (adapted from Gaussand, 2007).

The other caspase activation pathway in mammals is the mitochondria pathway which is characterized by a depolarization of the mitochondrial membrane and a release of mitochondrial proteins (Danial and Korsmeyer, 2004) including pro-apoptotic proteins, such as cytochrome c, into the cytosol. A cytosolic complex, the apoptosome, is formed which consists of oligomerised Apaf-1 (apoptotic protease-activating factor 1), ATP/dATP, cytochrome c and the initiator caspase, pro-caspase-9 (Riedl and Shi, 2004). Oligomerisation of Apaf-1 allows the recruitment and autocatalytic activation of caspase-9, and consequently the propagation of a death signal by proteolytic processing and activation of effector caspases (Li *et al*., 1997).

Apart from the pathways now described, there is another cell death pathway. That pathway involves the endoplasmic reticulum (ER), and it is known as the apoptotic pathway of ER stress-mediated cell death (Momoi, 2004). The ER is the site of assembly of polypeptide chains that are destined for secretion or routing into various subcellular compartments. The ER-initiated PCD pathway comprises the activation of caspase-12 and/or the cytochrome c-dependent apoptotic pathway.

1.9 Yeast serves as a useful model organism to study the phenomenon of cell death

Saccharomyces cerevisiae has been successfully used as model system to solve complex biological questions related to the mechanism of action of several molecules or genes or proteins. Fundamental results unraveling the deadly function of mitochondria during apoptosis execution in yeast have been achieved (Skulachev, 2006). Yeasts, both fission and budding, have been used as tools to examine the functions of bonafide regulators/effectors of metazoan apoptosis and this approach has proved valuable in shedding light on the obscure functions of the proapoptotic Bcl-2 family homologues of the CED-9 of *Caenorhabditis elegans*. Like metazoan cells, yeast cells undergo cell death showing characteristic apoptotic markers such as externalization of phosphatidylserine to the outer leaflet of the plasma membrane, DNA fragmentation and chromatin condensation (Madeo *et al*., 1997). Expression of either of the two mammalian proapoptotic Bcl-2 family members, BAX and BAK, in *S. cerevisiae* and

Schizosaccharomyces pombe results in cytotoxicity with similar phenotypes. Moreover, the yeast genome codes for many proteins of the basic molecular machinery executing cell death, including orthologues of caspases (Madeo *et al.*, 2002), apoptosis inducing factor (Wissing *et al*., 2004), HtrA2/Omi (Fahrenkrog *et al*., 2004), and inhibitor of apoptosis (IAP) proteins (Walter *et al*., 2006). Notably, histone phosphorylation, which is considered to be a universal prerequisite for apoptosis execution (Cheung *et al*., 2005), was shown to be necessary for cell death induction upon oxidative stress in yeast. Ahn *et al,* (2006) suggested that a regulated cross-talk between deacetylation and phosphorylation within Histone H2B tails was required for induction of apoptosis in yeast. Physiological scenarios of yeast apoptosis have been demonstrated during ageing (Fabrizio *et al*., 2004; Herker *et al*., 2004), the mating process (Severin and Hyman, 2002), and also the development of yeast multicellular colonies (Vachova and Palkova, 2005).

Some features of PCD appear to be conserved from bacteria to fungi to plants and animals (Ameisen, 1996). The accumulated evidence strongly suggests that the cytotoxic effects of the expression in the yeast of mammalian BAX or BAK are relevant to the mechanism of their proapoptotic action in mammalian cells (Fraser and James, 1998) and thus yeast has become an important model to investigate the conserved steps of apoptosis. The programmed death of yeast has been linked to complex mitochondrial processes, such as cytochrome *c* and AIF release, channel opening upon human Bax expression, depolarization of mitochondrial membrane potential, and mitochondrial fragmentation. These mitochondrial events are more or less common to various scenarios of yeast apoptosis, namely chronological and replicative ageing, decreased actin dynamics, as well as apoptosis induced by acetic acid (Ludovico *et al*., 2001), H_2O_2 (Madeo *et al*., 1997), amiodarone, or α-factor. Especially in the fields of ageing and neurodegeneration, intricate experimental and genetic problems present in higher organisms were addressed in yeast. The discovery of an apoptotic yeast strain carrying a *CDC48* mutation (Madeo *et al*., 1997) shed light on its mammalian orthologue VCP (Shirogane *et al*., 1999), which is involved in several polyglutamine triggered neurodegenerative disorders and the crucial involvement of mitochondria in the *CDC48* connected yeast cell death pathway

was also observed (Braun *et al*., 2006; Zischka *et al*., 2006). Galactose-induced expression of harpin$_{Pss}$ caused yeast cell death indicating that the yeast might share, with plants, conserved components in cell death pathway (Podile *et al.,* 2001) and in both, harpin$_{Pss}$-induced YCD as well as plant HR, oxidative burst seems to play a prominent role. Partial characterization of harpin$_{Pss}$-induced YCD has been carried out by Sripriya (2004), and reported the following:

- Galactose-induced expression of harpin$_{Pss}$ caused cell death in *S. cerevisiae* Y187.
- Harpin$_{Pss}$ has no extracellular effect on the yeast cells.
- Chromosomal condensation or genomic DNA fragmentation was not observed during harpin$_{Pss}$-induced YCD.
- Loss of membrane integrity was observed in yeast cells during harpin$_{Pss}$ expression.
- Harpin$_{Pss}$-induced YCD is independent of the stage of cell cycle.
- Yeast 'petite' mutants (lacking functional mitochondria) were insensitive to harpin$_{Pss}$-induced YCD, indicating the possible involvement of mitochondria in this form of cell death.
- Cytochrome c release from mitochondria was not observed in harpin$_{Pss}$-induced YCD.

Thus many discoveries made originally in yeast have been experimentally validated in higher eukaryotic cells, suggesting that yeast-based strategies for studying apoptotic genes will continue to provide more insights into conserved cell death mechanisms.

1.10 Bio-physical features of harpin may provide clues on the structure-function relationship of this enigmatic protein

Harpins are hydrophilic in nature, rich in leucine & glycine and highly thermal stable proteins (He *et al*., 1993) which retain their activity even after boiling to 90^0 C for 10 min. Report from Alfano *et al*, (1996) demonstrated that four different truncations of harpin$_{Pss}$ elicit similar HR activity that is indistinguishable with that of the HR elicited by full length harpin$_{Pss}$ in tobacco. Similarly, Sripriya (2004), also showed that, truncation of the protein either towards the *N*-terminal or *C*-terminal region caused cell death during in

yeast. Since these *hrpZ* fragments represent non-overlapping regions, it could be concluded that the activity of harpin is not confined to a specific region of the protein.

Harpins exhibit the property of forming amyloid like fibrils and possess helical structure (Oh *et al.,* 2007) and the predicted α-helix in the *N*-terminal region of HpaG (harpin from *Xanthomonas axonopodis*) was supposed to be responsible for the HR elicitor activity and mutations in the α-helix region of HpaG abolished the HR elicitation activity (Kim *et al*., 2004 and Wang *et al*., 2008). $Harpin_{Pss}$ exists as a polydispersed, multimeric protein in nature, the forms include, dimer, trimer, tetramer and octamer (Chen *et al.,* 1998) and the functional significance for the existence of the protein in many oligomeric forms, still remains unclear. Interestingly $harpin_{Pss}$ has a single 'Tryptophan' (W167) residue which makes it a protein of special interest for fluorescence quenching studies. $Harpin_{Pss}$ sequence analysis reveals the dissimilarity in amino acid sequence (He *et al*., 1993) or the absence of homology with any known protein in the protein data base, which makes it a peculiar biological molecule for functional or structural studies. Above all, the crystal structure of harpin (any of the known harpins) has not been elucidated till date and which really makes it a challenging biological molecule and one of the top proteins on the earth. Biophysical techniques like circular dichroism (CD), differential scanning calorimetry (DSC) and dynamic light scattering (DLS) have been extremely useful in revealing the structural and functional aspects of many biological macromolecules with special reference to proteins. CD was extensively used in studying the secondary structural confirmations of proteins like Cytochrome c and its interactions with Cytochrome c oxidase (Michel *et al*., 1989). DSC and DLS have been used for studying the thermal denaturation and light scattering or protein-ligand interactions of hexokinase (Barone *et al*., 1995) and calmodulin (Andriyka *et al*., 2002). Although $harpin_{Pss}$ has been extensively characterized biochemically and *via* mutational analysis, speculation of HR elicitation and high thermal stability of the protein have not been well addressed from a structural point of view. It would be quite interesting to look at the reasons for oligomerization from a structural point of view. CD analysis reveals that the protein is predominantly α-helical (51.5%) and the amino acid sequence shows high percentage (13.5%) of leucine (He *et al.*, 1993). These two clues suggested that a leucine-zipper like

motif might be present in harpin$_{Pss}$ as leucine-zipper is a motif, responsible for the dimeric or oligomeric form in many α-helical proteins (Landschulz *et al.*, 1988). A leucine zipper is a super secondary structural motif found in proteins that creates adhesion forces in parallel alpha helices (Landschulz *et al*., 1988). Each half of a leucine zipper consists of a short alpha-helix with a leucine residue at every seventh position, known also as the heptad repeat. The standard 3.6 residues per turn alpha-helix structure changes slightly to become 3.5 residues per turn alpha-helix. Leucine zipper motifs are protein-protein dimerization or oligomerization motifs consisting of heptad repeats of leucine or hydrophobic amino acid residues that form a coiled-coil structure (O'Shea *et al*., 1989; Gonzalez *et al.*, 1996). Classical coiled-coil proteins share a characteristic seven-amino acid repeat containing hydrophobic side chains at the first (a) and fourth (d) positions (Lupas *et al*., 1991, Conway and Parry, 1990). The lack of structure-activity relationship prompted us to take up the bio-physical studies of the protein and to look for common structural motifs among harpins which might be responsible for the functional nature of the molecule.

1.11 Objectives of the present study

Against this background, we have set two major objectives to understand more about the harpin$_{Pss}$-mediated cell death and the structure-function relationship of this protein viz.

1) Study of harpin-mediated cell death events:

   a) in yeast as a model system to decipher the physiological mechanism of action of harpin$_{Pss}$.

   b) on Jurkat cell lines (human T-cell lymphoma cell line) to test the effectiveness of harpin$_{Pss.}$

2) Investigation on the bio-physical features of harpin$_{Pss}$ for a better understanding of the structure- function relationship of the protein.

2.1 Yeast media

Strains were grown with aeration at 30^0 C in YEPD medium (1% (w/v) yeast extract, 2% (w/v) bactopeptone, and 2% (w/v) glucose) and Yeast Minimal Medium (YMM) containing a yeast nitrogen base (Difco), ammonium sulfate (Sigma), and tryptophan/uracil dropout supplement (Clontech) with raffinose or galactose (2%) (Sigma-aldrich) as the source of carbon (referred to as raffinose/galactose-containing medium, respectively) were used.

2.1.1 *E. coli* medium: Luria- Bertani medium (1% tryptone, 0.5% yeast extract and 1% sodium chloride) was used to grow *E. coli* cultures with appropriate antibiotic.

2.2 Strains, plasmids and growth conditions *Saccharomyces cerevisiae* Y187 (Clontech) strain was used in the present study. The plasmid constructs pYEUT and pYEUT-*hrpZ* were generated by Podile *et al,* (2001). *S. cerevisiae* Y187-pYEUT-*hrpZ* was grown in yeast minimal medium (YMM) with raffinose or galactose (2%) as the carbon source with aeration at 28^0 C. To induce *hrpZ* expression, the transformed cells grown to an early exponential phase (OD_{600} ~0.5) in 2% raffinose medium were washed and resuspended in tryptophan drop-out supplement medium containing 2% galactose (induction of GAL 1 promoter). Either H_2O_2 or acetic acid in raffinose medium was used as a positive control to induce cell death in *S. cerevisiae*.

LB medium with kanamycin was used to culture *E. coli* BL 21 (Rosettae) cells harboring pET28a-*hrpZ* at 37^0 C and induced with 1mM IPTG for $harpin_{Pss}$ expression.

2.3 *hrpZ* cloning, expression and purification

The *hrpZ* gene (1.02 kb) encoding full length $harpin_{Pss}$ was cloned under *Nde1* and *Xho1* sites of pET 28a vector (Novagen) (primers used and PCR conditions are listed in table 2.1 and table 2.2). *E. coli* BL 21 (Rosettae) cells transformed with pET 28a-*hrpZ* was grown in Luria Bertani (LB) broth with Kanamycin (50 µg/ml) to OD_{600} ~ 0.5 and induced with 1mM IPTG. After 3 h of induction, bacterial cells were pelleted, washed and resuspended in 10 mM sodium phosphate buffer (pH 7.5) and immediately sonicated (1min pulse on and 30 sec pulse off, 7 cycles, Bandelin MS-72 probe). The sonicate was

boiled for 10 min, then centrifuged at 14,000 rpm for 20 min to remove cell debris and the supernatant was loaded on to a Ni-NTA column (sigma-aldrich). Protein was eluted with 200 mM imidazole in phosphate buffer after washing the column with 20 mM imidazole of the same buffer and then perfectly dialyzed against 10mM sodium phosphate buffer (pH 7.5). Purity of both the proteins was checked on a 12 % SDS-PAGE. The dialyzed protein was concentrated using amicon filter (10 kDa cut off, Millipore) and used after estimation by Bradford's method (1976).

Table 2.1

Primers used in the present study

Primer sequence (5' to 3')	Target gene	5'/3'	Restriction site
CGAATCCCATATGCAGAGTCTCAGTCTTAAC	full length harpin$_{Pss}$	5'	*Nde* I
CGGGATCCTCGAGGGCTGCAGCCTGATTGC	full length harpin$_{Pss}$	3'	*Xho* I

Table 2.2

PCR conditions to amplify full length harpin$_{Pss}$ sequence

Steps	Full length harpin$_{Pss}$
Step 1	94^0 C- 5 min
Step 2	94^0 C- 1 min
Step 3	65^0 C- 1 min
Step 4	72^0 C- 1 min
Step 5	Go to step '2' for 30 times
Step 6	72^0 C- 10 min
Step 7	Hold at 16^0 C

2.3.1 Raising of polyclonal antibodies

Polyclonal antibodies were raised against harpin$_{Pss}$. The antibodies were raised by injecting harpin$_{Pss}$ into rabbit subcutaneously after mixing with Freund's complete adjuvant and emulsification. Prior to immunization, the lateral ear vein was bled to collect pre-immune serum. After two weeks, a booster injection of protein emulsified

with Freund's incomplete adjuvant was given. The second booster injection was given after a week of first booster injection and finally the blood was collected after 10 days of the second booster injection. The collected blood was left overnight at 4^0 C for clotting and serum was collected for centrifuging at 7,000 rpm for 20 min. The serum was aliquoted and stored at -20^0C after adding 0.01% sodium azide.

2.3.2 Western blot analysis

The protein was resolved in 12% SDS-PAGE along with protein molecular weight standards and then transferred onto nitrocellulose membranes (Bio-rad). The membranes were blocked with 5% (w/v) non-fat dry milk, incubated with harpin primary antibody in 10ml of antibody-diluted buffer (1x Tris buffered saline and 0.5% Tween with 5% milk) with gentle shaking at 4^0C for 8-12 h and then incubated with anti-rabbit IgG-ALP conjugate secondary antibody. The immunoblot was visualized using BCIP-NBT substrate.

2.3.3 Mass spectrometry of harpin$_{Pss}$

Two microliters of the purified (Ni-NTA) protein solution (~ 3 µg) was mixed with 2 µl of 2% TFA (trifluoroacetic acid) and 2 µl of the matrix solution (2,5 dihydroxyacetophenone with 10 mM di-ammonium citrate). Mass measurements were performed on a Autoflex III TOF/TOF spectrometer (Bruker) in the positive linear mode of operation. About 1000 single spectra were added. Spectra were processed using 10 Da Gauss filter smoothing and baseline subtraction.

2.4 Harpin$_{Pss}$-mediated yeast cell death

2.4.1 H_2DCFDA staining for ROS detection in yeast cells expressing pYEUT-*hrpZ*

S. cerevisiae cells, transformed with pYEUT-*hrpZ* were cultured in raffinose-containing medium with tryptophan drop out to an OD_{600} of 0.5 at 30^0C. The cells were pelleted, washed and resuspended in minimal medium supplemented with raffinose or galactose. A positive control with yeast cells treated with 80 mM acetic acid in raffinose containing medium was also set up. After 90 min of induction, cell culture (~ $1x10^6$ cells ml^{-1}) from

each sample was pelleted, resuspended in phosphate buffered saline (PBS) and incubated with 15 µM H_2DCFDA (2'7'-Dichloro dihydro fluorescein diacetate) for 30 min in dark at 28^0 C (Ludovico *et al.,* 2002). The cells were then acquired in the FACS Calibur flow cytometer at 488-520 nm using FL1-H filter for measuring the reactive oxygen species (ROS). A total of 20,000 cells were analyzed per sample.

2.4.2 Measurement of O_2 consumption in an 'Oxygraph'

S. cerevisiae pYEUT-*hrpZ* cells grown to an OD_{600} of 0.5 were pelleted and resuspended in raffinose or galactose containing medium and cultured for 4h. Cells (~$5x10^6$) from both the samples were resuspended in 1ml of YMM, loaded into the oxygraph chamber and monitored for O_2 uptake for a period of 10 min. Prior to loading of cells in the oxygraph chamber, water at a constant temperature of 25^0 C was circulated through the outer jacket of the reaction chamber. Calibration of oxygen content in the electrode chamber was done with air saturated water, assumed to contain 253 nmol O_2 ml^{-1} at 25^0 C. O_2 consumption by yeast cells was monitored using a Clark type O_2 electrode (DW2, Hansatech Ltd, King's Lynn, UK).

2.4.3 Rhodamine-123 (Rh-123) staining for detection of mitochondrial potential

S. cerevisiae pYEUT-*hrpZ* cells cultured for 200 min and 12h were centrifuged (~ $1x10^6$ cells ml^{-1}), washed and resuspended in 1ml PBS and incubated with 100 nM Rhodamine-123 (Ludovico *et al.,* 2001) for 30 min in dark at 28^0C. A positive control was also set up by adding 80 mM acetic acid in raffinose- containing medium. After incubation, the cells were washed with PBS to remove the unwanted dye, suspended in 1 ml of PBS and acquired in the BD FACS calibur flow cytometer equipped with an argon ion laser at an excitation of 488 nm and an emission of 529nm using FL1-H filter. A total of 20,000 cells were analyzed per sample.

2.4.4 Annexin V and Propidium Iodide (PI) staining

S. cerevisiae pYEUT-*hrpZ* cells cultured for 200 min were harvested (~$1x10^6$ ml^{-1}), washed with PBS and treated with 15 U lyticase (Sigma-aldrich) ml^{-1} in sorbitol buffer

(pH 6.8) for 30 min at 28^0C (Madeo *et al.*, 1997). Cells were then washed with binding buffer (10 mM HEPES, 140 mM NaCl, 2.5 mM $CaCl_2$, pH 7.4), suspended in 200 µl of binding buffer and stained with 5 µl of annexin V- FITC (20 µg/ml) (BD Biosciences) and 10 µl of PI (50 µg/ml) for 20 min in dark at 30^0C. After incubation, the cells were washed with binding buffer and resuspended in 1 ml of PBS. The samples were then acquired in the BD FACS calibur flow cytometer using FL 1-H filter (λ_{exc}= 488 nm and λ_{em} = 529 nm) on X- axis and FL 2-H filter (λ_{exc}= 605 nm and λ_{em} = 640 nm) on Y-axis. A total of 20,000 cells were analyzed per sample. Acetic acid treated cell sample was used as a positive control.

2.4.5 Yeast cell cycle analysis by flow cytometry

S. cerevisiae Y187 pYEUT-*hrpZ* cells grown to an OD_{600} ~0.5 were centrifuged, resuspended in YMM and synchronized in the presence of 0.2 M hydroxy urea (sigma-aldrich) for 2 h. Cells were then pelleted, washed and resuspended in YMM containing raffinose and cultured for 3 h. Cells were then recentrifuged and suspended in YMM supplemented with raffinose or galactose or raffinose with 0.2 M hydroxy urea (S-phase blocker) as a positive control. After incubating for a period of 4h, 12h and 24h, cells (~1x 10^6) were collected from each sample, fixed with 70% ethanol for at least 30 min and resuspended in 0.5 ml of 50 mM sodium citrate containing 0.1 mg/ml RNase A and propidium iodide (Sigma-Aldrich) at a final concentration of 4 µg/ml, following the incubation of the sample at 30^0 C for 30 min. Then the cells were spin down and suspended in 1 ml of PBS and acquired in BD FACS calibur flow cytometer using FL 2-A filter (λ_{exc}= 605 nm and λ_{em} = 640 nm). A total of 20,000 cells were analyzed per sample.

2.4.6 Estimation of oxidized and reduced Glutathione

S. cerevisiae Y187 pYEUT-*hrpZ* cells cultured in the presence of raffinose or galactose for 12 h were pelleted and homogenized in a buffer consisting of 0.1 M sodium phosphate and 0.005 M EDTA (pH 8.0) with 25% phosphoric acid (HPO_3) which is used as protein precipitant. The total homogenate was ultracentrifuged at 36,000 rpm for 30

min at 4^0C to obtain the supernatant for the assay of oxidized glutathione (GSSG) and reduced glutathione (GSH) (Hissin and Hilf, 1976). Protein estimation (Bradford, 1976) was carried out to take equal amounts of protein from both the samples for the assay.

GSH assay: To 0.5 ml of the above supernatant, 4.5 ml of the phosphate-EDTA buffer, pH 8.0 was added. The final assay mixture (2.0 ml) contained 100 µl of the diluted supernatant, 1.8 ml of phosphate-EDTA buffer and 100 µl of the *O*-Phthalaldehyde (OPT) solution, containing 100 µg of OPT. After thorough mixing and incubation at room temperature for 15 min, OD was recorded in a fluorescence spectrophotometer with absorbance at 420 nm and excitation at 350 nm.

GSSG assay: A 0.5 ml portion of the original supernatant was incubated at room temperature with 200 µl of 0.04 M *N*-ethylmaleimide (NEM) for 30 min to interact with GSH present in the sample. To this mixture 4.3 ml of 0.1 N NaOH was added. A 100 µl portion of this mixture was taken for measurement of GSSG, using the procedure outlined for GSH assay, except that 0.1 N NaOH was employed as diluent rather than phosphate-EDTA buffer. Standard curve for GSH and GSSG was prepared according to the method of Hissin and Hilf (1976).

2.4.7 Detection of metacaspase activation

S. cerevisiae Y187 pYEUT-*hrpZ* cells cultured in the presence of raffinose or galactose were assessed for caspase activation using the fluorescent caspase inhibitor 'CaspACE, FITC-VAD-fmk *In Situ* Marker' (Promega) (Madeo *et al*., 2002). Briefly, 1x 10^6 cells were washed in PBS, suspended in 200 µl staining solution containing 10 µM of FITC-VAD-FMK and incubated for 30 min at 30^0 C in dark. Cells were then washed once and suspended in PBS. Sample analysis was performed in a BD FACS Calibur flow cytometer equipped with FL 1-H filter (λ_{exc}= 488 nm and λ_{em} = 529 nm). A total of 20,000 cells were analyzed per sample. Acetic acid treated cell sample was used as a positive control.

2.4.8 Mitochondrial enzyme assays

Isolation of mitochondria

Mitochondria were isolated following the protocol of Daum *et al.,* (1982) from both the raffinose grown (control) yeast cells, and galactose grown ($harpin_{pss}$ expressed) yeast cells. *S. cerevisiae* Y187 cells cultured in raffinose or galactose-supplemented medium for 15 h at 28^0 C were harvested by centrifugation (5 min, 5000 rpm), washed with distilled water, suspended to 0.5 g, wet weight / ml in 0.1 M Tris.SO_4, pH 9.4, 10 mM dithiothreitol (DTT), and incubated for 10 min at 30^0 C. They were then washed once with 1.2 M sorbitol, 20mM potassium phosphate buffer, pH 7.4, to give 0.15 g of cell, wet weight/ml. Lyticase (Sigma-aldrich) (5mg/g of wet weight) was added and the suspension was incubated at 30^0 C with gentle shaking. After 50 – 60 min, all the cells had usually been converted to spheroplasts. Spheroplasts were harvested by centrifugation for 5 min at 3000 rpm, washed twice with 1.2 M Sorbitol. For homogenization, spheroplasts were suspended in 0.6 M Mannitol, 10 mM Tris Cl, pH 7.4, 0.1% bovine serum albumin (BSA), 1 mM phenylmethylsulfonylfluoride (PMSF), to a concentration of 0.15 g of spheroplasts (wet weight/ml). After chilling on ice, spheroplasts were homogenized by 10-15 strokes in a tight fitting Dounce homogenizer. From this point, all operations including centrifugations were carried out at 0 - 4^0 C. The homogenate was diluted with one volume of the homogenization buffer and centrifuged for 5 min at 3500 rpm. The supernatant was saved, and the pellet was rehomogenized as before and recentrifuged at 3500 rpm. The supernatants were combined and crude mitochondria were sedimented at 9000 rpm for 10 min. The mitochondrial pellet was washed twice by resuspension and recentrifugation at 9000 rpm for 10 min; for the last wash, BSA and PMSF were omitted from the washing buffer. Mitochondria were suspended in 0.6 M Mannitol, 10mM Tris-Cl, pH 7.4, to give an approximate final concentration of 10 mg of protein/ ml.

Visualization of mitochondria by confocal microscopy

Isolated mitochondria were suspended in 10mM Tris-Cl buffer, pH 7.4 and 10µl of JC-1 (1.5mg/ml) fluorescent dye was added and incubated for 20 min in dark at 4^0 C. A drop of the suspension was placed on a glass slide, covered with a coverslip and observed under

the confocal microscope (Leica) at λ_{exc}= 605 nm and λ_{em} = 640 nm for red filter, and λ_{exc}= 514 nm and λ_{em} = 529 nm for green filter.

Mitochondrial protein estimation

The protein content of the mitochondria, isolated from the raffinose or galactose grown yeast cells was estimated by Bradford's method (1976) against BSA standard.

2.4.8a Assay for NADH dehydrogenase (Complex I) activity

NADH dehydrogenase assay was carried out following the protocol of Sottocasa *et al*, (1967). Mitochondrial suspension (i.e. 0.1 mg mitochondrial protein) from yeast cells cultured in raffinose-supplemented medium or the mitochondrial protein (i.e. 0.1 mg) from the yeast cells cultured in galactose-supplemented medium was taken into 1 ml quartz cuvettes and the volume was made up to 0.98 ml with potassium phosphate buffer, pH 7.4 (50 mM monobasic potassium phosphate and 50 mM dibasic potassium phosphate). To this 10 µl of potassium ferricyanide (100 mM) was added and the reaction was initiated by adding 10µls of NADH (100 mM) to each of the cuvettes. Absorbance changes were measured at 420 nm at regular intervals of 50 sec for 3 min. The molar extinction coefficient of NADH is 6.22 x 10^{-3}. The activity of NADH dehydrogenase is expressed as µ moles of NADH oxidized or reduced per min per mg protein. Activity of NADH dehydrogenase = Slope (ΔAbs/min) x 1 mg / 6.22 x 10^{-3} x amount of mitochondrial protein taken in mg for assay. Percentage difference in activity = [(activity of glu-mit) – (activity of gal-mit)] x 100 / activity of glu-mit.

2.4.8b Assay for Cytochrome c oxidase activity

Cytochrome C oxidase activity assay from yeast mitochondria was performed following the standard instructions given in the Sigma-aldrich kit. To a final volume of 1ml, 0.85 ml of 1x assay buffer, 50 µl of Ferrocytochrome c substrate solution (reduced with 0.5 mM DTT, sigma kit) along with 20 µg of yeast mitochondrial protein was added followed by the addition of 1x enzyme dilution buffer to make up the remaining volume. Assay reaction was monitored by the oxidation of ferrocytochrome c to ferricytochrome c

at 550 nm at regular intervals of 50 sec for 5 min in an UV-Visible spectrophotometer. Reaction mixture containing all the above components, except mitochondrial protein, was used as a blank. The difference in molar extinction coefficient between reduced and oxidized cytochrome c is 21.84 at 550 nm. The activity of Cytochrome c oxidase is expressed as µ moles of Ferrocytochrome c oxidized per min per mg protein. Activity of Cytochrome c oxidase = Slope (ΔAbs/min) x 1 mg / 21.84 x amount of mitochondrial protein taken in mg for assay. Percentage difference in activity = [(activity of Raf-mit) – (activity of gal-mit)] x 100 / activity of Raf-mit.

2.4.8c Assay for yeast mitochondrial ATPase activity

Mitochondrial ATPase activity was measured following the protocol of Pullman *et al*., (1960). To a final volume of 1ml, 50 mM Tris Cl (pH 8.0), 1 mM ATP, 0.3 mM NADH, 3.3 mM $MgCl_2$, 2 µg/ml antimycin A, 1mM Phosphoenol pyruvate, 5 U/ml Lactate dehydrogenase and 2.5 U/ml Pyruvate kinase were added along with 20 µg of yeast mitochondrial protein (measured by Lowry method) at 28^0 C. Assay reaction was monitored by the oxidation of NADH at 360 nm at regular intervals of 50 sec for 5 min in an UV-Visible spectrophotometer. Reaction mixture containing all the above components except mitochondrial protein was used as a blank. The molar extinction coefficient of NADH is 6.22×10^{-3}. The activity of Mitochondrial ATPase is expressed as µ moles of NADH oxidized or reduced per min per mg protein. Activity of ATPase = Slope (ΔAbs/min) x 1 mg / 6.22×10^{-3} x amount of mitochondrial protein taken in mg for assay. Percentage difference in activity = [(activity of Raf-mit) – (activity of gal-mit)] x 100 / activity of Raf-mit.

2.5 Animal cell culture

2.5.1 Chemicals: RPMI 1640 cell culture medium (sigma-aldrich), Fetal bovine serum (FBS) (sigma-aldrich), Phosphate buffered saline (PBS), MTT (3-(4,5-dimethyl thiazol-2yl)-2,5-diphenyl tetrazolium bromide) (Himedia) were used.

2.5.2 Jurkat cell culture

Jurkat cells (human T-cell lymphoma cell line) were grown in RPMI 1640 supplemented with 10% heat inactivated fetal bovine serum (FBS), 100 IU/ml penicillin, 100 µg/ml Streptomycin and 2 mM L-glutamine. Cultures were maintained in a humified atmosphere with 5% CO_2 at 37^0 C. The cultured cells were passed twice a week seeding at a density of about 2x 10^5 cells/ml. Cell viability was determined by the trypan blue dye exclusion test.

2.5.3 Harpin$_{Pss}$ treatment/cell proliferation assay

Cell proliferation was determined using the MTT assay. Jurkat cells (25x10^3 cells/well) were incubated in 96 well plates in the presence (10 – 80 µM) or absence of harpin$_{Pss}$ (control) for 24h in a final volume of 200 µl. After treatment, 20 µl of MTT (5 mg/ml in PBS) was added to each well and incubated for an additional 4h at 37^0 C. The purple blue MTT formazan precipitate was dissolved in 100 µl of dimethyl sulfoxide (DMSO) and the absorbance values were recorded at 570 nm on a multiwell plate ELISA reader (Lab systems, Multiskan, 355).

2.5.4 DNA fragmentation assay

Jurkat cells treated with 40 µM harpin$_{Pss}$ for 12 and 24 h were used for the isolation of the DNA. DNA laddering was detected by isolating fragmented DNA using the SDS/ Proteinase K/ RNase A extraction method (Sambrook *et al*., 1989), which allows the isolation of only fragmented DNA without contaminating genomic DNA. Five million cells were pelleted, washed in cold PBS and lysed in a buffer containing 50 mM Tris-HCl (pH 8.0), 1 mM EDTA, 0.2 % Triton X-100 for 20 min at 4^0 C. After centrifugation at 14,000 g for 15 min, the supernatant was treated for 1 h at 37 °C with RNase A (0.5 mg/ml) and then with proteinase K (0.5 mg/ml) for 1 h at 50 °C. DNA was extracted with buffered phenol and precipitated with ethanol and DNA was resolved on 1 % agarose gel in TBE (44.6 mM Tris, 44.5 mM boric acid and 1 mM EDTA). DNA fragmentation was visualized upon staining gel with ethidium bromide (0.5 mg/ml) and exposed to UV light.

2.5.5 Quantification of apoptosis by flow cytometry

To quantitate apoptosis (sub G0/G1 cells), flow cytometric analysis using propidium iodide (PI) was performed. Jurkat cells treated with 40 µM harpin$_{Pss}$ for 12 and 24 h, were prepared as single cell suspension in 200 µl PBS, fixed with 2 ml of ice-cold 70% ethanol, and maintained at 4 ^{0}C overnight. The cells were harvested by centrifugation at 500 x g for 10 min, resuspended in 500 µl PBS supplemented with 0.1 % Triton X-100 and RNase A (50 µg/ml), incubated at 37 °C for 30 min, and stained with 50 µg/ml propidium iodide (PI) in dark at 4 °C for 30 min. The red fluorescence of individual cells was measured with a FACS Calibur flow cytometer using FL 2-H filter (λ_{exc}= 605 nm and λ_{em} = 640 nm) (BD Biosciences). A minimum of 20,000 events were counted per sample.

2.5.6 Preparation of whole cell extracts and immunoblot analysis

The cell lysis was carried out as described by Sambrook *et al*., (1989). To prepare the whole cell extract, cells after treatment were washed with PBS and suspended in a lysis buffer (20 mM Tris, 1 mM EDTA, 150 mM NaCl, 1% NP-40, 0.5% sodium deoxy cholate, 1 mM β-glycerophosphate, 1 mM sodium orthovanadate, 1 mM PMSF, 10 µg/ml leupeptin, 20 µg/ml aprotinin). After 30 min of shaking at 4^{0}C, the mixtures were centrifuged (9,000 rpm) for 10 min, and the supernatants were collected as the whole-cell extracts. The protein content was determined according to Bradford, (1976). An equal amount of total cell lysate was resolved on 8-12 % SDS-PAGE gels along with protein molecular weight standards, and then transferred onto nitrocellulose membranes. Membranes were stained with 0.5% Ponceau *S* in 1% acetic acid to check the transfer. The membranes were blocked with 5% w/v nonfat dry milk and then incubated with the primary antibodies (Bax and Bcl 2) in 10 ml of antibody-diluted buffer (1X Tris-buffered saline and 0.05% Tween-20 with 5% milk) with gentle shaking at 4 ^{0}C for 8-12 h and then incubated with ALP conjugated secondary antibodies. Signals were detected by using substrate BCIP-NBT. The blots were probed with β-actin antibodies to confirm equal loading.

2.5.7 Detection of cytochrome *c* release using Western blot analysis

After exposure to 40 µM $harpin_{Pss}$ for various time periods, cells were collected and washed with PBS and subsequently with buffer A (0.25 M sucrose, 30 mM Tris-HCl, pH 7.9, 1 mM EDTA). Cells were then resuspended in buffer A containing 1 mM PMSF, 1 mg/ml leupeptin, 1 mg/ml pepstatin, 1 mg/ml aprotinin and homogenized with a glass dounce homogeniser. After centrifugation for 10 min at 16,000 rpm, protein concentration of the cytosolic extract was determined using Bradford method. Approximately, 30 µg of cytosolic protein was used for Western blot analysis as described above. Cytochrome c was detected using the mouse monoclonal antibody directed against human cytochrome c.

2.6 Bio-physical studies

2.6.1 Circular dichroism spectroscopy (CD)

Circular dichroic (CD) spectra were recorded on a Jasco J-810 spectropolarimeter (Jasco International Co., Ltd., Tokyo, Japan, website: http://www.jascoint.co.jp) equipped with a Peltier thermostat supplied by the manufacturer. Samples were placed in a 2-mm path length rectangular quartz cell. Spectra were recorded at a scan rate of 20 nm/min with a response time of 0.5 sec and a band width of 2 nm. Protein concentration was 2.25 µM for measurements in the far UV region (250–190 nm). Each spectrum was the average of 4 accumulations. In order to study the effect of temperature on the secondary structure of the protein, CD spectra were recorded in the near UV region at different temperatures.

2.6.2 Fluorescence spectroscopy

Emission spectra were recorded on a Spex Fluoromax-3 fluorescence spectrometer from Jobin-Yvon (Edison, JJ. USA, website: http:// www.jobinyvon.com). Slit width of 3 nm and 6 nm were used on the excitation and emission monochromators respectively. Measurements were performed by irradiating protein ($harpin_{Pss}$) samples ($OD_{280} \leq 0.1$) with light of 295 nm wavelength, in order to selectively excite tryptophan residues of the protein and emission spectra were recorded above 300 nm. In fluorescence quenching experiments, small aliquots of 5 M quencher stocks (acrylamide or potassium iodide)

were added to protein samples and fluorescence spectra were recorded after each addition. The final quencher concentration attained in each case was 0.52 M. The iodide stock solution contained 0.2 M sodium thiosulphate to prevent the formation of triiodide. All the measurements were performed in duplicate at 25^0 C and yielded reproducible results. The average values have been reported.

2.6.3 Differential scanning calorimetry (DSC)

DSC experiments were performed on a MicroCal VP-DSC differential scanning microcalorimeter (MicroCal Inc., Northampton, MA, USA) equipped with two fixed cells, a reference cell and a sample cell. Sample and reference solutions were properly degassed with stirring in an evacuated chamber for 5 min at room temperature and then carefully loaded into the calorimeter cells. A background scan collected with buffer in both cells was subtracted from each scan. The temperature dependence of the molar heat capacity of the proteins was further analyzed by using the Origin DSC software package supplied by the manufacturer.

2.6.4 Dynamic light scattering (DLS)

DLS measurements were performed at a protein concentration ranges from 0.5-1.0 mg/ml at pH 7.5. Before the DLS measurements, the solutions were passed through a 0.22 μm filter and centrifuged at 14,000 rpm for 10 min. All experiments were performed at a 90° scattering angle on a PDExpert (Precison Detectors, Inc. Bellingham, MA, USA) DLS instrument at a wavelength of 685 nm with a power of 30 mW. The measurements were carried out at various temperatures ranges between 25-61°C using a built-in temperature controller. The diffusion coefficient (D) was calculated from the autocorrelation function, using the accessory 'PrecisonAcquire' software provided with the instrument. The experimentally measured hydrodynamic radius, (R_h) of the protein was determined from the Stokes–Einstein relationship.

2.6.5 Congo red binding

To measure congo red binding, 100 μg of protein was added to a 10 μM congo red (Sigma-aldrich) solution in 5 mM sodium phosphate buffer at pH 7.5. The absorbance

spectrum was measured from 400 to 600 nm using a Cary 100 UV-Vis spectrophotometer (VARIAN) equipped with a Peltier thermostat supplied by the manufacturer.

2.6.6 Atomic Force Microscopy (AFM)

A drop of 0.1 mg/ml protein solution was placed on a freshly cleaved mica sheet and dried immediately under nitrogen gas. The salt deposits were washed extensively by washing with miliQ water. The samples were once again dried with nitrogen gas. All the images were recorded in air under ambient conditions in semi-contact mode with a scan rate of 80 Hz using a NTMDT (Moscow) AFM instrument. The force was kept at the lowest possible value by continuously adjusting the set-point and feed-back gain during imaging. Image analysis was performed using NOVA software, supplied by NTMDT along with the instrument.

2.6.7 Crystallization of harpin$_{Pss}$

Protein (5-6 mg/ml) exchanged in 20 mM Tris-Hcl, pH 7.0 was used to set up for intial screening. 'Crystal screen high throughput' and 'Index screen high throughput' (Hampton research) were the most commonly used commercial screens for screening. Classic screens of 'Jena Bioscience' (JBS) were also used for screening. Crystallization was done by 'Sitting-drop vapor diffusion' for all the commercial screens. Sitting drop screens were set up in 96 well Greiner plates with three sub wells for holding the sample. 100 µl of screening solution (various combinations) was used per well. Drops containing 2 µl of protein and reservoir solution was placed in each sub well in a ratio of 1:1 using 'Hydra I- e Drop'. Three different concentrations of the protein (1.5, 3, 5 mg/ml) were used in the sub wells. Plates were sealed after being set up and placed in a 277 K and 293 K 'Rigaku robo' incubator and imaged using a 'Minstrel' plate reader. Plates were observed for nucleation or crystal growth over a period of 2 months. Conditions giving micro crystalline precipitates were further expanded using 'Crystal track' software and dispensed using 'Alchemist'. 96 screens were thus prepared and drops were set up and imaged. A total of 2016 set ups were screened for crystallization.

3.1 Harpin$_{Pss}$-induced cell death events in yeast

3.1.1 Detection of ROS in *S. cerevisiae* cells expressing harpin$_{pss}$

S. cerevisiae Y187 cells harboring pYEUT-*hrpZ* were cultured in raffinose-supplemented medium, pelleted and resuspended in YMM containing raffinose or galactose or treated with acetic acid. ROS is detected using 2'7'-dichloro dihydro fluorescein diacetate, a non-fluorescent cell-permeable compound, which is changed to fluorescent compound 2'7'-dichlorofluorescein upon oxidation by ROS. Cells with ROS release exhibit greenish yellow fluorescence which could be detected in the flow cytometer using FL1-H filter at λ_{exc} = 488 nm and λ_{em} = 520 nm. Only 1.7% cells cultured in raffinose-supplemented medium exhibit ROS levels where as 45% of acetic acid treated cells exhibit ROS levels (Fig.3.1) and 39% of yeast cells cultured in galactose-supplemented medium shows ROS levels indicating that reactive oxygen species (ROS) are involved in harpin$_{pss}$-mediated yeast cell death.

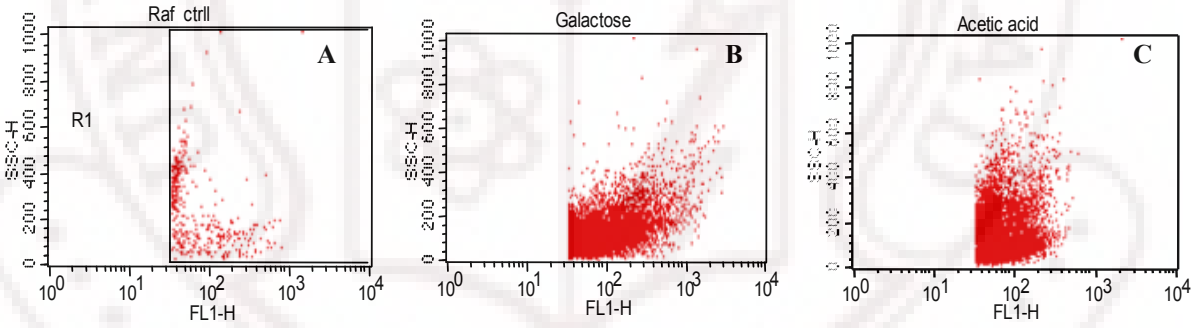

Fig 3.1 Detection of ROS in harpin$_{pss}$-mediated yeast cell death

S. cerevisiae Y187 cells harboring pYEUT-*hrpZ* were cultured in raffinose-supplemented medium with tryptophan drop out to an OD_{600} of 0.6. Cells were then pelleted, washed and resuspended in minimal medium containing raffinose or galactose or treated with 80 mM acetic acid. After 90 min of induction, cell culture (~ $1x10^6$ cells ml^{-1}) was pelleted, resuspended in PBS and incubated with 15 µM H_2DCFDA for 30 min in dark at 28^0 C. The flow cytometry pictures of cells cultured in media supplemented with A) raffinose B) galactose C) 80 mM acetic acid in raffinose. Data represent the result from one of three similar experiments.

3.1.2 Determination of O_2 consumption during harpin$_{pss}$- induced YCD

S. cerevisiae Y187 pYEUT-*hrpZ* cells cultured in raffinose-containing medium were shifted to raffinose or galactose-supplemented medium to induce harpin$_{Pss}$ expression. Oxygen consumption of yeast cells was monitored using an 'Oxygraph' consisting of a 'Clark O_2 electrode' that measures the amount of dissolved oxygen in the medium. After 4h incubation, O_2 consumption by yeast cells expressing harpin$_{pss}$ was determined to be 0.9 $\pm$ 0.2 nmoles/min/5 million cells (Fig 3.2), where as the O_2 consumption by control cells cultured in raffinose-supplemented medium was determined to be 3.4 $\pm$ 0.3 nmoles/min/5 million cells. Harpin$_{pss}$ -expressed yeast cells exhibit a four-fold reduction in the rate of oxygen consumption which indicates the impairment of mitochondrial function, thus leading to respiratory deficiency in harpin$_{pss}$-induced yeast cell death.

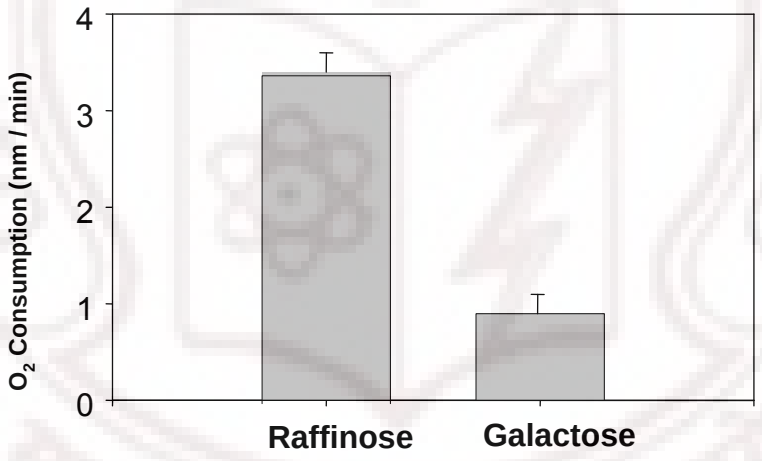

Fig 3.2 Estimation of O_2 consumption during harpin$_{pss}$-induced yeast cell death

S. cerevisiae Y187 transformed with pYEUT-hrpz was grown in raffinose-supplemented medium with tryptophan drop out to an OD_{600} of 0.6 at 30^0 C. The cells were then centrifuged and suspended in raffinose or galactose containing medium and incubated for 4h. Cells (~$5x10^6$) from both the samples were pelleted and resuspended in 1ml of YMM containing 2% raffinose or galactose. The 1ml cell suspension was loaded into the oxygraph chamber and monitored for O_2 uptake for equal period of time. Vertical bars on the histogram indicate standard error of three independent experiments.

3.1.3 Assessment of mitochondrial membrane potential (ψ) in yeast cells expressing harpin$_{Pss}$

S. cerevisiae Y187 pYEUT-*hrpZ* cells cultured in raffinose or galactose or acetic acid treated cells were monitored for changes in mitochondrial potential using rhodamine-123, a lipophilic cationic dye that is accumulated by intact mitochondria possessing negative charge. The rate of accumulation of the dye depends on the mitochondrial membrane potential. Rh-123 could be detected in the flow cytometer using FL1- H filter at λ_{exc}= 488 nm and λ_{em} = 529 nm. Yeast cells expressing harpin$_{Pss}$ and acetic acid treated cells exhibit hyperpolarization (Fig 3.3A) during the initial hours of culturing as compared to that of control cells grown in raffinose-containing medium. During the late hours of induction (i.e. 12 h), harpin$_{Pss}$- expressed yeast cells and acetic acid- treated cells showed depolarization (Fig 3.3B) of mitochondrial membrane as compared to that of control cells.

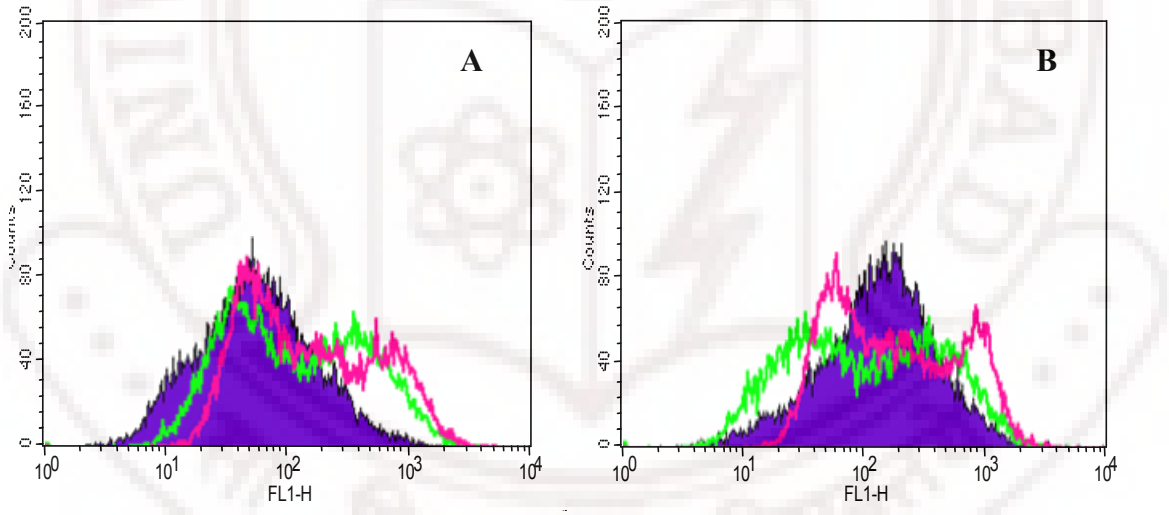

Fig 3.3 Detection of mitochondrial membrane potential (ψ) in harpin$_{pss}$-induced YCD

S. cerevisiae Y187 pYEUT-hrpZ cells cultured in raffinose-supplemented medium were pelleted and resuspended in minimal medium containing raffinose or galactose or treated with 80 mM acetic acid. After 3 h of induction, ~1x10^6 cells ml^{-1} was pelleted, resuspended in PBS and incubated with 100 nM Rh-123 for 30 min at 30^0 C and then acquired in the flow cytometer. The area in violet color represents the cells cultured in raffinose-supplemented medium, the green colored line represents the cells cultured in galactose-supplemented medium where the expression of harpin$_{Pss}$ is induced and the pink colored line represents the cells cultured in raffinose containing medium with acetic acid induced cell death. Cells cultured for A) 3 h and B) 12 h after induction. Data represent the result from one of three similar experiments.

3.1.4 Assessment of yeast cell death induced by harpin$_{Pss}$

S. cerevisiae Y187 pYEUT-*hrpZ* cells cultured in raffinose-supplemented medium were pelleted and resuspended in minimal medium containing raffinose or galactose or treated with acetic acid. Nature of cell death (whether apoptotic or necrotic) was assessed using annexin V, a protein of 36 kDa that binds to the phosphotidyl serine residues and detected by the conjugated fluorescent molecule FITC in the flow cytometer or fluorescent microscope. Cells which show the binding of annexin V are said to be in the phase of apoptotic cell death. Annexin V-FITC is detected using FL 1-H filter at an excitation of 488 nm and an emission of 529 nm. Cells were simultaneously counter stained with another fluorescent dye propidium iodide which is taken up by cells in the phase of necrotic cell death. PI is detected in flow cytometer using FL 2-H filter at an excitation of 605 nm and an emission of 640 nm. In harpin$_{Pss}$- induced YCD 29% of galactose-supplemented cells (fig 3.4) and 53% of acetic acid treated cells have taken up PI showing a shift towards the upper left quadrant as compared with 3% of control cells cultured in raffinose-supplemented medium. Only 1.6 % of acetic acid treated cells and 0.2 % of harpin$_{Pss}$- induced cells tested positive for annexin V staining (upper right quadrant). Hence the yeast cell death induced by harpin$_{Pss}$ expression and acetic acid (130mM) treatment has more orientation towards necrosis rather than apoptosis.

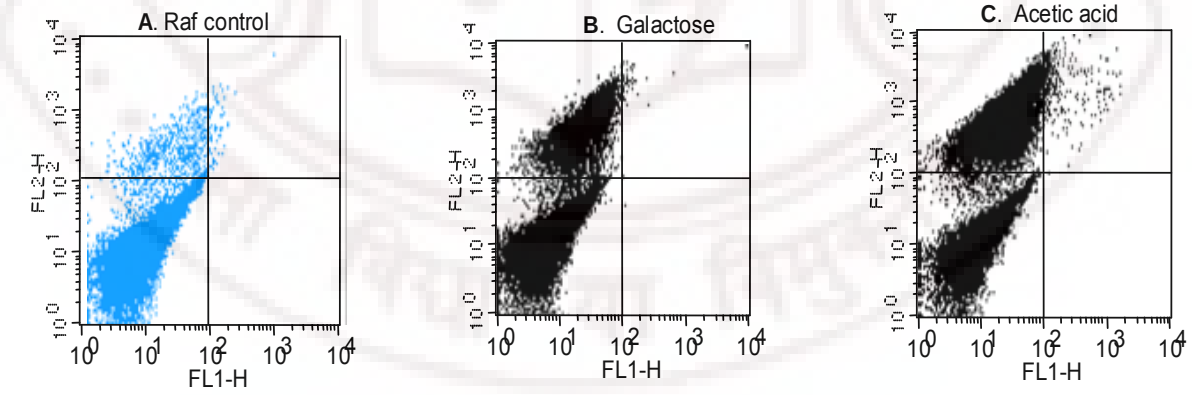

Fig 3.4 Assessment of yeast cell death induced by harpin$_{Pss}$

S. cerevisiae Y187 transformed with pYEUT-*hrpz* was grown in raffinose medium, centrifuged and resuspended in raffinose or galactose or treated with acetic acid. After 4h culturing cells were pelleted and treated with lyticase for 30min and stained with annexin V- FITC (20µg/ml) and PI (50µg/ml). The flow cytometry pictures of cells (A) cultured in raffinose served as control, (B) galactose-supplementation where harpin expression was induced and (C) cells treated with acetic acid. Data represent the result from one of three similar experiments.

3.1.5 Yeast cell cycle analysis

S. cerevisiae Y187 pYEUT-*hrpZ* cells cultured in raffinose-containing medium were shifted to raffinose or galactose-supplemented medium or treated with hydroxy urea. Harpin$_{Pss}$-induced YCD was verified by flow cytometric analysis of cellular DNA content stained with propidium iodide which directly represents different phases of the cell cycle. PI could be detected in the flow cytometer using FL2- A filter at λ_{exc}= 605 nm and λ_{em} = 640 nm. The cell cycle histograms of *S. cerevisiae* Y187 cultured in different conditions and time points are illustrated in Fig 3.5 and the percentage of cells in different phases of the cell cycle at three different time points are represented in table 3.1. The FACS analysis of control cells (cultured in raffinose) showed prominent G1, followed by S and G2/M phases except in late hour (24h) sample where more number of cells are in stationary phase showing increased accumulation in the G1 phase. Harpin$_{Pss}$-expressing yeast cells (galactose cultured) showed increased accumulation in G0/G1 sub phase (resembling positive control) with increase in culturing time as compared to the control cells. Yeast cells cultured in presence of hydroxy urea (positive control) exhibit blockage of cell cycle at the S-phase showing more accumulation of cells at the G1-phase. Thus harpin$_{Pss}$- expression in yeast leads to DNA damage resulting in cell cycle blockage ultimately leading to yeast cell death.

Cell cycle phase	Cells cultured in Raffinose (%)			Cells cultured in Galactose (%)			Cells cultured in Hydroxy urea ('S' block) (%)		
	4h	**12h**	**24h**	**4h**	**12h**	**24h**	**4h**	**12h**	**24h**
G0 (M4)	0.89	1.9	3.3	3.6	19.64	48.1	7.1	43.05	4.15
G1 (M1)	54.7	58.8	62.1	61.4	55.93	43.8	61.9	49.3	65.78
S (M2)	13.1	16.1	13.4	10.3	17.5	5.3	14.1	6.0	13.3
G2M (M3)	31.1	22.3	21.3	23.8	7.3	3.2	15.0	2.3	16.7

Table 3.1 Percentage of yeast cells in different phases of the cell cycle at three different time points

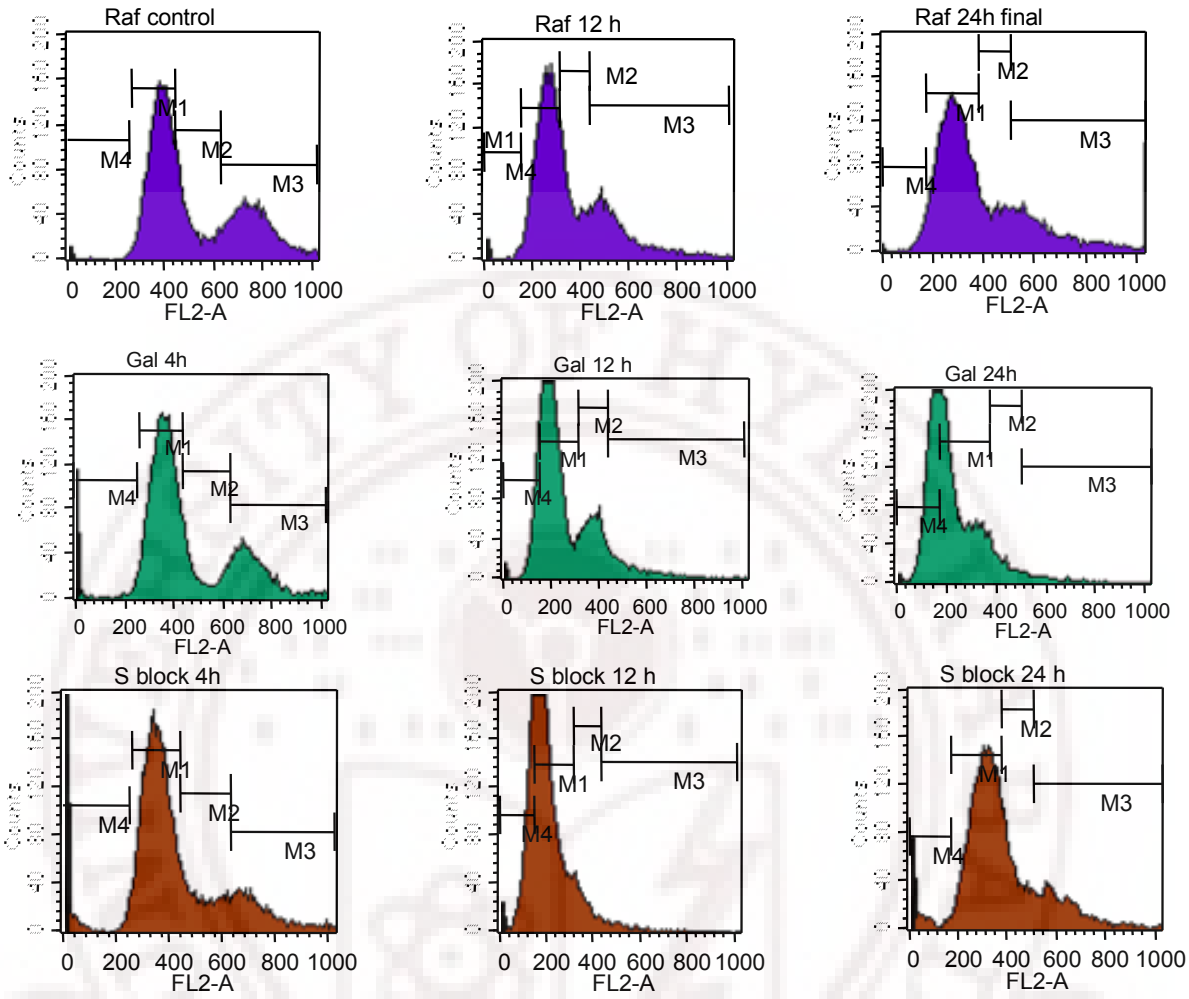

Fig 3.5 Cell cycle analysis in harpin$_{pss}$-mediated yeast cell death.

S. cerevisiae Y187 pYEUT-*hrpZ* cells were grown in raffinose-containing medium with tryptophan drop out to an OD ~0.6 at 30^0 C. Cells were then pelleted and resuspended in YMM containing raffinose or galactose or raffinose with 0.2M Hydroxy urea. After incubating for a period of 4h, 12h and 24h, cells were collected from each sample, fixed with 70 % ethanol and stained with PI (4µg/ml) and then acquired in flow cytometer. Violet colored histograms represents cells grown in raffinose-containing medium, green and brown histograms represent cells grown in galactose (harpin$_{Pss}$-expressing) and in presence of S-phase blocker. Data represent the result from one of three similar experiments.

3.1.6 Determination of GSH and GSSG content

S. cerevisiae Y187 harboring pYEUT-*hrpZ* was grown in raffinose-supplemented medium, pelleted and resuspended in YMM containing raffinose or galactose. After incubation for 12 h, cell extracts were prepared and used for the estimation of glutathione. Glutathione is present in the oxidized form (GSSG) which is readily converted to the reduced (GSH) form by the enzyme glutathione reductase. Reduced

glutathione is predominant in biological tissues than oxidized glutathione. During oxidative stress, GSH gets oxidized and is converted to GSSG. The relative comparison of GSH/GSSG ratio between the control and stress samples indicates the extent of oxidative stress. The ratio of GSH/GSSG for raffinose grown cells was 0.77, while it was 0.43 for cells expressing harpin$_{Pss}$. *S. cerevisiae* Y187 expressing harpin$_{Pss}$ exhibit 37% reduction in GSH levels (Fig 3.6) and significant decrease in the GSH/GSSG ratio compared to the control cells indicating the extent of oxidative stress in cells expressing harpin$_{Pss}$.

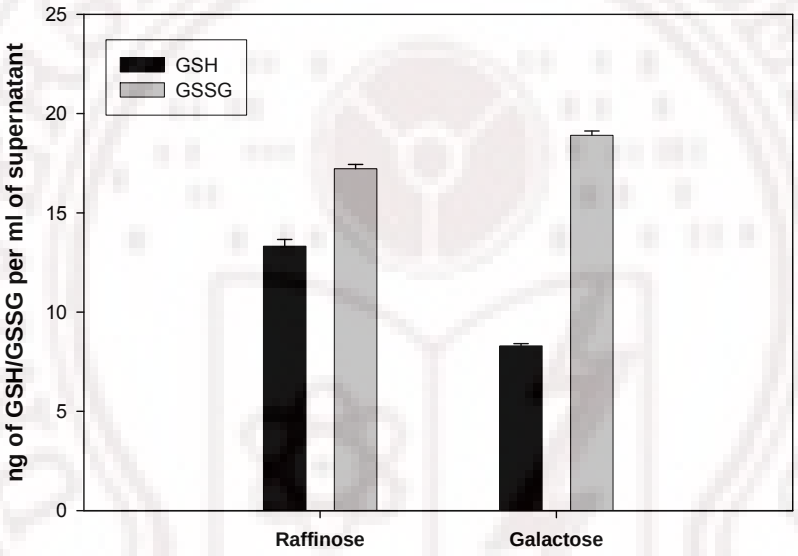

Fig 3.6 GSH and GSSG estimation in harpin$_{Pss}$-induced YCD

S. cerevisiae Y187 transformed with pYEUT-*hrpZ* was grown in raffinose-containing medium with tryptophan drop out to an OD ~0.6 at 30^{0}C. Cells were then pelleted and resuspended in YMM containing raffinose or galactose. After incubation for a period of 12h, the cell extracts were prepared by homogenization and ultracentrifuged followed by the estimation of reduced and oxidized glutathione. Vertical bars on the histogram indicate standard error of three independent experiments.

3.1.7 Assessment of metacaspase activity

S. cerevisiae Y187 pYEUT-*hrpZ* cells cultured in raffinose-supplemented medium were transferred to minimal medium containing raffinose or galactose or treated with acetic acid for 4 h. In order to confirm caspase activation in harpin$_{Pss}$-induced YCD, cells were incubated with CaspACE, FITC-VAD-fmk *in situ* marker that binds to the active site of caspases and detected using flow cytometry. In comparison, galactose cultured yeast cells (harpin$_{Pss}$-expressed) and acetic acid treated cells exhibit higher metacaspase activity than

the control cells (Fig 3.7) indicating the elevation of metacaspases in harpin$_{Pss}$-induced yeast cell death.

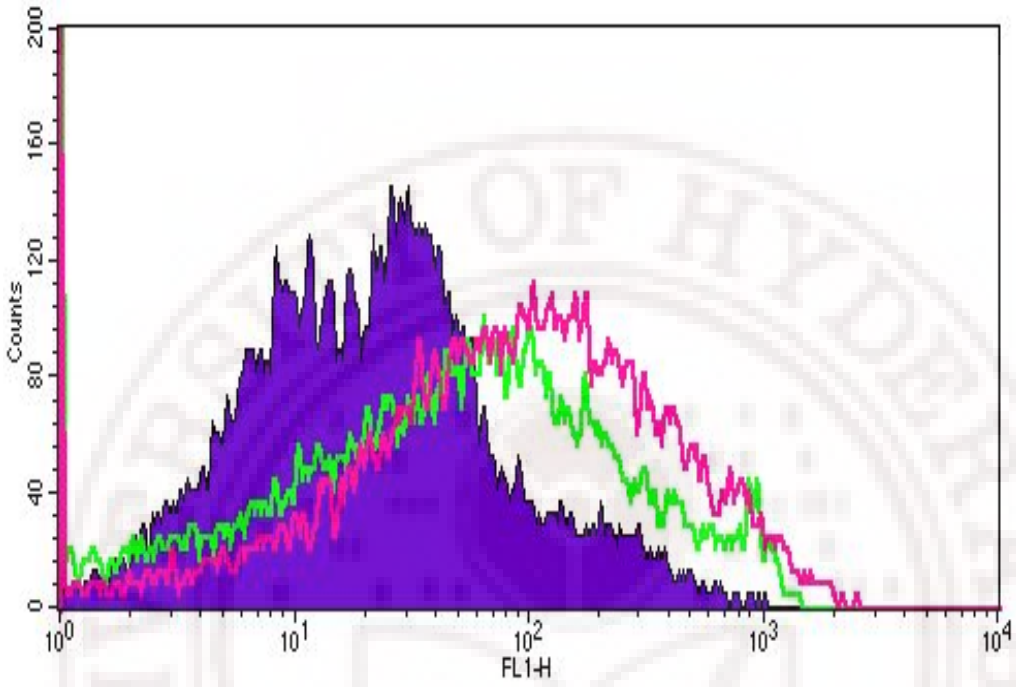

Fig 3.7 Detection of metacaspase activity in harpin$_{Pss}$-induced yeast cell death.

S. cerevisiae Y187 cells harboring pYEUT-hrpZ were cultured in raffinose-supplemented medium with tryptophan drop out to an OD_{600} of 0.6. Cells were then pelleted, and resuspended in minimal medium containing raffinose or galactose or treated with 80 mM acetic acid. After 4h of induction, ~1x10^6 cells ml^{-1} were pelleted, resuspended in PBS and incubated with FITC-VAD-fmk for 30 min at 30^0 C and then acquired in flow cytometer. Area in blue represents cells cultured in raffinose-supplemented medium (control), green line for cells cultured in galactose (harpin$_{Pss}$ expressed) and pink for acetic acid treated cells. Data represent the result from one of three similar experiments.

3.1.8 Mitochondrial enzyme assays

A) Isolation of mitochondria

The mitochondria were isolated (Daum *et al*, 1982) as described in materials and methods and suspended in 100 µls of 0.6 M Mannitol and 10 mM Tris-Cl, buffer pH 7.4.

B) Visualization of mitochondria by confocal microscopy

The yeast mitochondria isolated were stained with a fluorescent dye, JC-1, which enters the mitochondria exhibiting a fluorescence shift from red to green, observed at λ_{exc}= 605

nm and λ_{em} = 640 nm for red filter (Fig 3.8B) and λ_{exc}= 514 nm and λ_{em} = 529 nm for green filter (Fig 3.8A), along with the transmission image (Fig 3.8C) taken under the confocal microscope.

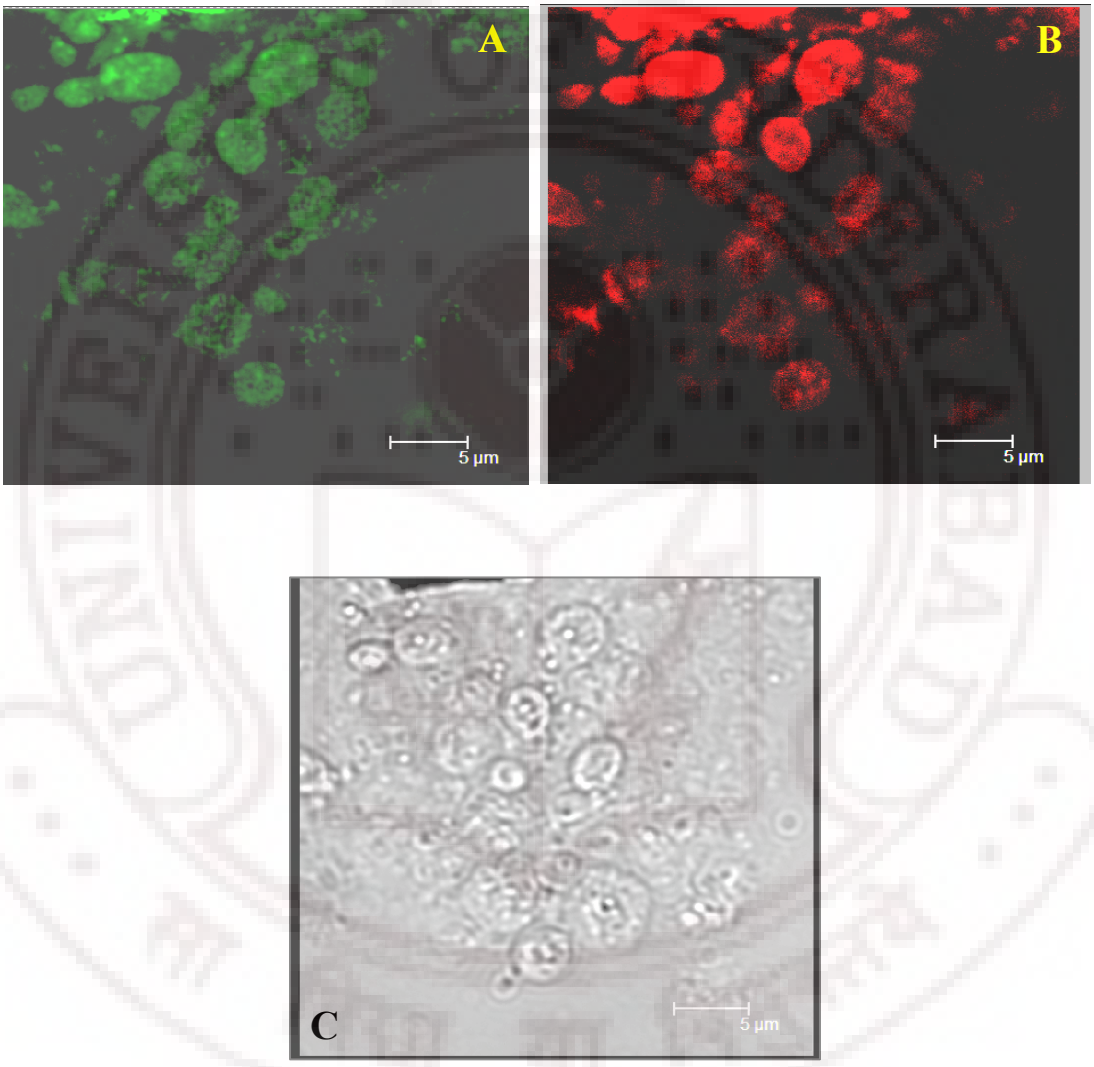

Fig 3.8 Confocal image of yeast mitochondria stained with JC-1 showing green (A) and red (B) fluorescence respectively, shown along with the transmission image (C).

C) Assay for NADH dehydrogenase (Complex I) activity

Assay for NADH Dehydrogenase activity was done by recording the change in absorbance (OD measured at 420 nm) plotted on Y-axis against the time (in sec) taken on

X-axis (Fig 3.9). The specific activity of the NADH dehydrogenase enzyme from yeast grown in raffinose-supplemented medium is 150.48 µ moles of NADH oxidized or reduced / min/mg protein and for yeast grown in galactose-supplemented medium, it was 101.76 µ moles of NADH oxidized or reduced / min/ mg protein. *S. cerevisiae* Y187 expressing harpin$_{Pss}$ exhibited 32% reduction in the NADH dehydrogenase levels compared to the control cells.

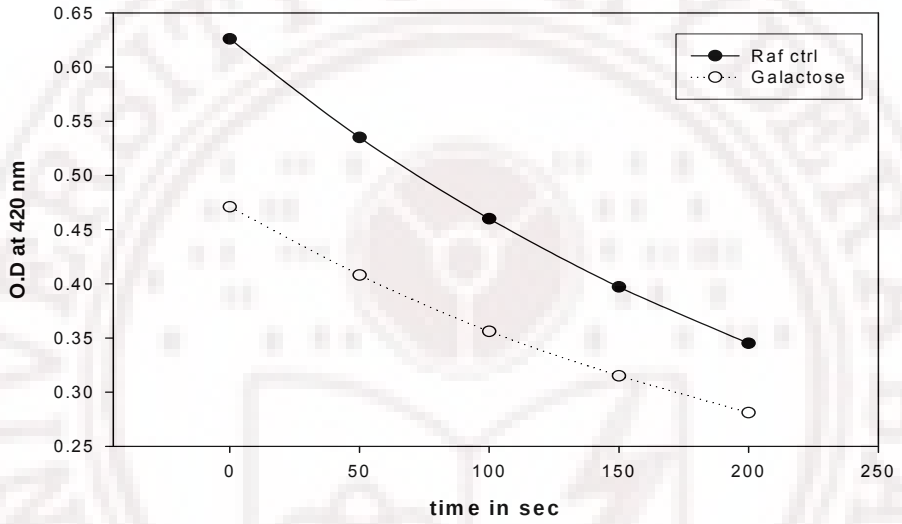

Fig 3.9 Assay for NADH dehydrogenase activity

NADH dehydrogenase activity of the mitochondria isolated from cells cultured in galactose-supplemented medium or raffinose-supplemented was estimated spectrophotometrically at 420 nm on a time based scale for 200 sec.

D) Assay for Cytochrome c oxidase (Complex IV) activity

Assay for Cytochrome c oxidase activity was done by recording the change in absorbance (OD measured at 550 nm) plotted on Y-axis against the time (in sec) taken on X-axis (Fig 3.10). The specific activity of Cytochrome c oxidase from the control cells cultured in raffinose-supplemented medium was 43.4 µ moles of Fe Cytochrome c oxidized/min/mg protein, while it was 24.2 µ moles of Fe Cytochrome c oxidized/min/mg protein for the cells induced with harpin$_{Pss}$ expression i.e. in galactose-supplemented medium.

S. cerevisiae Y187 expressing harpin$_{Pss}$ exhibited 44% reduction in complex IV activity compared to the control cells.

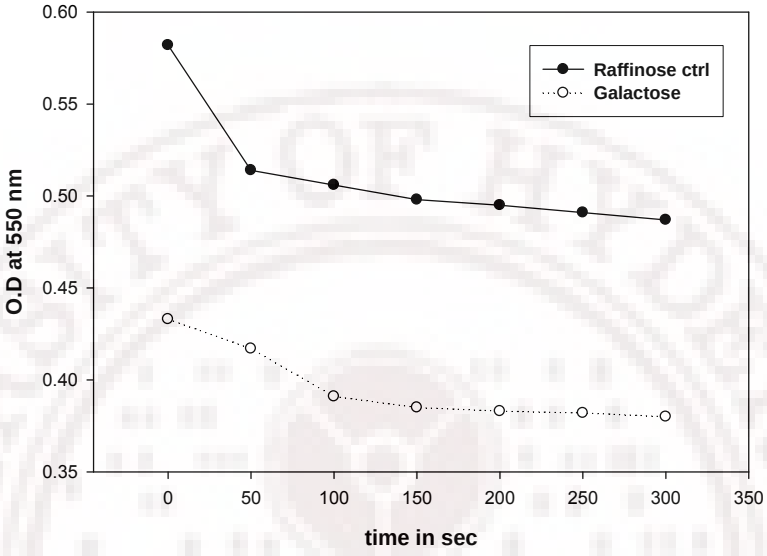

Fig 3.10 Assay for Cytochrome c oxidase activity

The Cytochrome C oxidase activity of mitochondria isolated from cells cultured in galactose-supplemented medium or raffinose-supplemented was estimated spectrophotometrically at 550 nm on a time based scale for 300 sec.

E) Assay for mitochondrial ATPase (Complex V) activity

Assay for mitochondrial ATPase activity was done by recording the change in absorbance (OD measured at 360 nm) plotted on Y-axis against the time (in sec) taken on X-axis (Fig 3.11). The specific activity of mitochondrial ATPase from the control cells cultured in raffinose-supplemented medium was 253 µ moles of NADH oxidized / min/mg protein, while the cells cultured in galactose-supplemented medium had 176.8 µ moles of NADH oxidized /min/mg protein. *S. cerevisiae* Y187 expressing harpin$_{Pss}$ exhibit 30% reduction in complex V activity compared to the control cells.

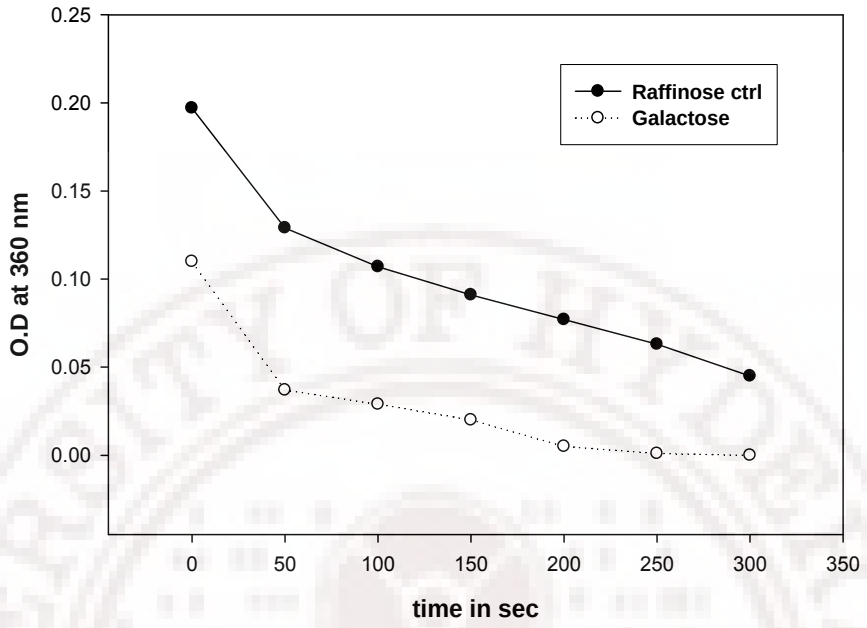

Fig 3.11 Assay for mitochondrial ATPase activity

The mitochondrial ATPase activity of mitochondria isolated from cells cultured in galactose-supplemented medium or raffinose-supplemented was estimated spectrophotometrically at 360 nm on a time based scale for 300 sec.

3.2 Harpin$_{Pss}$-induced cell death events in Jurkat cell lines

3.2.1 Effectiveness of Harpin$_{Pss}$ on cancer cell lines

The effectiveness of harpin$_{Pss}$ has been tested on animal cell lines (Jurkat cells-T-cell lymphoma cell line). Cell proliferation, on harpin$_{Pss}$ treatment was evaluated using MTT assay which is based on the mitochondrial reduction of the MTT salt to formazan crystals by living cells. Jurkat cells were cultured (serum free) with or without harpin$_{Pss}$ (10 –80 μM) for 24h. A dose dependent decrease in Jurkat cell proliferation was observed at 24h of harpin$_{Pss}$ treatment with maximum decrease in cell proliferation at a concentration of 40 μM (1.5 mg/ml) where the percent inhibition (IC_{50}) was 50% (Fig. 3.12). Thus harpin$_{Pss}$ treatment appears to be efficient causing cell death in Jurkat cells.

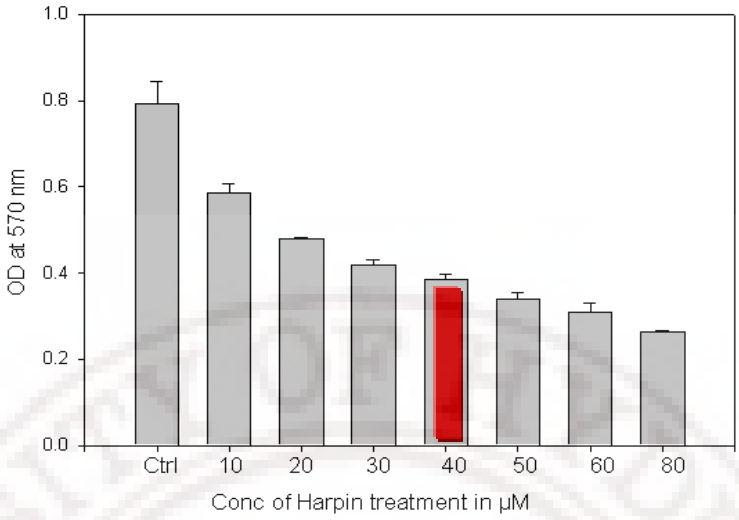

Fig. 3.12 MTT assay for determination of cell viability

Jurkat cells were cultured in presence (10 – 80 µM) or absence (control) of harpin$_{Pss}$ for 24h. After treatment, cell viability was determined by the addition of MTT followed by recording the absorbance values at 570 nm on an ELISA reader. Vertical bars on the histogram indicate standard error of three independent experiments.

3.2.2 Morphological changes

Harpin$_{Pss}$ treated Jurkat cells showed typical features of cell death compared to the untreated control cells. Phase contrast microscopic observations revealed changes in cell shape, organelle distribution and membrane blebbing ultimately resulting in cell burst and release of small cell fragments (Fig.3.13) called as the apoptotic bodies.

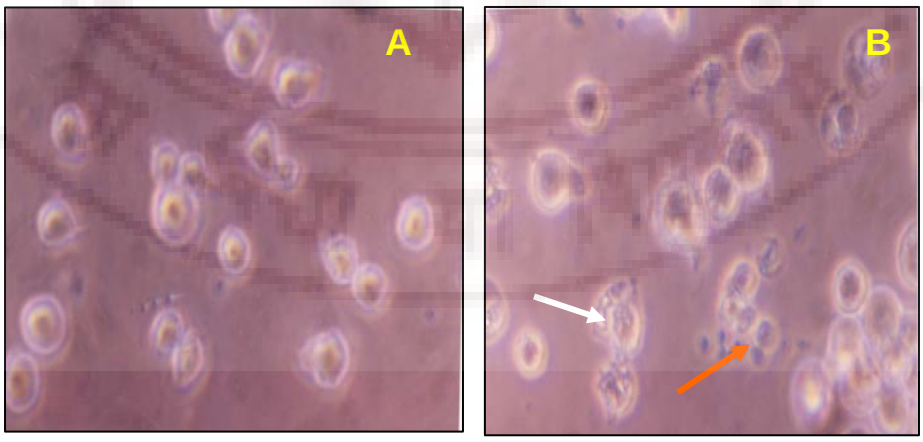

Fig. 3.13 Photomicrographs of Jurkat cells (A) untreated control cells and (B) cells treated with harpin$_{Pss}$ showing features of cell death. White arrow points to membrane blebbing and red arrow shows the apoptotic bodies.

3.2.3 DNA fragmentation induced by harpin$_{Pss}$ in Jurkat cells

Induction of apoptosis in Jurkat cells treated with harpin$_{Pss}$ was further evaluated by DNA fragmentation, a hallmark feature of apoptosis. Jurkat cells treated with 40 µM harpin$_{Pss}$ showed DNA fragmentation (Fig 3.14) evidenced by a ladder of 180-200 base pairs which corresponds to internucleosomal cleavage, a characteristic feature of apoptotic cells. Untreated Jurkat cells (lane 1) did not show any such fragmentation pattern.

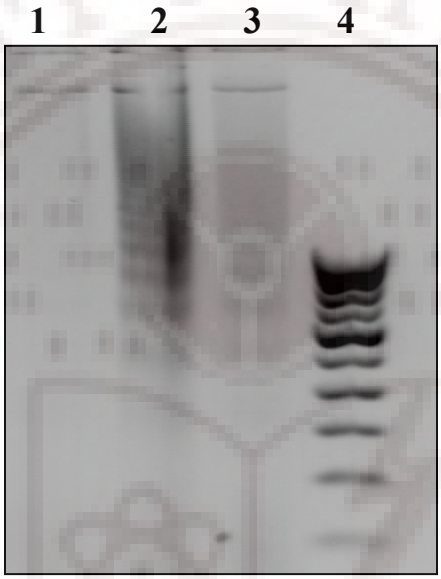

Fig. 3.14 Analysis of DNA fragmentation in Jurkat cells treated with harpin$_{Pss}$

Jurkat cells were treated with 40 µM harpin$_{Pss}$ for 24 h and 12 h. DNA was isolated from the treated cells and separated on 1.5% agarose gels. DNA was stained and visualized under UV light. Lane 1: Untreated control cells; Lane 2: Cells treated with harpin for 24h; Lane 3: Cells treated with harpin for 12h; Lane 4: 100 bp marker.

3.2.4 Effect of harpin$_{Pss}$ on cell cycle profile of Jurkat cells

The induction of apoptosis in cells treated with harpin$_{Pss}$ was further evaluated by flow cytometric analysis of DNA content. Jurkat cells treated with or without 40 µM harpin$_{Pss}$ were stained with propidium iodide (50µg/ml) for 30 min and subjected to FACS analysis. The FACS analysis of control cells, showed prominent G1, followed by S and G2/M phases. Only 3 % of untreated cells showed hypodiploid DNA (sub G0/G1 peak). The percentage of hypodiploid DNA increased gradually to 12 % (Fig. 3.15) in the cells treated for 12 h with harpin$_{Pss}$ which further increased to 27 % at 24 h.

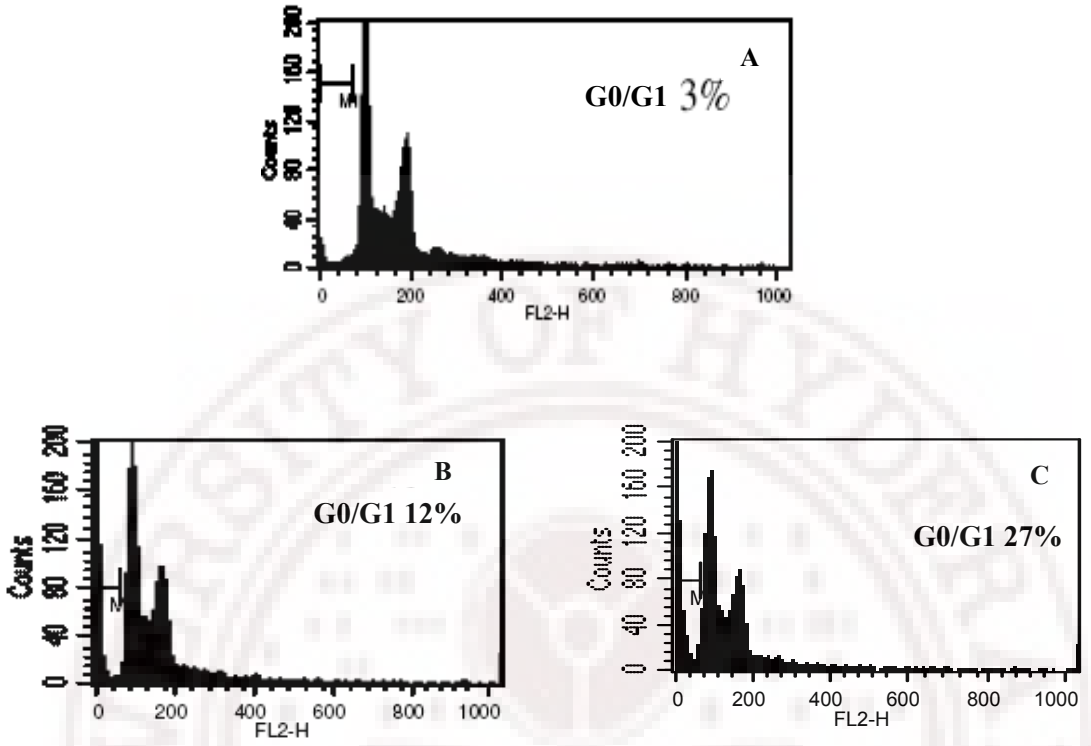

Fig. 3.15 Cell cycle analysis of Jurkat cells treated with harpin$_{Pss}$.

Jurkat cells (1 x 10^6) treated with 40 µM harpin$_{Pss}$ for 12h (B) and 24h (C) along with untreated cells (A) were fixed in 1ml of 70% ethanol and suspended in PBS. The cells were then stained with PI solution for 30 min and analyzed for DNA content by flow cytometer. Data represent the result from one of three similar experiments.

3.2.5 Effect of harpin$_{Pss}$ treatment on Cytochrome c release, Bcl-2 and Bax proteins in Jurkat cells

The process of apoptosis is associated with the disruption of mitochondrial membrane potential, which results from the opening of permeability transition pores in the mitochondrial membrane, leading to the release of cytochrome c. The expression levels of Bcl-2 and Bax proteins was associated with mitochondrial membrane integrity and play a crucial role in the regulation of apoptosis. No appreciable change in the levels of Bax protein was observed at all the time periods (Fig. 3.16A) but a time dependent decrease of Bcl-2 protein levels was observed after treatment with harpin$_{Pss}$ (Fig 3.16B). These results suggest an altered Bcl-2/Bax ratio (Fig. 3.16C) in the cells treated with harpin$_{Pss}$. Furthermore, to determine whether there is any release of cytochrome c from the mitochondria into the cytosol, cytosolic fractions from the cells treated with 40 µM

harpin$_{Pss}$ for 3, 6, 12 or 18h were subjected to western blot analysis. A time dependent elevation in the levels of cytochrome c with maximum increase at 12 and 18 h was observed (Fig. 3.17).

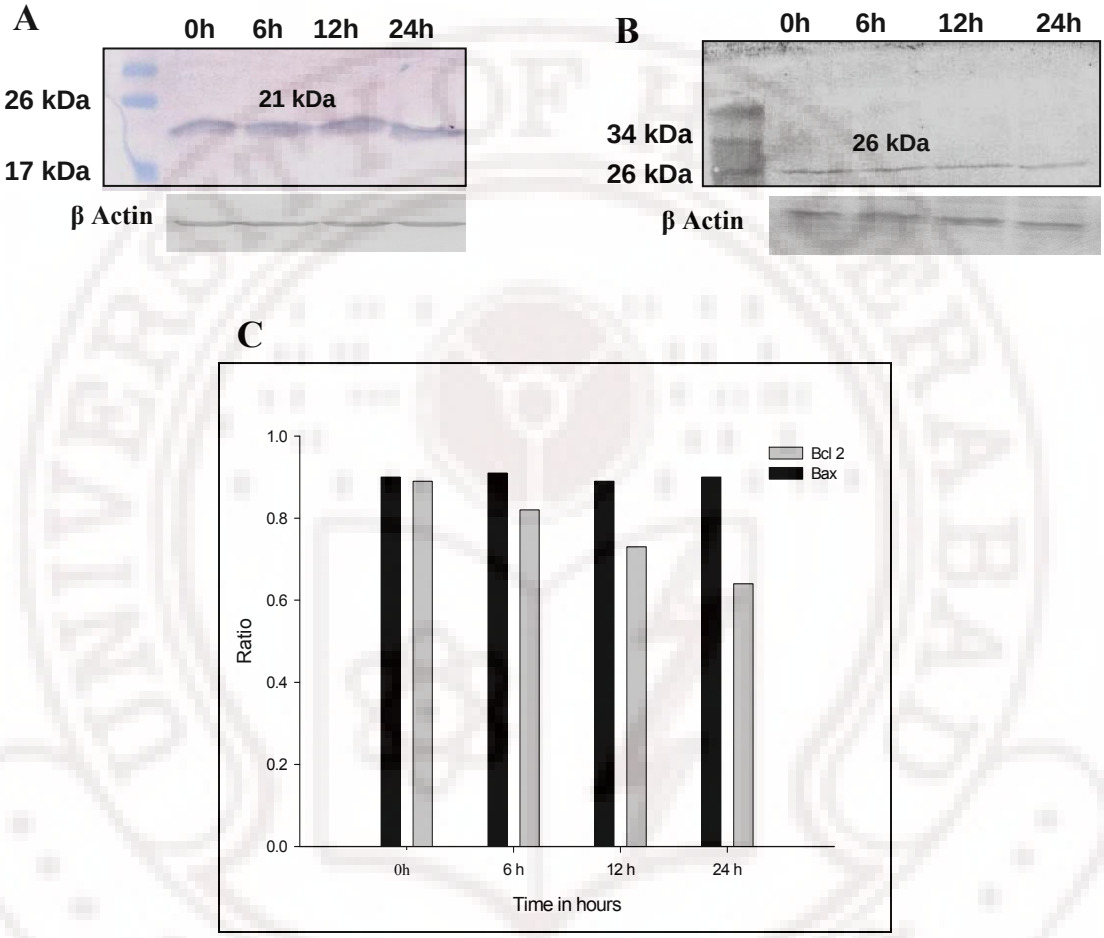

Fig. 3.16 Western blot analysis of Jurkat cells treated with harpin$_{Pss}$

The cell extracts of Jurkat cells treated with 40 µM harpin$_{Pss}$ at 0, 6, 12 and 24 h were resolved on 15% SDS-PAGE and probed against Bax (A) and Bcl-2 (B) antibodies followed by incubation with anti-mouse IgG secondary antibody and developed using BCIP-NBT substrate. β actin was used as loading control. The histograms (C) represent the altered Bcl2/Bax ratio analyzed with Scion imaging.

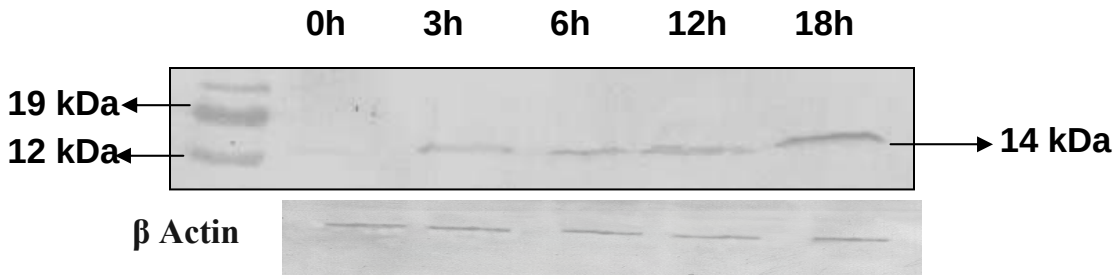

Fig. 3.17 Cytochrome *c* release from Jurkat cells

Jurkat cells were treated with 40 µM harpin$_{Pss}$ for 0, 3, 6, 12 and 18 h. Equal quantities of cytosolic protein (30 µg) was resolved on a 15% SDS-PAGE and immunoblotted with cytochrome c antibody. β actin was used as loading control.

3.3 Bio-physical studies on harpin$_{Pss}$

3.3.1 Harpin$_{Pss}$ expression and purification

Harpin$_{Pss}$ was expressed in *E. coli*. The *hrpZ* gene (1.02 kb) encoding full length harpin$_{Pss}$ was PCR amplified as a single band (Fig. 3.18A) and cloned under *NdeI* and *XhoI* sites of pET 28a vector. Cloning was confirmed by release of 1 kb insert upon double digestion of the cloned plasmid on a 1% agarose gel (Fig.3.18B). *E. coli* BL 21 competent cells were prepared and transformed with pET 28a-*hrpZ* and selected on an LB kanamycin (50µg/ml) plate. A single colony of pET 28a-*hrpZ* transformant of *E. coli* BL 21 (Rosettae) was grown in LB broth to OD_{600} ~ 0.5 and induced with 1mM IPTG, with hourly sample collection for confirmation of expression on a 12% SDS PAGE (Fig.3.18C). After 3h of induction, the cells were pelleted and sonicated for protein extraction. Antibodies were raised against harpin$_{Pss}$ and the reactivity was tested on an immunoblot. The membrane was incubated with harpin$_{Pss}$ antibody and then with the secondary antibody, anti-rabbit IgG- ALP conjugate. The blot was visualized with alkaline phosphatase color reaction using BCIP-NBT substrate. Band corresponding to harpin$_{Pss}$ was detectable, confirming the specificity of the antibody (Fig.3.18D). Harpin$_{Pss}$ was purified from the protein extract by passing through Ni-NTA column to obtain pure protein shown on a 12% SDS gel (Fig. 3.18E). The polydispersed, oligomeric nature of harpin$_{Pss}$ resolved on an 8% native PAGE is also shown in Fig. 3.18F.

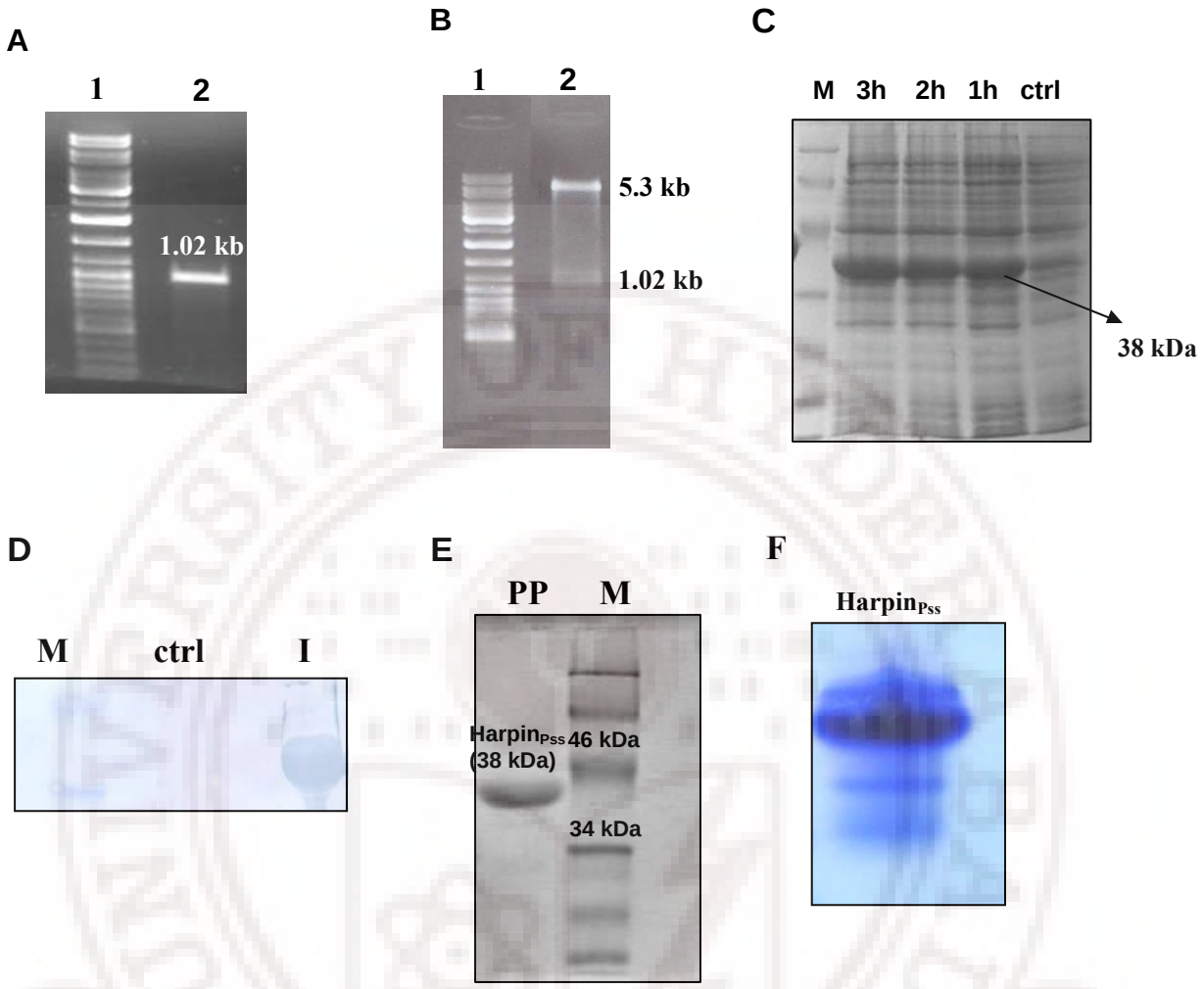

Fig. 3.18 PCR amplification, cloning, expression and purification of harpin$_{Pss}$.

A) 1.02 kb *hrpZ* gene encoding full length harpin$_{Pss}$ was PCR amplified using gene specific primers and resolved on a 1% agarose gel. Lane 1: 1 kb DNA ladder. Lane 2: A 1.02 kb *hrpZ* amplicon.

B) Confirmation of *hrpZ* cloning in pET 28a vector by double digestion shown on a 1% agarose gel. Lane 1: 1 kb DNA ladder. Lane 2: Double digestion of pET 28a-*hrpZ* showing the release of 1.02 kb harpin$_{Pss}$ fragment along with the 5.3 kb pET 28a vector.

C) 12% SDS PAGE showing hourly expression of harpin$_{Pss}$ (shown with arrow) from *E. coli* BL 21 cells along with the un-induced control (ctrl) and protein molecular weight marker (M).

D) Western blot analysis carried out with alkaline phosphatase color reaction showing the specific detection of harpin$_{Pss}$, i.e. induced expression (I), uninduced control (ctrl) and protein marker (M).

E) Ni-NTA purified protein (PP), harpin$_{Pss}$ (38 kDa) showed on a 12% SDS gel along with the protein molecular weight marker (M).

F) 8% native PAGE showing the polydispersed, multimeric (mono, di, trimeric etc) nature of harpin$_{Pss}$.

3.3.2 MALDI-TOF analysis of harpin$_{Pss}$

The Gauss filter-smoothed mass spectrum (TOF/TOF) of harpin$_{Pss}$ shows a singly charged ($[M_1+H]^+$) fundamental peak corresponding to a mass of 38,138 Da (Fig 3.19) and the other two major peaks represent a double charge ($[M_1+2H]^{2+}$) at 19,070 Da, as well as the triple charge ($[M_1+3H]^{3+}$) corresponding to a peak of 12,715 Da. The very low intensity tiny peaks could be due to minute impurities. Of the 367 amino acid residues in the expressed recombinant protein, 26 residues, including the twelve histidines [one His(6) tag at N-terminus and other at C-terminus) are due to the pET 28a Vector, where as the calculated molecular weight of the actual 341 amino acid harpin$_{Pss}$ is 34,700 Da at pH 7.0.

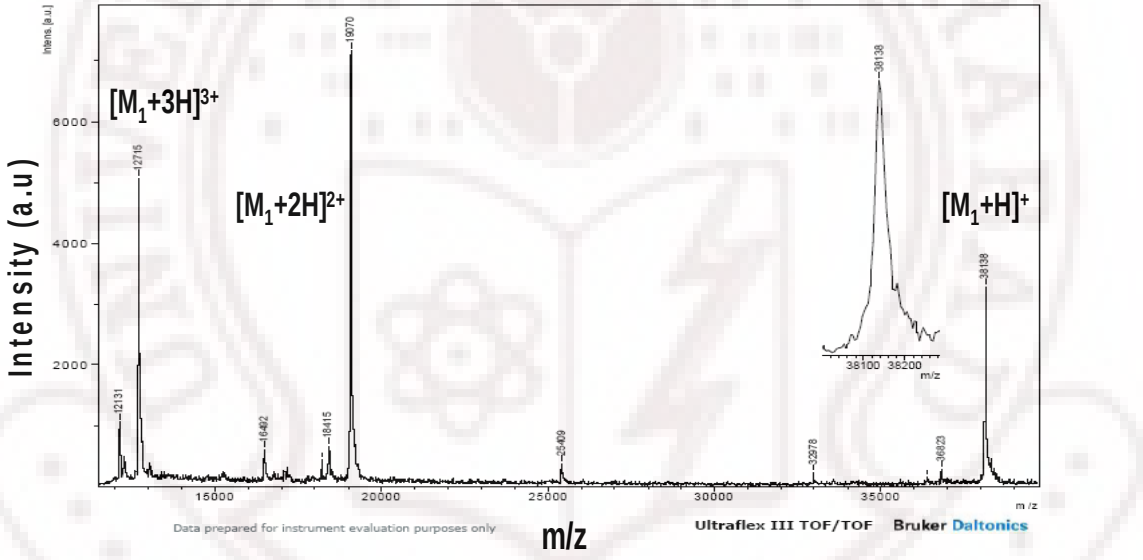

Fig.3.19 MALDI-TOF spectrum of harpin$_{Pss}$ indicating the molecular mass at 38,138 Da and the other peaks showing the double and triple charged status of the protein

3.3.3 Secondary structure and CD spectroscopy

CD spectrum of native harpin$_{Pss}$ in the far UV region (240-190 nm) is shown in Fig. 3.20. Two minima centered around 206 nm and 223 nm are clearly discernible in the spectrum, suggesting the presence of helical structure along with other secondary structural elements. To estimate the content of different types of secondary structures in harpin$_{Pss}$, the CD spectrum shown in Fig. 3.20 has been analyzed by three different programs, namely CDSSTR, CONTINLL, SELCON3 using the routines available at

DICHROWEB. Reference set 4 containing 43 proteins was used for fitting the experimental spectra. The calculated fit obtained using CDSSTR program is in excellent agreement with the experimentally obtained spectrum of harpin$_{Pss}$, indicating high accuracy in the estimates obtained from this analysis. The values obtained for the different types of secondary structures are: α-helix (51.5%), β-sheet (8.6%), β-turns (15.6%) and unordered structures (25.8%) (Table 3.2).

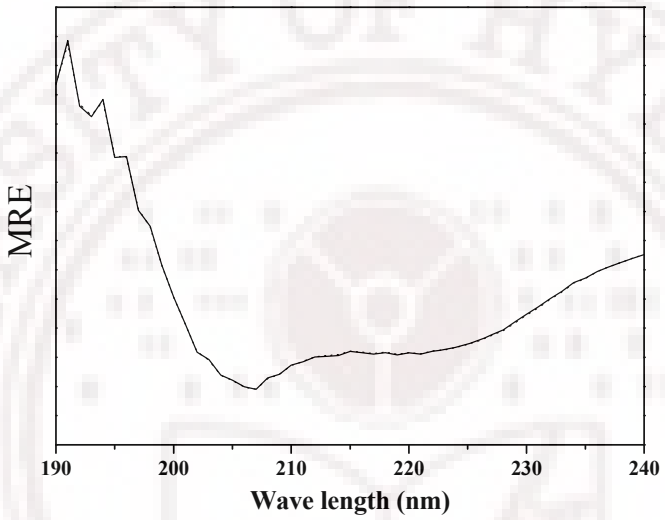

Fig. 3.20 CD spectrum of harpin$_{Pss}$

Circular dichroic spectrum of harpin$_{Pss}$ at far UV region. The spectrum was recorded at 25 °C and validated with the calculated fit obtained from the CDSSTR program which indicates that α-helix is more predominant in the protein. MRE indicates mean radial elipticity.

Programme	α-Helix (%)	β-sheet (%)	Turn(%)	Coil(%)
CDSSTR	54.4	9.2	12.2	24.4
CONTINLL	53.0	2.5	17.5	27.0
SELCON3	47.2	14.3	17.3	26.0
Total	51.5	8.6	15.6	25.8
Theoretical	45.3	3.8	6.7	44.1

Table 3.2 Results of CD spectral analysis of Harpin$_{Pss}$.

3.3.4 Fluorescence quenching of harpin$_{Pss}$

Fluorescence quenching study was carried out with harpin$_{Pss}$ using a neutral quencher, acrylamide or an anionic quencher, iodide (I^-). The fluorescence emission spectra of native harpin$_{Pss}$, recorded in the absence or in the presence of increasing concentrations of acrylamide or KI are shown in Fig 3.21A and 3.21B respectively. In both cases, spectrum 1 is that of the native harpin$_{Pss}$ in the absence of quencher and spectra 2- 20 correspond to harpin$_{Pss}$ in the presence of increasing concentrations of acrylamide or iodide. The significantly lower quenching observed with iodide in the native harpin$_{Pss}$ indicates that the tryptophan residue (W167) in this protein is buried in the hydrophobic core of the protein, where as the higher quenching observed with the neutral quencher, acrylamide also confirms the non-polar environment around the tryptophan residue in the protein.

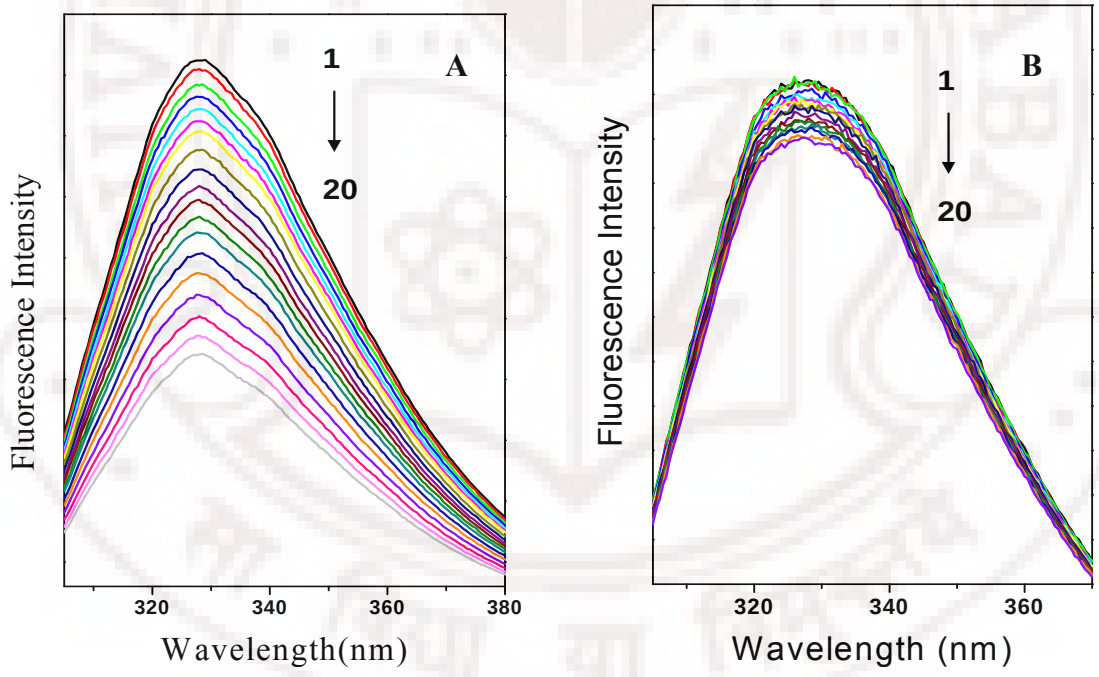

Fig. 3.21 Fluorescence quenching of harpin$_{Pss}$

Fluorescence spectra of native harpin$_{Pss}$ in the absence and presence of acrylamide (A) or potassium iodide (B). Spectral line 1 corresponds to harpin$_{Pss}$ alone and spectral lines from 2- 20 corresponds to harpin$_{Pss}$ with increasing concentrations of acrylamide or iodide.

3.3.5 Differential scanning calorimetry

In order to characterize the thermal unfolding mechanism and to rationalize the high thermal stability of $Harpin_{Pss}$ we have performed differential scanning calorimetric studies. A heating thermogram of the protein in PBS (pH 7.5) is given in Fig. 3.22. The thermogram indicates the presence of three distinct transitions centred at 50.0 °C, 59.9 °C and 93.6 °C, respectively. Changing the protein concentration between 0.1 mg/ml and 1.5 mg/ml did not alter the overall features of the thermogram. Deconvolution of the thermogram of $harpin_{Pss}$ is also shown (dotted lines) in the same figure. Thermodynamic parameters, viz, change in calorimetric enthalpy (ΔH_c), change in van't Hoff enthalpy (ΔH_v) and transition temperature (T_m) for individual transitions obtained from the deconvolution analysis, are listed in Table 3.3. Deconvolution analysis shows that the first, second and third transitions start at 26 °C, 44 °C, 76 °C and end at 72 °C, 76 °C and 108 °C, respectively.

To check the reversibility of heat induced $harpin_{Pss}$ unfolding, sample was heated to 90 °C in the DSC cell, and then cooled rapidly to room temperature. After an equilibration period of 10 minutes the sample was subjected to a second heating scan. The resulting thermogram contained all the three endothermic transitions, which establishes the reversibility of transitions 1 and 2 in $harpin_{Pss}$. The calorimetric enthalpy (ΔH_c) corresponding to transition 1 was found to vary considerably when repeated experiments were performed (involving protein obtained in different batches of purification) whereas enthalpy corresponding to transitions 2 and 3 were reproducible. These thermodynamic data strongly suggest that transition 1 most likely corresponds to dissociation of a polydisperse, oligomeric aggregate of $harpin_{Pss}$ and transitions 2 and 3 correspond to temperature induced structural changes in the protein. A hypothetical diagram representing the probable mechanistic pathway for thermal dissociation of $harpin_{Pss}$ is shown in Fig. 3.23.

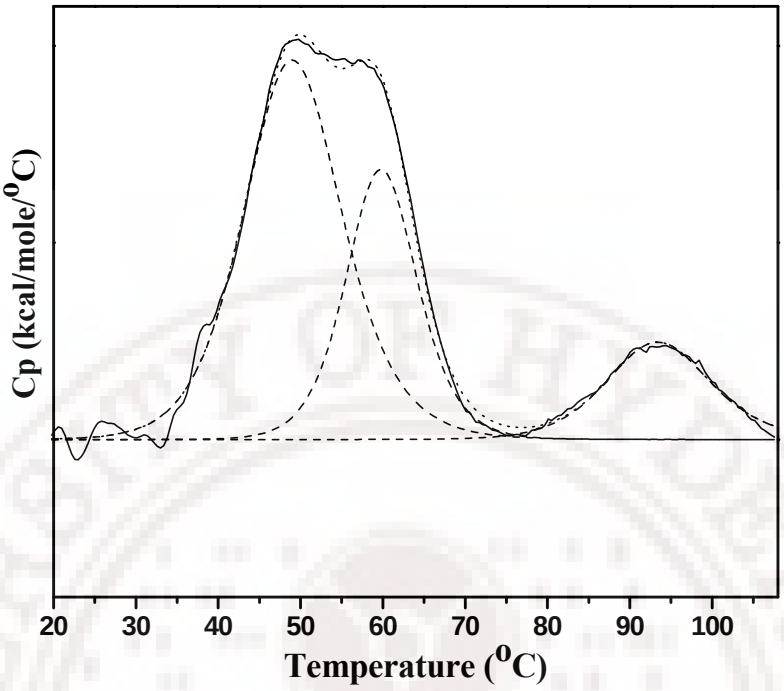

Fig. 3.22 Differential scanning calorimetry of harpin$_{Pss}$

DSC scan of a 0.545 ml sample of 0.028 mM (monomer)/0.014 mM (dimer) of harpin$_{Pss}$ protein in 0.5 M sodium phosphate, pH 7.5 at a scan rate of 60 K h^{-1}. Deconvolution analysis of DSC data is also shown.

	T_m (°C)	ΔH_c (kcal.mol^{-1})	ΔH_v (kcal.mol^{-1})	$\Delta H_c/\Delta H_v$
Transition 1	50.0	217.3±69.3	224.1±7.2	-
Transition 2	59.9	154.5±10.0 309.1±20.1*	330.2±42.5	0.47 0.94*
Transition 3	93.6	59.1±4.4	258.1±11.0	-

*In analysis protein was considered as dimeric and dimer concentration was used.

Table 3.3 Thermodynamic parameters of thermal unfolding of Harpin$_{Pss}$.

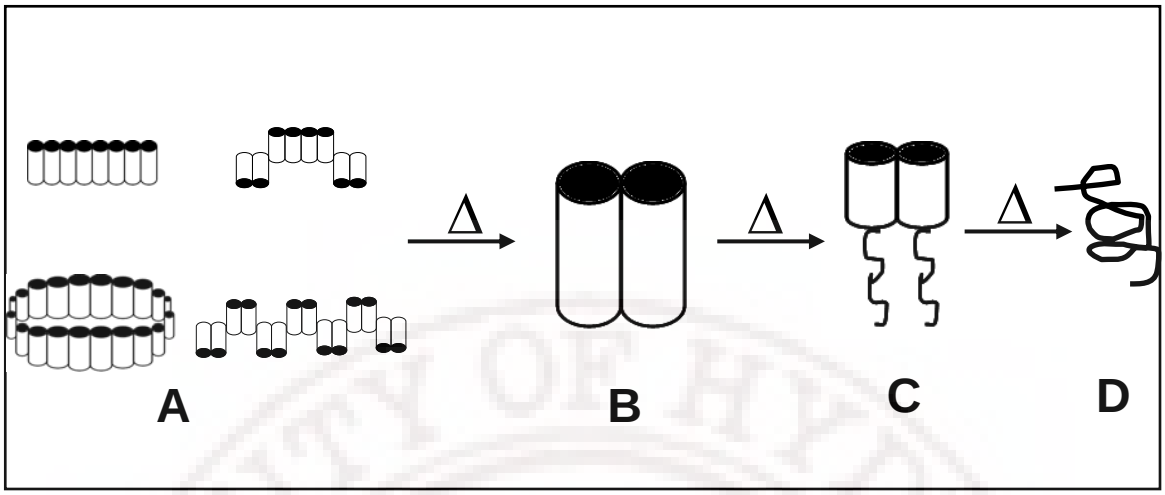

Fig. 3.23 Probable mechanistic pathway for thermal unfolding of harpin$_{Pss}$.

An oligomeric protein (A) unfolding to a dimer (B), then to a semi/partially unfolded dimer (C) and finally to a fully unfolded monomer (D). Cylinders represent folded helices, whereas curved lines represent unfolded random coils.

3.3.6 Temperature dependent CD

To understand the structural basis of the complex nature of the thermal unfolding process of harpin$_{Pss}$ as revealed by the DSC thermograms, CD spectra of the protein were recorded at various temperatures. Each spectrum was analysed using the CDSSTR program to get the average α-helical content and β-sheet content at different temperatures. Fig. 3.24 presents the dependence of α-helical content and β-sheet structure on temperature. Up to 45 °C, before the onset of transition 2, there is no obvious change in helical and sheet content, suggesting that no change in secondary structure occurs below this temperature. The changes observed in the helical content at higher temperatures suggest the temperature-induced unfolding of the protein. Temperature-dependent CD shows that at high temperature the α-helical content is reduced, whereas β-sheet structure increases with temperature.

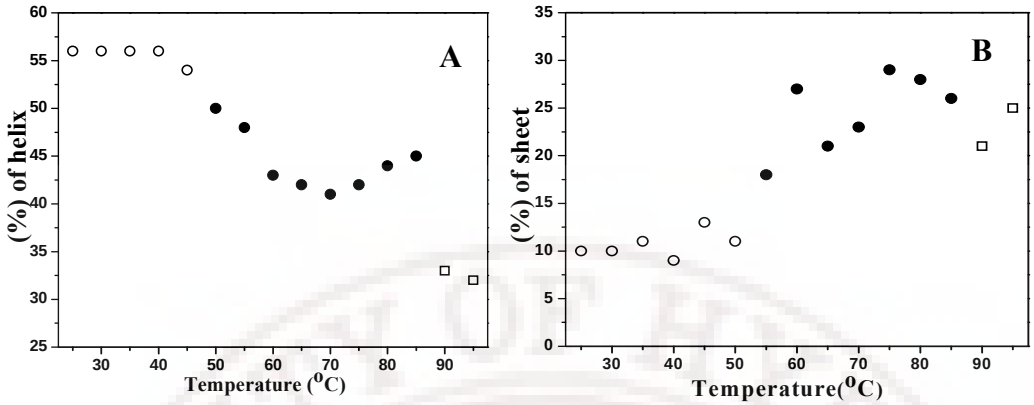

Fig. 3.24 Temperature dependence CD of harpin$_{Pss}$

Temperature dependence CD of harpin$_{Pss}$ shows no significant change in α-helical or β-sheet content up to 45-50 °C. Increase in temperature results in (A) decrease of α-helix and (B) increase in β-sheet content.

3.3.7 Reversible aggregation of harpin$_{Pss}$

Oligomeric structures of protein can be easily detected via native polyacrylamide gel electrophoresis (PAGE). Generally proteins with oligomeric form give a smear instead of distinct bands. To demonstrate the reversibility of aggregate formation in thermal unfolding, gel electrophoresis was performed by heating harpin$_{Pss}$ at 90 °C for 5 min, cooled to RT and again loaded on to the gel. Fig. 3.25 shows the reversibility of the protein in aggregate formation. The aggregate formation is relatively a fast process as the gel electrophoresis was carried out immediately after cooling the heated sample. Therefore the aggregate formation is an inherent property in harpin$_{Pss}$ and the phenomena may play an important role for its thermal stability and biological activity.

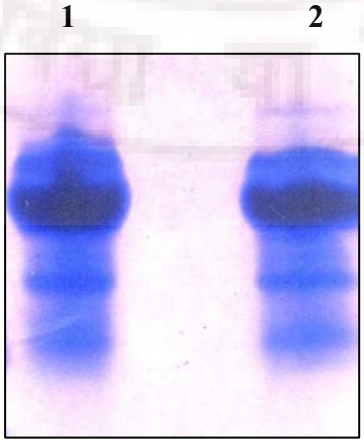

Fig. 3.25 Electrophoretic profile of harpin$_{Pss}$ resolved on an 8 % native-PAGE showing reversible aggregation of the protein. Lane 1, Harpin$_{Pss}$, lane 2, Harpin$_{Pss}$ heated at 90 ^{o}C for 10 min, cooled and loaded on the gel.

3.3.8 Dynamic light scattering

The hydrodynamic radius of $Harpin_{Pss}$ as a function of temperature (up to 61 ^{0}C, which is the highest temperature where the DLS experiments could be carried out) is shown in Fig. 3.26. The data presented here indicates that the hydrodynamic radius (R_h) decreases with increase in temperature which is quite interesting, because for a monomeric protein the R_h is expected to increase with increase in temperature. The average R_h of the native protein is 20.54 ± 6.19 nm, which is significantly higher than the predicted value of 2.58 nm (according to Equation 1). The predicted R_h of native protein and unfolded protein comes from two empirical equations. Equation (1) is for native protein, equation (2) is for fully unfolded protein and N is the number of residues in the protein.

$$R_h = 4.75N^{0.29} Å \quad (1)$$

$$R_h = 2.21N^{0.57} Å \quad (2)$$

Here, large R_h of $Harpin_{Pss}$ at room temperature may be attributed to the aggregation of monomeric protein. The decrease in R_h with temperature suggests the dissociation of oligomeric structure, which is consistent with the DSC and temperature dependent CD data. For a thermostable protein like harpin it is obvious that total thermal unfolding can't be accomplished at 60-65 °C. At 61 °C the R_h is 9.35 ± 1.04 nm which is also much higher than R_h value of 6.14 nm predicted by Eqn. 2 for the denatured protein (monomer). It may be possible that higher R_h at 61 °C is due to partially unfolded dimeric structure as estimated R_h for fully unfolded dimeric $harpin_{Pss}$ falls in the range of 12-13 nm. The partially unfolded dimeric protein may convert to fully unfolded monomeric protein at higher temperatures.

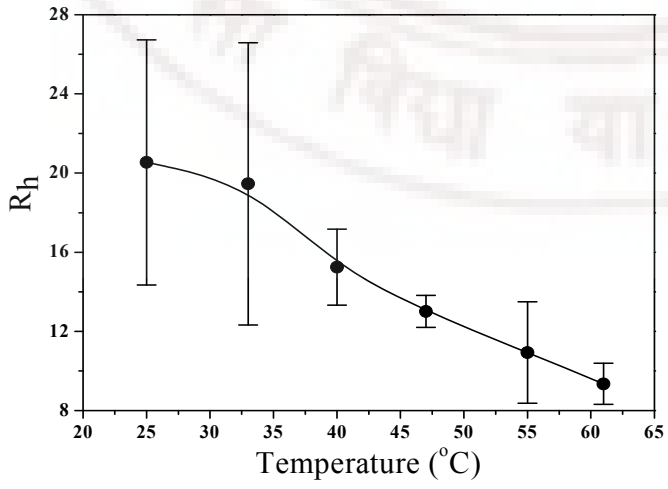

Fig. 3.26 DLS study of $harpin_{Pss}$

Temperature dependence of the hydrodynamic radius (R_h) of $harpin_{Pss}$ showing the decrease in R_h of the protein with increase in temperature. Vertical lines represent standard error in R_h measurement, taken out of three independent observations.

3.3.9 Congo red binding

The β-sheet fibrils referred to as amyloids typically bind azo dye congo red (CR). Binding of CR to amyloids leads to a characteristic red shift of the absorption spectrum. At room temperature a blue shift of the absorption maxima (λ_{max}) from 499 to 485 nm was observed with harpin$_{Pss}$ while at 55 °C there was no shift in λ_{max} (Fig. 3.27). The blue-shift of the absorption spectrum indicates aggregation of the dye.

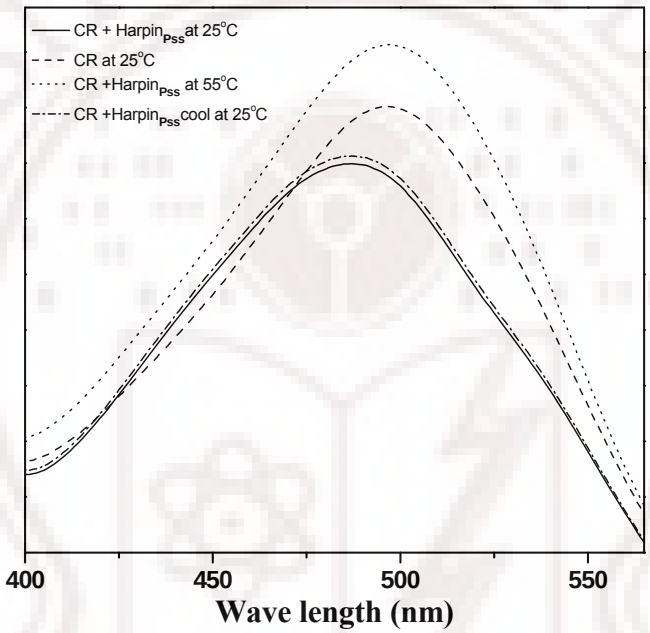

Fig. 3.27 Congo red binding of harpin$_{Pss}$ oligomer.

Solid line (—) represents CR with harpin$_{Pss}$ at 25°C, dashed line (−−)CR alone, dotted line (····) represents CR with harpin$_{Pss}$ at 55°C, dash-dot line (−·−)CR with harpin$_{Pss}$ after cooling the heated sample to 25°C.

3.3.10 Atomic force microscopy

To visualise the morphology of aggregates and corroborate the above DLS data, the harpin$_{Pss}$ samples were imaged using atomic force microscopy (AFM). Fig. 3.28 gives four different AFM images of harpin$_{Pss}$ and all the images show the heterogeneity in size and shape among aggregates of this protein. Small rod-like structures (Fig 3.28 B) may correspond to protofibrils or rod like aggregates. However, the sizes of the aggregates

shown in the AFM picture appears to be slightly bigger than the R_h values obtained from DLS measurements. This could be due to the fact that the solutions for DLS studies were filtered through a 0.22 µm filter, resulting in the removal of larger aggregates that might have been present in the samples before filtration. Also it should be kept in mind that DLS measures average size of the aggregates present in solution.

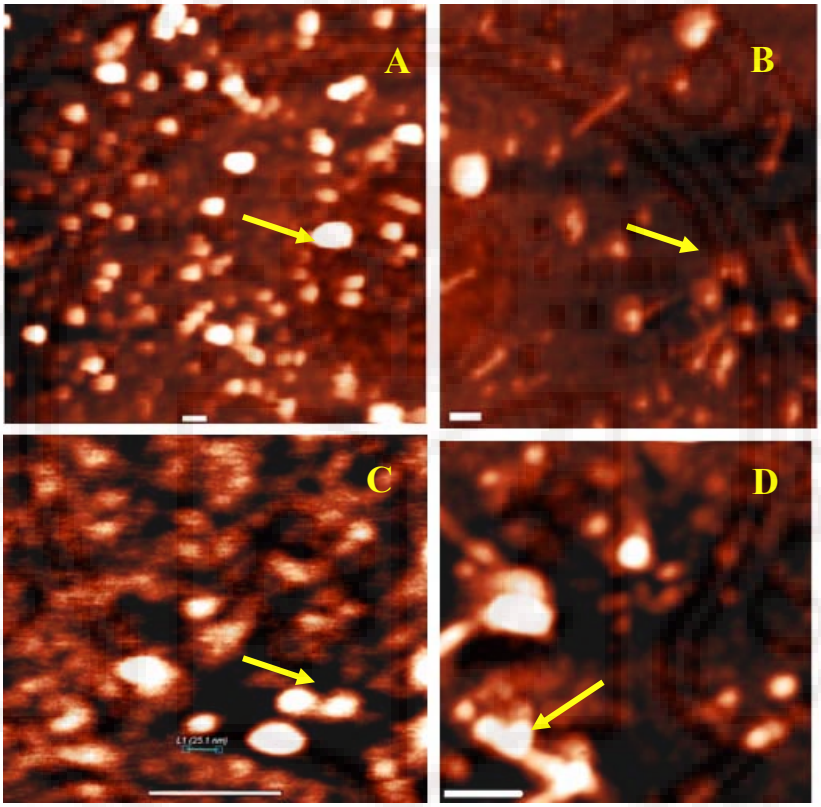

Fig. 3.28 AFM image of harpin$_{Pss}$ showing heterogeneity in size and shape (shown with arrows) among the aggregates of the protein.

3.3.11 Crystallization of harpin$_{Pss}$

Harpin$_{Pss}$ was set up for crystallization by 'Sitting drop' method as described in materials and methods and the plates were observed for crystal growth for 2 months. Most of the set ups had precipitation of the protein and some contained micro crystalline precipitates

which apparently resulted from the polydispersed, oligomeric and non-specific aggregation of the protein.

3.3.12 Oligomeric form and leucine-zipper

Examination of the primary structure of harpin$_{Pss}$ revealed the presence of two leucine zipper-like motifs (amino acids 71-90 and 302–323) in harpin$_{Pss}$ (Fig 3.29) Sequence alignment, shown in Fig. 3.30 A and B clearly describes that these particular segments consists of heptadic repeat of leucine or other hydrophobic amino acids such as isoleucine, phenylalanine, alanine, methionine and valine. Analysis of primary structure of other harpins also shows the existence of one or more leucine-zipper like motifs (Fig. 3.30 A and B). Some of the harpins have coiled-coil motif where the first (a) and fourth (d) positions of heptad repeats were occupied by hydrophobic amino acids (Fig. 3.30 C). The presence of at least two leucine-zipper like motif in harpins can in principle nucleate a variety of different oligomerization states (Fig. 3.31).

MQSLSLNSSSLQTPAMALVLVRPEAETTGSTSSKALQEVV

VKLAEELMRNGQLDDSSPLGKLLAKSMAADGKAGGGIED

VIAALDKLIHEKLGDNFGASADSASGTGQQDLMTQVLNGL

AKSMLDDLLTKQDGGTSFSEDDMPMLNKIAQFMDDNPAQ

FPKPDSGSWVNELKEDNFLDGDETAAFRSALDIIGQQLGN

QQSDAGSLAGTGGGLGTPSSFSNNSSVMGDPLIDANTGP

GDSGNTRGEAGQLIGELIDRGLQSVLAGGGLGTPVNTPQT

GTSANGGQSAQDLDQLLGGLLLKGLEATLKDAGQTGTDV

QSSAAQIATLLVSTLLQGTRNQAAA

Fig 3.29 Primary structure of harpin$_{Pss}$ (341 aa) with leucine zippers.

Amino acid sequence analysis of harpin$_{Pss}$ reveals the presence of two leucine zipper like motifs in the protein.

Panel A

```
71 GKAGGGIEDVIAALDKLIH          --------          P.s.pv syringae
12 STMQISIGGAGGNNGLLGTSRQNAGLGGNSALG  --- --  Erwinia amylovora
31 NGASPSQSGFGGQRSNIAEQLSDIMTTMMFMGS  ----  Erwinia carotovora
23 QGLKGLNSAASSLGSSVDKLSSTIDKLTSALTS  -----  Erwinia chrysanthemi
11 STMQISIGGAGGGNGLLGTSRQNAGLGDHSALG ---  Erwinia pyrifoliae
106 SALGGGLGGALGAGMNAMNPSAMMGSLLFSALE ---  Pectobacterium
58 SPLGKLLGKAMAASGKAGGGLEDIKAALDTLIH  ----  P. s. pv phaseolicola
41 QLLTQLIMALLQQSNNAEQ          ---------  Xanthomonas axonopodis
```

Panel B

```
300 KGLEATLKDAGQTGTDVQSSAAQIAT          ----------  P.s.pv syringae
380 SSLGIDAMMAGDAINNMAL          ----------  Erwinia amylovora
191 AILGNGLSQAQGQNSPLQLGNNGLQG          ----------  Erwinia carotovora
209 SALSNVSTHVDGNNRHFVD  --- ----------  Erwinia chrysanthemi
312 SFVNKGDRAMAKEIGQFMDQYPEVFG          -------  Erwinia pyrifoliae
300 GSMDKFMKAVGMIKSAVAG          ----------  Pectobacterium
304 KGLEATLQDAGQTGTGVQSSAAQVALLLVNMLL  ---P.s. pv. phaseolicola
91 QALMNIVGDI LQAQNGGGF          ---------  Xanthomonas axonopodis
322 TNLNIKNSSAKGADDKVVQ          ------  Pseudomonas syringae pv. tomato
```

Panel C

```
        a   d   a   d   a   d   a   d   a
23  QGLKGLNSAASSLGSSVDKLSSTIDKLTSAL  --- Erwinia chrysanthemi
27  TTGSTSSKALQEVVVKL          -------  P.s.pv. syringae
300  GSMDKFMKAVGMIKSAVAG          ----------  Pectobacterium
91 QALMNIVGDI LQAQNGG          ---------  Xanthomonas axonopodis
58  SPLGKLLGKAMAASGKAGGGLEDIKAALDTL  ----  P. s. pv. phaseolicola
301 VHAQNVGEDLITVKGEGGAAVTNLNIKNSSAKGADDKVVQL  ----  P.s pv. tomato
        a   d   a   d   a   d   a   d   a   d   a   d
```

Fig. 3.30 Occurrence of leucine zipper like motifs and heptad repeats in harpins.

Panel A and B, showing amino acid sequence alignment of one or more leucine-zipper like motifs in several harpins including harpin$_{Pss}$. Panel C, some harpins are also have coiled-coil motifs, where each (a) and (d) position of heptad repeat are occupied by hydrophobic amino acids. Heptadic amino acids are marked in bold letters.

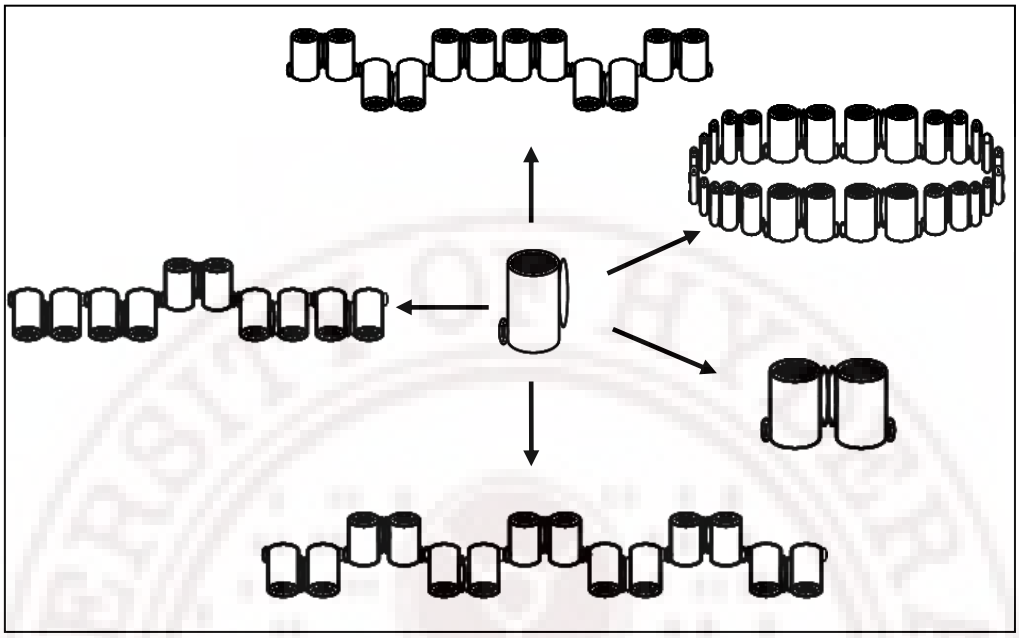

Fig. 3.31 Hypothetical model showing the different oligomeric forms of harpins.

Harpins have at least two leucine-zipper like motifs and hence can nucleate variety of different oligomerization states. Cylinders represent folded helices and two small distorted ellipsoids attached to cylinder are the leucine-zipper like motifs.

4.1 Harpin$_{Pss}$-induced yeast cell death

Initial database searches indicated that the yeast genome lacks genes with obvious homology to many critical components of metazoan apoptotic death machinery, including Bax/Bcl-2 family, Apaf-1/Ced-4, p^{53}, or caspases. This led to a conclusion that PCD does not exist in yeast, however, information has accumulated implying that yeast can undergo PCD and that many components of the yeast PCD and the metazoan apoptosis can be conserved by yeast (Fleury *et al*., 2002). In addition, more detailed analysis of the yeast genome has shown that several yeast proteins share homology with metazoan apoptotic proteins and may be members of an evolutionary conserved family of cell-death proteins (Jin and Reed, 2002).

Evidence suggesting that at least part of the apoptotic machinery may be present in yeast comes from studies on the overexpression of mammalian apoptotic genes in yeast. Owing to the absence of homologs of major genes involved in apoptosis, yeast system was used extensively to study the role of individual molecular components in apoptosis. Surprisingly, expression of several proteins involved in metazoan apoptosis, induced cell death in both the budding yeast *Saccharomyces cerevisiae* and the fission yeast *S. pombe* (Frohlich and Madeo, 2000). Heterologous expression of the pro-apoptotic Bcl-2 family proteins, Bax and Bak, caspases, Ced-4/Apaf-1, or p^{53} in yeast triggered apoptosis like cell death. Further more, cell death induced by pro-apoptotic genes was suppressed by anti-apoptotic Bcl-2 family proteins. Co-expression of several members of Bcl-2 family that are anti-apoptotic in animals, including Bcl-X_L, Bcl-2, Mcl-1, and A1 suppressed yeast lethality induced by Bax and Bak (Ink *et al*., 1997). The identification of specific mutation (S565G) in the cell division cycle gene CDC48 (Madeo *et al*., 1999) that can trigger cell death further indicated the presence of genetically controlled PCD machinery in yeast. Cell death in the CDC48 mutant resembled many features typical to apoptosis that include exposure of phosphotidyl serine on the outer layer of the cytoplasmic membrane, DNA fragmentation and chromatin condensation. PCD has also been implicated as a mechanism of eliminating senescing yeast cells (Laun *et al*., 2001).

Although, there are no homologs of metazoan apoptotic proteins in yeast, recent investigations suggested that some yeast proteins have regions with similarity to mammalian proteins involved in cell death. The Pbh1p protein from *S. pombe* (Rajagopalan and Balasubramanian, 1999) and the Bir1p from *S. cerevisiae* (Yoon and Carbon, 1999) share homology with members of the evolutionary conserved cell death proteins. Another protein SpRad9 from *S. pombe* shares similarity with a human apoptotic protein Rad9 and induces apoptosis in human cells by interacting with Bcl-2 through the region similar to BH3 domain (Komatsu *et al*., 2000). Madeo *et al*., (2002) identified a yeast protein with structural homology to mammalian caspases and named it YCA1, which mediates apoptosis induced by hydrogen peroxide and some other forms of yeast cell death. Thus, yeast as a model system has revealed novel insights into the understanding of evolutionary and functional aspects of genes or proteins involved in cell death.

Reactive oxygen species (ROS) are important mediators of cell death in many organisms. Formation of ROS is common to both apoptotic and necrotic forms of cell death, and plays a central role in the induction and execution of PCD in yeast (Frohlich and Madeo, 2000). Cell death can be triggered in yeast by various treatments that result in ROS production such as hydrogen peroxide, depletion of glutathione, lipid hydroperoxide or exposure to acetic acid. In harpin$_{Pss}$-induced YCD, we have observed extensive ROS generation (Sripriya *et al*., 2009) which likely results from the changes in the electron transport chain events (complex I & III) of the mitochondria. Diphenylene iodonium (DPI), an inhibitor of complex I, completely suppressed ROS generation from the mitochondria during harpin treatment in tobacco cell cultures (Amirsadeghi *et al.,* 2007; Xie and Chen, 2000). The protective effect of catalase in yeast cells expressing the lethal phenotype in galactose-supplemented medium indicated the involvement of oxidative burst in YCD (Podile *et al.,* 2001), a feature similar to plant HR. In our attempt to compare the biochemical events of plant HR and YCD, the use of protein kinase inhibitor K252a completely suppressed the YCD (Podile *et al.,* 2001), as observed in some forms of plant HR (Adam *et al.,* 1997). The amount of cell death greatly increased when the H_2O_2 production was enhanced by inhibiting catalase, similarly harpin$_{Pss}$-induced cell

death decreased significantly in the presence of catalase. The difference between the protective effect of K252a and catalase in harpin$_{Pss}$-induced YCD, also observed by Desikan *et al.,* (1996) in *Arabidopsis* suspension cultures, suggests the importance of protein phosphorylation and oxidative burst as the major events in harpin$_{Pss}$-induced cell death.

Mitochondria play a crucial role in apoptosis in animals. Disruption of mitochondrial membrane releases apoptogenic factors such as cytochrome *c* and apoptosis-inducing factor (AIF), activating cell death pathways. The mechanism of mitochondrial membrane disruption in yeast has resemblance to animals, the discovery of a mammalian ion channel, named mitochondrial apoptosis-induced channel, whose activity correlates with the onset of apoptosis and a similar channel activity in the mitochondrial outer membrane of yeast expressing human Bax, indicates the similar mechanism of release of cell death-inducing factors in both yeast and mammals (Pavlov *et al*., 2001). Harpin$_{Pss}$ expressed yeast cells exhibited transient hyperpolarization during initial hours of induction and depolarization during late hours of induction (Sripriya *et al*., 2009) similar to acetic acid-treated cells indicating that there was loss of mitochondrial membrane potential ($\Delta\Psi_m$) in harpin$_{Pss}$-induced YCD. Since 'petite' mutants of *S. cerevisiae* were insensitive to expression of harpin$_{Pss}$ (Sripriya *et al*., 2009), mitochondria were playing a major role in harpin$_{Pss}$-induced YCD similar to Bax-induced YCD (Greenhalf *et al.,* 1996), while there was no evidence of Cyt C release. Cyclosporine A (PTP blocker) that inhibits apoptosis in yeast (Severin and Hyman, 2002), did not protect *S. cerevisiae* Y187 pYEUT-*hrpZ* cells, probably because of the non-involvement of Cyt C leakage (Sripriya *et al*., 2009). A central feature of mitochondrial dysfunction during animal apoptosis is the opening of permeability transition pore (PTP), releasing Cyt C and intermembrane space proteins into the cytosol, but in harpin$_{Pss}$-induced YCD, PTP seems to have no prominent role as evidenced by the effect of CsA and no release of Cyt C. In *Arabidopsis* cells, harpin$_{Pss}$ treatment resulted in decline of mitochondrial membrane potential ($\Delta\Psi_m$) with the appearance of cytosol-localized Cyt C from the mitochondria (Krause and Durner, 2004). Bax expression induced the release of Cyt C from mitochondria and decreased Cyt C oxidase in yeast (Manon *et al.,* 1997), similar to its effect in mammals. Roucou *et al.,*

(2000) showed that the Cyt C-green fluorescent protein fusion was not released from mitochondria into cytosol upon expression of Bax in the yeast cell, indicating that mitochondrial release of Cytochrome *c* was not mandatory for YCD.

S. cerevisiae contains a few orthologues of mammalian cell death regulators such us the YCA1/MCA1 coding for metacaspases which are supposed to be involved in yeast cell death triggered by different stimuli (Silva *et al*., 2005). In mammalian cells, caspase activity also stimulates several non-death functions like cell cycle, proliferation, inflammation and differentiation (Li *et al*., 2007). Yeast metacaspase (MCA1) was also shown to accelerate G1/S phase of cell cycle and antagonize G2/M transitions (Lee *et al*., 2008). The role of YCA1 in yeast cell death remains elusive, YCA1 independent cell death (Buttner *et al*., 2007) and YCA1 independent caspase like activities (Vachova and Palkova, 2005) have also been reported, yet the involvement of metacaspases remains debatable in yeast cell death. YCA1 seems to have a prominent role in acetic acid induced yeast cell death, in a manner unrelated to its caspase activity (Guaragnella *et al*., 2006) indicating that it could be associated with other cellular functions. Khan *et al*, (2005) suggested that oxidative stress in yeast might be interlinked with metacaspase activation and the same appears to hold good for harpin$_{Pss}$-induced YCD as oxidative stress is the major factor involved in this form of cell death.

Cytochrome *c* and caspases are the key factors for induction of apoptosis in animal cells but in yeast the absence of cytochrome *c* or metacaspase may only reduce but not abolish the cell death processes. Unlike in animal cells, the release of cytochrome *c* upstream of metacaspase activation is not very much essential in yeast (Silva *et al*., 2005) or caspase activation may not be always associated with the release of cytochrome *c* and yeast might possess alternative death pathways which do not involve the role of cytochrome *c* (Pereira *et al*., 2007).

In the present study, FITC-labelled caspase, *in-situ* marker VAD-fmk, that binds specifically to the active site of metazoan caspases was used and detected by flow cytometry. Harpin expressing yeast cells showed elevated metacaspase activity (similar to acetic acid treated cells) compared with the control cells. This forms the first report on

the induction of metacaspase activity during harpin-induced YCD (Sripriya *et al*., 2009) or even in plant cells where caspase activation during harpin expression has not been reported earlier.

Of all the eukaryotic cell cycles, the budding yeast *Saccharomyces cerevisiae* has been one of the most extensively studied and characterized both from an experimental and modelling perspective. *S. cerevisiae* differs slightly from other eukaryotes in the way the cell grows during the cell cycle. As the cell grows, a bud forms from the side of the cell and holds one pole of the mitotic spindle, the bud then eventually becomes the daughter cell, after cell division, with one copy of the genetic material being sent there during anaphase (the original cell is called the mother cell). In response to genotoxic agents and cell cycle blocks, all eukaryotic cells activate a set of surveillance mechanisms called checkpoints. DNA structure checkpoints are integrated with the DNA damage response pathways and the cell cycle transition exhibited by many cells impaired in checkpoint functions may be a result of the cells inability to mediate the efficient repair of DNA lesions. The DNA structure checkpoint pathways are usually implicated in recombination or repair mechanisms in both yeast and human cells (Grushcow *et al*., 1999; Morrison *et al*., 2000). The cell cycle is transiently arrested at different stages depending on the phase at which DNA alterations occur (G1, S and G2). Three responses have been characterized in budding yeast, which are known as the G1/S, intra-S and G2/M DNA damage checkpoints. *RAD9*, *RAD17*, *RAD24*, *RAD53 MEC3* and *DDC1* gene products are specifically required for a proper DNA damage response (Longhese *et al*., 1998) and are proposed to act at an early step of damage recognition at any stage of the cell cycle. Genetic studies in fission yeast have shown that both recovery and checkpoint controls are abolished by mutations in the *rad* genes, while mutations in cell cycle control genes only affect the checkpoint function (Enoch *et al*., 1991; Khodairy *et al*., 1994).

Specific effects triggered by hydrogen peroxide, menadione and diethylmaleate (a thiol oxidant that depletes glutathione) on yeast cells are observed at the level of cell cycle arrest, hydrogen peroxide causes Rad9p-dependent arrest in G2, while menadione causes Rad9p-independent arrest in G1 (Flattery and Dawes, 1998). Diethylmaleate induces primarily G1 arrest but some cells are arrested as budding G2 cells (Wanke *et al*., 1999).

In harpin$_{Pss}$-induced YCD, we have observed increase in accumulation of cells in the G0/G1 sub-phase of the cell cycle, resembling the cells treated with hydroxy urea (S-phase blocker) indicating that harpin$_{Pss}$ expression in yeast leads to DNA damage resulting in cell cycle blockage probably at the G1/S check points, ultimately leading to cell death. Thus, most of the checkpoint mechanisms that have been identified using budding yeast as a model organism have been conserved throughout evolution and can potentially be exploited to search for therapeutic agents with increased selectivity for cancer cells.

In yeast, as in mammalian cells, phosphatidylserine (PS) has an asymmetric distribution in the lipid bilayer of the cytoplasmic membrane. The exposure of PS residues at the outer surface of the cytoplasmic membrane occurs at the early stages of apoptosis (Martin *et al.,* 1995) when membrane integrity is still retained. In the present study more percentage of harpin$_{Pss}$-expressed cells stained positive for PI than for annexin V similar to acetic acid-treated cells (induced for a necrotic response) suggesting that the harpin$_{Pss}$-induced YCD was more necrotic rather than apoptotic.

A *Nicotiana sylvestris* mitochondrial mutant lacking complex I of the electron transport chain was found to produce more transcript levels of antioxidant enzymes (APX, CAT, SOD) during harpin-induced hypersensitive response (Garmier *et al*., 2002) compared to the wild type, indicating that lack or impairment in the functioning of complex I results in more of ROS production and ultimately leading to elevation of antioxidant mechanisms in the plants. Complex I of mitochondrial ETC was also supposed to be an important target for salicylic acid-induced respiratory inhibition in tobacco cells (Xie and Chen 1999). Also the inhibition of mitochondrial Complex I by tumor necrosis factor affects electron flow through other complexes resulting in cytochrome *c* release by an antioxidant pathway and caspase activation followed by the induction of membrane permeability transition (Higuchi *et al*., 1998). During harpin$_{Pss}$ expression in yeast, we found ROS production (Fig 3.1) and changes in glutathione levels (Fig 3.6) which could be the result of down regulation of complex I activity in harpin$_{Pss}$-induced yeast cell death.

During oxidative stress, despite the induction of antioxidant defenses, the levels of oxidatively modified proteins (protein carbonyls and glutathione-protein mixed disulphides) are considerably increased in the yeast cells. The induction of *UB14* gene expression during cellular adaptation to respiratory metabolism suggests an important role of the ubiquitin pathway in the turnover of oxidized proteins under these conditions (Watt and Piper, 1997). H_2O_2 decreases the GSH/GSSG ratio and increases the levels of low molecular weight thiols and protein mixed disulphides between cysteine residues (Grant *et al*., 1998). Similarly, in harpin$_{Pss}$-induced YCD also, we observed a decrease in the glutathione levels and reduction in the GSH/GSSG ratio indicating the extent of oxidative stress built up in the system. *S. cerevisiae* DNA is also a target for oxidative damage after exposure to peroxides or hydroxyl radicals, leading to an increase in the frequency of intra-chromosomal recombination (Brennan *et al*., 1994). The decrease of glutathione levels and superoxide dismutase activity concomitant with an increase in ROS production and the accumulation of oxidized proteins may, therefore, account for cell death and aging (Jakubowski *et al*., 2000).

The hypoxic response for most organisms comprises a complex biochemical and genetic program that includes the differential expression of a large number of genes (Hochachka *et al*., 1996; Bunn and Poyton, 1996). Thus oxygen availability affects the intracellular levels and activities of a large number of proteins in most organisms including yeast. Superoxides and subsequently ROS may act as second messengers, controlling the activity of the trans-acting factors that regulate the transcription of hypoxic genes (Bunn and Poyton, 1996; Bunn *et al*., 1998; Ratcliffe *et al*., 1998). In harpin$_{Pss}$-induced YCD, the hypoxic condition seems to be evident, the oxygen consumption capacity of cells expressing harpin$_{Pss}$ decreased four-fold, compared with that of the control cells grown in raffinose-supplemented medium (Fig 3.2). It was also proved that varying oxygen concentrations affects the expression of several *S. cerevisiae* genes (Kwast *et al*., 1998; Burke *et al*., 1997). Cytochrome c oxidase has been implicated as a probable oxygen sensor and in the regulation of hypoxic genes in a number of mammalian cells (Chandel *et al*., 1997; Budinger *et al*., 1998). The mitochondrial respiratory chain and cytochrome *c* oxidase are well suited for their role in oxygen sensing, because they are consumers of

most of the oxygen that is taken up by the eukaryotic cells, and the varying oxygen concentrations affects the flux of electrons through both the respiratory chain and cytochrome *c* oxidase in several cell types (Wilson *et al*., 1988; Rumsey *et al*., 1990) including yeast (Burke *et al*., 1998). Also the V_{max} of cytochrome *c* oxidase in several cells decreases in response to hypoxia (Chandel *et al*., 1996), and this decrease in V_{max} increases the reduction state of mitochondrial electron carriers that are upstream of cytochrome *c* oxidase and ROS generation (Duranteau *et al*., 1998). ROS are also involved in the cross talk between mitochondria and nucleus (Poyton and McEwen, 1996) which would function to activate members of signal transduction pathways. Unlike complex I and II, which generate superoxide into the mitochondrial matrix (Turrens and Boveris, 1980; Zhang *et al*., 1998), complex III releases superoxide into the mitochondrial intermembrane space and subsequently into the cytosol (Boveris *et al*., 1976; Turrens *et al*., 1985; Muller *et al*., 2004). Evidences indicate that ROS generated by complex III are required for activation of certain transcription factors called hypoxia-inducible factors (HIF) (Semenza *et al*., 1994). The functional integrity of cytochrome *c* oxidase or other components of the respiratory chain is compromised during hypoxic conditions and there is a coordinate loss of cytochromes during hypoxia (Rep and Grivell, 1996). Harpin treatment in tobacco cells was associated with the inhibition of cytochrome c oxidase pathway (Xie and Chen 2000) and the inhibitory targets in harpin-treated cells are the complex III or complex IV of mitochondrial ETC. Also the inhibition of these two complexes, particularly complex IV (cytochrome oxidase) has been linked to animal apoptosis induced by various stimuli (Green and Reed, 1998; Gudz *et al*., 1997; Scaife, 1996). Bax expression in yeast lead to decrease in cytochrome c oxidase activity (Manon *et al*., 1997), similarly, $harpin_{Pss}$ expression in yeast also resulted in reduction of cytochrome *c* oxidase activity compared to that of the control cells, which could be the consequence of severe hypoxia.

Harpin and salicylic acid treatments in tobacco cells resulted in altered mitochondrial functions leading to drop in ATP levels (Xie and Chen 2000). Xie and Chen (1999) suggested that ATP synthesis is linked to respiratory O_2 uptake and reported that salicylic acid or its analogs that inhibited ATP synthesis also inhibited respiratory O_2

consumption. During harpin treatment in tobacco cells, inhibition of ATP synthesis precedes cell death revealing the affect on electron transport or cytochrome pathway respiration, ultimately resulting in the depletion of high energy phosphates which could be the basic cause for induction of cell death. Even in *Arabidopsis* cells, treated with harpin$_{Pss}$, cellular ATP levels were found to be declined (Krause and Durner, 2004). Also, in harpin$_{Pss}$-induced yeast cell death, we observed a reduction in the activity of mitochondrial ATPase (Complex V) indicating the effect on respiratory electron transport system as well as the reduced capability of the cells for ATP synthesis or O_2 consumption.

As a whole the results presented here revealed the basic physiological changes in harpin$_{Pss}$-induced yeast cell death giving an indication that this is a necrosis-like PCD, although caspase activation has been observed (Vachova and Palkova, 2007). Harpin has a rapid and dramatic impact on mitochondria, in functioning, that it binds and triggers ion currents in lipid bilayers (Lee *et al*., 2001) and forms ion conducting pores and probably disrupting the function of mitochondria in the cell. The necrosis seen in this YCD could be the consequence of severe oxidative-stress, involving the paralyses of mitochondrial ETC events. This necrosis-like PCD seems to be comparable to the cellular events during HR response in plants. Thus the possibility of using yeast as a model organism throws light in elucidating the mechanism of action of several molecules in higher eukaryotic systems, however there might be little variations from one system to another due to its evolutionary genetic make up and environmental influences.

4.2 Harpin$_{Pss}$-induced cell death in Jurkat cell lines

Apoptosis is under strict genetic control and a distinct cellular morphology is detectable. It is an essential process of the development and tissue homeostasis of most multicellular organisms and the deregulation of apoptosis has been implicated in the pathogenesis of many diseased conditions such as cancers. In contrast, necrosis is a random process and results in cell lysis. During classical apoptosis, caspase proteins are recruited for activation of the apoptotic pathway (Ha *et al*., 2003; Tibbetts *et al*., 2003). Another hall mark feature of classical apoptosis is the fragmentation of genomic DNA or chromatin

condensation. There is also a tight relationship between cell cycle and apoptotic responses, cell cycle components such as P^{53}, P^{Rb} and E2F, have been shown to participate in both cell cycle progression and apoptosis. Apoptotic stimuli affect both cell proliferation and death through these regulators. Moreover, in recent years the regulation of cell cycle and apoptosis has received much attention as a possible means of eliminating excessively proliferating cancer cells. Cancer occurrence requires mutations for the failure of the apoptotic safeguard mechanisms as well as the deregulation of the cell cycle (King *et al*., 1998). Virtually many anticancer approaches including chemotherapy, hormones and radiation induce cytotoxicity of tumor cells by apoptosis (Djavaheri *et al*., 2003; Hostanska *et al*., 2003). Initiation of apoptosis is controlled by regulation of the balance between life and death signals received by the cells, therefore, specific therapies designed to change the balance between life and death signals in cancerous cells, could be of therapeutic benefit. In our study, we have chosen T-cell lymphoma cells (Jurkat cell line) which is an aggressive malignancy of thymocytes characterized by high numbers of bone marrow and circulating blast cells, enlargement of mediastinal lymph nodes, and often central nervous system involvement. Similar to other types of leukemias, T-cell leukemia is caused by genetic alterations in hematopoietic precursor cells leading to a variety of changes, including loss of cell cycle control, unlimited self-renewal capacity, impaired differentiation, hyperproliferation and loss of sensitivity to death signals. The present study investigating the effect of $harpin_{Pss}$ on animal cells, indicated that this protein could induce cell death in Jurkat cells in concentration and time dependent manner. The results from the flow cytometric detection of Propidium iodide stained cells and DNA fragmentation assay indicated that the cells treated with $harpin_{Pss}$ were undergoing apoptosis. Cell death was also assayed by studying the release of Cytochrome c and also the alteration in Bcl2/Bax levels.

Cell viability with $harpin_{Pss}$ treatment was evaluated by MTT assay which is based on the reduction of MTT salt to formazan crystals by the mitochondria (NADH dehydrogenase or Succinate dehydrogenase) in living cells. A dose dependent decrease in Jurkat cell proliferation was observed with $harpin_{Pss}$ treatment at 24h of incubation period and the IC_{50} was determined to be at a concentration of 40 µM (1.5 mg/ml) of the protein. The

high concentration of the protein required to induce cell death is due to the fact that, harpin exists as an oligomeric and polydispersed protein (monomer, dimer, trimer, tetramer and octamer). Among all these forms, the monomeric or dimeric forms of the protein retain more functional activity (Chen *et al*., 1998) and in the total oligomeric protein concentration of 1.5 mg/ml, the monomeric or dimeric forms could account for a low quantity in the solution compared to all the other forms of the protein, apparently, which cannot be calculated.

Jurkat cells treated with $harpin_{Pss}$ showed the clear formation of apoptotic bodies and cell burst when observed under the phase contrast microscope where as untreated cells are healthy showing bunches of cells. Flow cytometric analysis of $harpin_{Pss}$ treated cells showed an arrest in G_0/G_1 sub-phase of the cell cycle indicating the anti-proliferation or apoptosis induction by the protein. Proliferation and apoptosis are tightly coupled and cell cycle regulators can influence both cell division and cell death. The timing and order of cell cycle events are monitored during cell cycle check points that occur at G1/S phase boundary, in S phase, and during the G2/M phases (Murray and Hunt, 1993). Cell cycle progression can be blocked at these checkpoints in response to the status of both the intracellular and extracellular environment. The cell cycle control system is based on two protein families, the cyclin dependent protein kinases (Cdks) and the cyclins, activation of specific cyclin/Cdk complexes and their phosphorylation of particular proteins permits the cell cycle processes to continue. Numerous genes, including c-*myc*, are known to inhibit or activate cell proliferation by affecting the formation and activity of Cdk complexes (Evan *et al*., 1992). p53 also arrests the cell cycle or activates apoptosis (Yontsh *et al*., 1991), thus, some types of programmed cell death are coupled to the cell cycle. PCD induction is linked to cell cycle progression as suggested by studies of p*34cdc2* a serine-threonine kinase that controls the G0-G1 checkpoint (Shi *et al*., 1994).

During apoptosis, nucleus of the cell undergoes dramatic morphological changes, including chromatin condensation, peripheral margination, nuclear shrinkage and subsequent fragmentation (Kerr *et al*., 1972). The changes are apparently driven by biochemical processes that become active during apoptosis. Key proteins responsible for maintaining nuclear structure and chromatin integrity are proteolysed during apoptosis,

releasing specific fragments. In addition, DNA breaks, including internucleosomal cleavage are generated and have been recognized as a biochemical hallmark of apoptosis. Cleavage of DNA at internucleosomal sites is recognized to be the primary biochemical feature for apoptosis. This specific cleavage leads to the formation of nucleosomal fragments of 180-200 bp lengths, which upon electrophoresis resolve into a 'DNA ladder'(Wyllie, 1980). Harpin$_{Pss}$-treated Jurkat cells also showed DNA fragmentation, resembling the above features, which further substantiates the induction of apoptosis in Jurkat cells. Specific endonucleases including DNA fragmentation factor (DFF) or Caspase-activated DNase (CAD) are activated during apoptosis and are responsible mainly for this type of DNA breakdown (Wyllie, 1998). Internucleosomal DNA cleavage, although a late event, is considered as an indicator of apoptosis and is a qualitative measure rather than quantitative.

In the intrinsic cell death or in the mitochondrial pathway, the Bcl-2 family proteins are perhaps the most important regulators. These proteins could also be responsible for bridging signals from the extrinsic pathway to the mitochondrial pathway. The Bcl-2 family of proteins consists of both anti-apoptosis and pro-apoptosis members. The Bcl-2 family proteins can interact with each other and also with several other cellular proteins. The interaction between Bcl-2 and Bax is one such example, enabling proper confirmation on the membranes *in vivo* which could be the result of activation by death signals (Hsu and Youle, 1998; Nechushtan *et al*., 1999; Desagher *et al*., 1999). Another example comes from the fact that the antideath molecules Bcl-2 or Bcl-x_L inhibits the regulation of cell cycle progression (Chao and Korsmeyer, 1998) but promoted by pro-death molecules Bax (Knudson *et al*., 2001) or Bad (Chattopadhyay *et al*., 2001). The pro-death multidomain proteins, Bax or Bak are responsible for the induction of mitochondrial apoptosis, the ability of Bax or Bak to oligomerize has been considered an important factor in the formation of a mitochondrial channels for release of apoptotic factors such as Cytochrome c (Wei *et al*., 2000; Eskes *et al*., 2000). Bax is usually localized in the cytosol and translocated to the mitochondria in response to death stimuli, where as Bak constitutively resides in the mitochondria. Deletion of both Bax and Bak renders the cell resistant to all major mitochondrial death signals, including DNA

damage, growth factor deprivation, ER stress and to the extrinsic pathway signals mediated by Bid (Wei *et al*., 2001; Zong *et al*., 2001; Cheng *et al*., 2001; Lindsten *et al*., 2000). In the present study, harpin$_{Pss}$-treated Jurkat cells showed the expression of both Bax and Bcl-2, tested in a time dependent manner. The Bcl-2 levels were found to be decreasing with increase in time points and an alteration in the Bcl-2/Bax levels was observed, indicating the reduction in anti-apoptotic effect and progression in apoptosis.

The mitochondrial intermembrane space (IMS) contains a heterogenous class of proteins whose release promotes cell death and the first molecule identified belonging to this class of pro-apoptotic proteins is the Cytochrome *c* (Ott *et al*., 2002). Using green fluorescent protein (GFP) tagged to Cytochrome *c*, Goldstein *et al*., (2000) demonstrated that cytochrome *c* release into the cytosol is a very rapid process, which initially occurs by detachment from the inner membrane and subsequently released after permeabilization of the outer membrane (Ott *et al*., 2002). Mitochondrial outer membrane permeabilization (MOMP) is mandatory for apoptotic cytochrome *c* release and depends on the activation of molecular machinery involved in mitochondrial fission. Preceding cytochrome *c* release, mitochondrial membranes undergo morphological changes that resemble the events associated with fission. Evidence exists that the proapoptotic protein Bax interacts with endophilin1, the main regulator of mitochondrial division (Karbowski *et al*., 2004) and thus, Bax might stimulate mitochondrial fission, which in turn favours MOMP (Perfettini *et al*., 2005). Harpin$_{Pss}$-treated Jurkat cells showed gradual release of cytochrome *c* into the cytosol with hourly time intervals indicating the feature of apoptosis observed with harpin$_{Pss}$ treatment in the cells. Thus, Cytochrome *c* release might induce caspase activation which subsequently cleave various substrates, leading to the characteristic morphological changes associated with apoptosis, such as DNA fragmentation, chromatin condensation and ultimately formation of apoptotic bodies and cell death.

In conclusion, these results showed that 'Harpin', a type III effector protein induces apoptotic cell death in Jurkat cell lines and we predict that nanoparticle derivatives of such proteins would be more effective at relatively low concentrations in inducing cell

death. Therefore, this work opens a new area in accelerating the development and usage of proteins like harpin as potent cytotoxic or anti-cancerous agents.

4.3 Bio-physical features of harpin$_{Pss}$

Harpin$_{Pss}$ is a bacterial protein secreted by *Pseudomonas syringae* pv. *syringae*. The protein is thermally stable, but there was no explanation regarding the high thermal stability of the protein. In the purification of the protein, the high thermal stability of harpin$_{Pss}$ was utilized to isolate it from a mixture of proteins present in the homogenate, by heating it above 90 °C in order to deactivate other mesophilic proteins (He *et al*., 1993). Differential scanning calorimetry (DSC) is an extremely useful technique for investigating thermal unfolding of proteins and for characterizing the associated energetics. DSC scan of harpin$_{Pss}$ show three peaks (Fig 3.22) indicating that the thermal unfolding of the protein is a rather complex process. The DSC thermogram reveals two distinct transitions below 90 °C and a third transition around 93 °C. These results seem to contradict earlier observations as it was reported earlier that harpin$_{Pss}$ is stable above 90 °C. We have investigated the reversibility of thermal unfolding and found that the two transitions below 90 °C are highly reversible in nature. So, it appears that due to reversibility of first two transitions the protein shows characteristic thermal stability at high temperature. Since earlier studies reported that harpin$_{Pss}$ is oligomeric in nature (Chen *et al.*, 1998), we propose that the transiton 1 is due to dissociation of multimeric form. Support for this argument comes from the temperature dependent CD, where we have shown that before the starting of transition 2, i.e. up to 44 ^{o}C there is no change in the α-helical or β-sheet component of the protein. As the secondary structural components remain unchanged, it appears that there is no structural change in the temperature range 26 °C to 44 °C. The high α-helical content in harpin$_{Pss}$ obtained from our results (following the analysis of Lobley and Wallace, 2001) is consistent with the predicted secondary structure from sequence analysis using theoretical approaches (Alfano *et al*., 1996). Recently the harpin from *Xanthomonas axonopodis* pv. *glycines* was reported to be predominantly α-helical based on CD spectral studies (Oh *et al.*, 2007). Fluorescence studies also showed that in the above temperature range (26- 44 °C), emission maximum of 'tryptophan' fluorescence does not change with temperature,

suggesting no structural change occurs in this temperature range or if any structural change occurs, it does not affect the 'Trp' environment since only one 'Trp' is present in the protein. Therefore, the endotherm of transition 1 comes from the dissociation of oligomeric structure. Transition 2 falls in the temperature range between 44 °C to 75 °C. In this temperature range the helical content decreases continuously while the β-sheet fraction increases. These changes in the secondary structure indicate some sort of unfolding and associated reorganization of the protein.

Dynamic light scattering (DLS) is a powerful tool to get the hydrodynamic radius of macromolecules (Wilkins *et al*., 1999). The R_h of $harpin_{Pss}$ (20.54 nm) at room temperature, obtained by DLS measurements, is considerably higher than the predicted value (2.58 nm) of R_h of a 341 amino acid protein. The high R_h at room temperature also supports the oligomeric nature of the protein. The R_h of $Harpin_{Pss}$ at 61 °C is estimated as 9.35 nm, which is also considerably high as compared to the R_h predicted for denatured monomeric form of $harpin_{pss}$ (6.14 nm). The high R_h at 61 °C can be explained if one assumes that the protein at this temperature exists as a partially unfolded dimer. Thus, light scattering results suggest that during transition 2 the protein starts to unfold, but it exists as a partially unfolded dimer after transition 2. So, at the final step the partially unfolded dimeric intermediate dissociates to a fully unfolded monomeric protein. Hence, we report the complex thermal unfolding behaviour of a thermostable protein via the oligomer→dimer/lower aggregate→semi unfolded dimer→unfolded monomer pathway and also report the reversibility of thermotropic transitions.

Apart from the thermal unfolding behaviour, DSC studies can also provide several thermodynamic features. These include ΔH_c, ΔH_v and T_m which are extremely useful to explain several thermodynamic properties. The calorimetric enthalpy change, ΔH_c, can be obtained by integration of the area beneath the experimental curve, the Van't Hoff enthalpy change, ΔH_v, can be obtained from the temperature dependence of the equilibrium constant. For $harpin_{Pss}$ ΔH_c of transition 1 was relatively high compared to ΔH_c of other two transitions. This may be due to the fact that first step is associated with dissociation of oligomeric states and the oligomers are tightly held with favourable interactions. The oligomers can consist of a variable number of different oligomerization

states instead of a well-defined quaternary structure. Support for our argument of different oligomerization states of native protein comes from the DSC and DLS experiments (Fig 3.26). We have seen in DSC experiments that the ΔH_c of transition 1 was not reproducible. The ΔH_c was found to vary in day to day experiments and the mean ΔH_c had a high standard deviation. DLS experiments also reflect the idea of different oligomerization states, as here again we have noticed high standard deviation in hydrodynamic radius for the native protein at 25°C. Now the question comes, why the native protein exhibits different oligomerization states? Why it is so thermostable? Why the reversibility in thermotropic transitions? And, why the thermal unfolding is so complex? Before discussing we summarise the extensive work done on harpin proteins, including $harpin_{Pss}$.

Although harpins were discovered long ago (Wei *et al*., 1992; Kim and Beer, 1998; Alfano and Collmer, 2004), their biochemical role and the mechanism by which they cause HR and affect the pathogenicity of plant bacteria remain largely unexplained. Harpins function in intercellular spaces and are known to possess pore-forming activity in cell-membranes (Pike *et al*., 1998; Ahmad *et al*., 2001; Lee *et al*., 2001). However, the biochemical basis of plant cell membrane destabilization by harpins is unknown. It has been well recognized that a protein adopts its unique, three-dimensional equilibrium structure spontaneously, under biological conditions, and that protein function depends upon the specific three-dimensional structure of the mature, folded form (Anfinsen, 1973; Gething and Sambrook, 1992). Most proteins are packed structures whose surface features establish their functions by presenting binding sites that are specific to some molecules. Interestingly, the amino acid sequences of harpins do not share any major homology with other proteins, or among themselves, and their functional regions cannot be determined by tertiary structure analysis. Here, we have identified a common structural feature in harpins. The common structural feature is the presence of at least two leucine-zipper like motifs in harpins including $harpin_{Pss}$. Presence of at least two leucine-zipper like motifs and presence of coiled coil motif in some harpins (Fig 3.31) can nucleate a variety of different oligomerization states. These oligomers can perturb the cell membranes as several earlier reports claim about the interaction between oligomers and

membrane. It has already been postulated that the leucine-zipper motif could contribute to the oligomeric structures of fusogenic viral glycoproteins and has an important role on virus fusion. Leucine zipper motifs have been proposed to be involved in the fusogenic assembly of influenza hemagglutinin (Carr and Kim, 1993), sendai virus fusion protein (Ghosh *et al*., 1997), newcastle disease virus fusion protein (Reitter *et al*., 1995), HIV transmembrane glycoprotein gp41 (Bernstein *et al*., 1995) etc. These proteins are shown to form aggregates in solution and it was believed that these aggregates can bind to the surface of membrane, they lie on the surface of the target membrane and assist in the apposition of the viral and target membranes. A similar role was suggested for leucine-zipper motifs in the *E. coli* toxin hemolysin E (Yadav *et al*., 2003), antibacterial melittin (Asthana *et al*., 2004) due to their ability to bind membrane. Our findings provide evidence that the presence of leucine-zipper-like helical motif in harpins can create aggregated structure, which can indeed stabilize an oligomeric membrane domain to form a coiled-coil structure with potential relevance to ion channels and the resulting perturbation/leakage in cell membrane can cause the HR elicitation.

Vieille & Zeikus (2001) showed that a number of hyperthermophilic proteins that have a higher oligomerization state than their mesophilic homologues is increasing. This suggests that intersubunit interactions provide a potentially major stabilization factor. Other studies (Kohlhoff *et al*., 1996; Clantin *et al*., 2001) also support that oligomerization is an important strategy, adopted for stabilizing proteins at very high temperatures. Since harpins tend to form oligomeric structures and that harpin$_{Pss}$ oligomerization has been detected experimentally, we propose the oligomeric nature of harpins is responsible for their high thermal stability. One important criterion of a thermostable protein is close packing or significantly reduced hydrophobic accessible surface areas (ASA). Internal packing could be involved in protein thermostability and statistical analysis suggests a number of hyperthermophilic proteins show significantly reduced hydrophobic ASA (Vieille and Zeikus, 2001). Binding experiment between ANS and harpin$_{Pss}$ suggests the absence of hydrophobic accessible surface areas, which can give some extent of thermal stability to the protein (data not shown). Harpins tend to form aggregates in native state and the ΔH_c of transition 1, where it is believed that the

transition is due to dissociation of aggregated protein to dimeric protein, is higher than other two transitions. Therefore the aggregated protein is thermodynamically stable, may be due to strong hydrophobic interactions and lack of ASA.

Congo red binding also shows a blue shift indicating aggregation of harpin$_{Pss}$. Binding of CR to amyloids leads to a red shift (Klunk *et al*., 1999). Red shift in the absorption spectrum (J aggregates) comes from head-to-tail stacking of dyes, while a parallel stacking arrangement leads to a blue shift (H aggregates) (Hirano *et al.*, 2007; Han *et al*., 1995, James, 1966). It was reported earlier (Lazar *et al*., 2005; Cooper and Stone, 1998) that some peptides show blue shift in CR binding instead of showing a red shift. These peptides are not classified as amyloids and the blue shift was explained in terms of the parallel stacking of CR. So at room temperature the aggregate of harpin$_{Pss}$ shows the blue shift due to formation of H type aggregate and reveals non-fibrilogenic nature of harpin$_{Pss}$. No obvious blue shift at high temperature suggests the dissociation of aggregate, which is consistent with other experiments. If the heated sample was cooled and the spectra were recorded again, characteristic blue shift again appeared, suggesting the reversibility in the process. Further studies are required to explain why CR takes an H aggregate in harpin. The highly stable aggregated form may also be responsible for the reversibility in thermal unfolding, as it is highly obvious that a great chance always exists to refold if the protein gets large enthalpic stability, large enthalpic stabilization can cancel out the unfavorable entropic contribution. We have reported here that harpin$_{Pss}$ is a protein with leucine-zipper like motif, it was reported earlier that unfolding of leucine-zipper is a complex process rather than a simple one step process (Dragan and Privalov, 2002). The complex thermal unfolding pathway of harpin$_{Pss}$ also reflects the presence of leucine-zipper like motif in the protein. The first step of transition is only dissociation of oligomeric protein rather than structural unfolding and the proposed transition 2 state indicates that the protein unfolds from a dimeric state to a semi-unfolded dimeric intermediate. If we put dimer concentration during DSC analysis, $\Delta H_c/\Delta H_v$ ratio for transition 2 is very close to unity, indicating that the observed step is a cooperative two-state transition (Nakagawa *et al*., 2002). Although this type of transition, which claims the existence of semi-unfolded dimeric intermediate state, is relatively uncommon, semi-

unfolded dimeric intermediate has been identified during the thermal unfolding of a number of leucine-zipper, coiled-coil and other proteins (Zhu *et al*., 2001; Makino *et al*., 2007; Ramstein *et al*., 2003).

In an attempt to solve the three dimensional structure of harpin$_{Pss}$, extensive crystallization trials were made resulting in precipitation of the protein and formation of micro crystalline precipitates. Crystallization is a process of slow and controlled precipitation of the protein, but an uncontrollable, rapid aggregation of the protein would never result in the formation of a crystal. The possible reason could be the polydispersed and oligomeric nature of the protein and also the existence of leucine-zipper like motifs or heptad repeats which would contribute for the coiled-coil confirmations, further resulting in the non-specific aggregation of the protein. AFM pictures (Fig 3.28), DLS and congo red binding studies also provide a good concrete evidence for the aggregative nature of the protein.

In conclusion, we have identified a conserved leucine-zipper like motif in harpins, which may have the potential to participate in the binding of the protein to the target cell membrane. Moreover, this segment may be involved in the assembly and protein induced destabilization of target cell membrane. We speculate that this conserved motif may have similar structural and functional roles in homologous proteins of the same family. Also the aggregated structure, formed by leucine-zipper like motifs, contributes for the thermal stability in the protein and results in the complex thermal unfolding behavior of the protein.

5.1 Background and Objective

Pseudomonas syringae pv. syringae 61 *hrpZ* encodes harpin$_{Pss}$, a 34.7 kDa extracellular protein that elicits hypersensitive response (HR) in plants. Galactose-induced expression of harpin$_{Pss}$ caused yeast cell death hypothesizing that yeast might share, with plants conserved components in cell death pathway (Podile *et al*., 2001). Extracellular treatment of harpin$_{Pss}$ did not affect the growth of yeast and the observed YCD was independent of the stage of cell cycle. Clear loss of membrane integrity was evident with the absence of nuclear fragmentation and chromosomal condensation. 'Petite' mutant of *S. cerevisiae* Y187 pYEUT-*hrpZ* was insensitive to cell death indicating the involvement of mitochondria in this YCD (Sripriya *et al*., 2009). Harpins are heat-stable, glycine-rich, amyloid forming proteins, secreted by plant pathogenic bacteria and can elicit hypersensitive response (HR), a defensive cellular suicide, in non-host plants. The biochemical mechanism of HR elicitation in non-host plants is still not clear. Absence of homology in amino acid sequence with other known proteins or among themselves makes it more difficult to predict the three-dimensional structure or to establish the structure-activity relationship in harpins.

With the above background, the present study was focused on the following objectives:

1) Harpin-mediated cell death events:

   a) To use yeast as a model system to decipher the physiological mechanism of action of harpin$_{Pss}$.

   b) To test the effectiveness of harpin$_{Pss}$ on Jurkat cell lines (human T-cell lymphoma cell line).

2) Investigation on the bio-physical features of harpin$_{Pss}$ for a better understanding of the structure- function relationship of the protein.

5.2 Harpin$_{Pss}$-induced yeast cell death

S. cerevisiae Y187-pYEUT-*hrpZ* was grown in YMM containing raffinose as the carbon source to an OD_{600} ~ 0.5, pelleted and resuspended in YMM supplemented with galactose or raffinose or acetic acid. Staining with H_2DCFDA confirmed ROS release

during harpin$_{Pss}$-induced YCD at 90 min of culturing time. Oxygraph study revealed that harpin$_{pss}$-expressed yeast cells exhibit a three-fold reduction in the rate of oxygen consumption compared to the control cells, indicating that the cells are in a state of respiratory deficiency during harpin$_{pss}$-induced YCD. Rhodamine 123 staining indicated, alteration in mitochondrial potential in cells expressing harpin$_{Pss}$, while dual staining with annexin V and PI showed that the yeast cells expressing harpin$_{Pss}$ exhibit necrosis rather than apoptosis. Cell cycle analysis with PI revealed that harpin$_{Pss}$-induced yeast cells showed increased accumulation in G0/G1 sub phase, resembling the cells treated with hydroxy urea (S-phase blocker) and thus harpin$_{Pss}$ expression in yeast leads to DNA damage resulting in cell cycle blockage leading to yeast cell death. Elevation of metacaspase activity has been reported for the first time in this form of yeast cell death induced by harpin$_{Pss}$ expression. Analysis of glutathione levels revealed that *S. cerevisiae* Y187 expressing harpin$_{Pss}$ exhibit 37% reduction in the GSH levels and significant decrease in GSH/GSSG ratio compared to the control cells indicating the extent of oxidative stress during harpin$_{Pss}$ expression.

Mitochondria seem to play an important role in harpin$_{Pss}$-induced YCD as evident by the testing on 'petite' mutants (Sripriya *et al*., 2009) and thus mitochondria have been isolated from *S. cerevisiae* Y187 cells expressing harpin$_{Pss}$ and tested for various enzymatic assays pertaining to the electron transport chain. The specific activity of NADH dehydrogenase in cells expressing harpin$_{Pss}$ is 32% reduced compared to the enzyme activity in the control cells. Similarly, *S. cerevisiae* Y187 expressing harpin$_{Pss}$ had 44% reduction in Cytochrome C oxidase activity compared to the control cells, while 30% reduction in mitochondrial ATPase activity was evident. Hence, harpin$_{Pss}$ expression results in oxidative stress and has a drastic impact on mitochondria resulting in the paralyses of ETC events ultimately leading to yeast cell death.

5.3 Harpin$_{Pss}$-induced cell death in Jurkat cell lines

Harpin$_{Pss}$, secreted by Gram –ve phytopathogenic bacteria, *Pseudomonas syringae* pv. *syringae* exhibits hypersensitive response in tobacco and other plants during host-pathogen interaction. On ectopic expression harpin$_{Pss}$ also caused cell death in yeast

(Podile *et al.*, 2001). For the first time, the effectiveness of harpin has been tested on animal cell lines and Jurkat cells (T-cell lymphoma cell line) have been used for the experiment. MTT assay for cell viability revealed a dose-dependent decrease in Jurkat cell proliferation, observed at 24 h of harpin$_{Pss}$ treatment with an optimum decrease in cell proliferation at a concentration of 40 µM (1.5 mg/ml) determined to be the IC_{50}. Phase contrast microscopy of cells treated with harpin$_{Pss}$ showed changes in cell shape, membrane blebbing resulting in cell burst and release of small cell fragments called as the apoptotic bodies. Cell cycle analysis of Jurkat cells treated with harpin$_{Pss}$ showed an arrest or prominent increase in the G0/G1 peak from 12 h to 24 h of treatment, compared with the untreated control cells. Genomic DNA analysis on a conventional agarose gel electrophoresis revealed genomic DNA fragmentation or laddering in cells treated with harpin$_{Pss}$ which is considered as the hall mark feature of apoptosis. Harpin$_{Pss}$ treatment in Jurkat cells showed a time dependent release of Cytochrome c and also an alteration in the Bcl-2/Bax ratio further confirming apoptotic cell death during harpin$_{Pss}$ treatment. Thus harpin$_{Pss}$-treatment on animal cells proved to be effective causing cell death in Jurkat cell lines.

5.4 Bio-physical studies on harpin$_{Pss}$

The *hrpZ* gene (1.02 kb) encoding full length harpin$_{Pss}$ was PCR amplified and cloned under *Nde I* and *Xho I* sites of pET 28a vector. The *E. coli* BL 21 (Rosettae) strain was then transformed with the pET 28a-*hrpZ* clone and induced with 1 mM IPTG for harpin$_{Pss}$ production. Harpin$_{Pss}$ was purified from the protein extract using Ni-NTA resin to obtain pure protein which could be seen as a single band on a 12% SDS gel. Harpin is a polydispersed, multimeric protein which resolves as a smear on an 8% native PAGE. MALDI-TOF analysis of harpin$_{Pss}$ showed a singly charged fundamental peak at a mass of 38,138 Da and two other major peaks representing a double charge at 19,070 Da and triple charge at 12,715 Da.

CD spectrum of native harpin$_{Pss}$ at far UV region (240-190 nm) was determined, which reveals that harpin$_{Pss}$ has 51.5% α-helix, 8.6% β-sheets, 15.6% and 25.8% turns and

random coils. Temperature-dependent CD shows that at high temperature the α-helical content of harpin$_{Pss}$ is reduced, whereas the β-sheet structure increases with temperature.

DSC scan for the thermal stability of harpin$_{Pss}$ shows the presence of three transitions at a temperature of 50.0 °C, 59.9 °C and 93.6 °C, respectively indicating that the protein initially unfolds from a higher oligomeric state to a lower oligomeric state or dimeric state followed by an unfolded dimeric state and then finally to an unfolded monomeric state. The whole thermal unfolding process is quite reversible as revealed by the reversible aggregation of harpin$_{Pss}$ shown on an 8% native PAGE.

DLS study of harpin$_{Pss}$ as a function of temperature shows that the hydrodynamic radius (R_h) of the protein decreases with increase in temperature as the partially unfolded dimeric protein may be converted to fully unfolded monomeric protein at higher temperatures. Congo red binding study shows that harpin$_{Pss}$ exhibits a blue shift, indicative of aggregative property but not amyloid nature. Atomic force microscopy of harpin$_{Pss}$ revealed the heterogeneity in size and shape among the aggregates indicating the polydispersed nature of this protein.

Amino acid sequence of harpin$_{Pss}$ showed high percentage (13.5%) of leucine residues in the protein. Two leucine-zipper like motifs were identified, each at the N-terminal and C-terminal regions of the protein which might be responsible for the dimeric or oligomeric status as seen in many α-helical proteins. Leucine zipper motifs are protein-protein dimerization/oligomerization motifs consisting of heptad repeats of leucine or hydrophobic amino acid residues such as isoleucine, phenylalanine, alanine, methionine and valine which may result in the formation of coiled-coil structure and also contributes for the thermal stability of the protein. Analysis of the primary structure of harpin$_{Pss}$ and other harpins from different bacterial species also showed the existence of leucine-zipper like motifs in this class of proteins. Leucine- zippers may have the potential to participate in the binding of the protein and destabilization of the target cell membrane.

5.5 Major findings of the work

- Oxidative burst seems to be the major factor and thus harpin$_{Pss}$-induced YCD is 'ROS' mediated.
- Yeast cells expressing harpin$_{Pss}$ become respiratory deficient with loss of mitochondrial potential.
- Elevation of metacaspase activity has been reported for the first time in this form of cell death induced by harpin$_{Pss}$ expression.
- Harpin$_{Pss}$-induced YCD seems to be mitochondria-dependent resulting in the paralyses of electron transport chain events leading to cell death.
- Harpin$_{Pss}$ induces apoptosis in Jurkat cell lines.
- CD studies revealed that harpin$_{Pss}$ is more α-helical in nature and rise in temperature results in the decrease of α helix and increase in β sheets.
- DSC studies revealed the thermal dissociation and thermal stability of the protein.
- Congo red binding and AFM studies showed the high aggregation property and polydispersed nature of harpin$_{Pss.}$
- At least two leucine-zipper like motifs were identified in harpins which can in principle nucleate oligomerization.
- Extensive crystallization trials resulted in micro crystalline precipitates and non-specific aggregation.

Abraham MC and Shaham S. (2004). Death without caspases, caspases without death. *Trends Cell Biol*.14: 184-193.

Abramovitch RB, Kim YJ, Chen S, Dickman MB and Martin GB. (2003). *Pseudomonas* type III effector AvrPtoB induces plant disease susceptibility by inhibition of host programmed cell death. *EMBO J.* 22: 60-69.

Adam AL, Pike S, Hoyos ME, Stone JM, Walker JC, Novacky A. (1997). Rapid and transient activation of a myelin basic protein kinase in tobacco leaves treated with harpin from *Erwinia amylovora*. *Plant Physiol*. 115: 853-861.

Ahmad M, Majerczak DR, Pike S, Hoyos ME, Novacky A, and Coplin DL. (2001). Biological activity of harpin produced by Pantoea stewartii subsp. stewartii. *Mol. Plant Microbe Interact*. 14: 1223-1234.

Ahn SH, Cheung WL, Hsu JY, Diaz RL, Smith MM, Allis CD (2005). Sterile 20 kinase phosphorylates histone H2B at serine10 during hydrogen peroxide-induced apoptosis in *Saccharomyces cerevisiae*. *Cell*. 120: 25–36.

Ahn SH, Diaz RL, Grunstein M, Allis CD (2006). Histone H2B deacetylation at lysine 11 is required for yeast apoptosis induced by phosphorylation of H2B at Serine 10. *Mol. Cell* 24: 211–220.

Alfano JR, and Collmer A. (2004). Type III secretion system effector proteins: double agents in bacterial disease and plant defense. *Ann. Rev. Phytopathol*. 42: 385-414.

Alfano JR, Charkowski AO, Deng W, Badel JL, Petnicki-Ocwieja T, van Dijk K and Collmer A. (2000). The *Pseudomonas syringae* Hrp pathogenicity island has a tripartite mosaic structure composed of a cluster of type III secretions genes bounded by exchangeable effector and conserved effector loci that contribute to parasitic fitness and pathogenicity in plants. *Proc. Natl. Acad. Sci. USA* 97: 4856-4861.

Alfano JR, Kim H-S, Delaney TP and Collmer A. (1997). Evidence that the *Pseudomonas syringae* pv. *syringae* hrp-linked hrmA gene encodes and Avr-like protein that acts in an hrp-dependent manner within tobacco cells. *Mol. Plant Microbe Interact*. 10: 580-588.

Alfano JR., Bauer DW, Milos TM, and Collmer A. (1996). Analysis of the role of *Pseudomonas syringae* pv. *syringae* HrpZ harpin in elicitation of the hypersensitive response in tobacco using functionally non-polar *hrpZ* deletion mutations, truncated *hrpZ* fragments, and *hrmA* mutations. *Mol. Microbiol*. 19: 715-728.

Alfano JR and Collmer A. (1996). Bacterial pathogens in plants: Life up against the wall. *Plant Cell*. 8: 1683-1698.

Ameisen JC. (1996). The origin of progammed cell death. *Science* 272: 1278-1279.

Amirsadeghi S, Robson CA, and Vanlerberghe GC. (2007). The role of the mitochondrion in plant responses to biotic stress. *Physiologia Plantarum*. 129: 253-266.

Andriyka LP, Leslie WT, and Hans JV. (2002). Dynamic Light Scattering Study of Calmodulin-Target Peptide Complexes. *Biophys. J.* 83: 1455–1464.

Anfinsen, C. (1973). Principles that govern the folding of protein chains. *Science*. 181: 223–230.

Arlat M., Van Gijsegem F, Huet JC, Pernollet J C, and Boucher CA. (1994). PopA1, a protein which induces a hypersensitivity-like response on specific Petunia genotypes, is secreted via the Hrp pathway of Pseudomonas solanacearum. *EMBO J*. 13: 543–553.

Ashkenazi A and Dixit VM. (1998). Death receptors: signaling and modulation. *Science*. 281: 1305-1308.

Asthana N, Yadav SP, and Ghosh JK. (2004). Dissection of antibacterial and toxic activity of Melittin: a leucine zipper motif plays a crucial role in determining its hemolytic activity but not antibacterial activity. *J. Biol. Chem*. 279: 55042-55050.

Baek D, Nam J, Koo YD, Kim DH, Lee J, Jeong JC, Kwak SS, Chung WS, Lim CO, Bahk JD, Hong JC, Lee SY, Kawai-Yamada M, Uchimiya H and Yun DJ. (2004). Bax-induced cell death of Arabidopsis is meditated through reactive oxygen-dependent and -independent processes. *Plant Mol. Biol*. 56: 15-27.

Baker CJ, Orlandi EW, Mock NM. (1993). Harpin an elicitor of the hypersensitive response in tobacco caused by *Erwinia-amylovora* elicits active oxygen production in suspension cells. *Plant Physiol*. 102: 1341–1344.

Barone G, Catanzano F, Del Vecchio P, Giancola C, and Graziano G. (1995). Differential scanning calorimetry as a tool to study protein-ligand interactions. *Pure & Appl. Chem*. 67: 1867-1872.

Bauer DW, Wei ZM, Beer SV, and Collmer A. (1995). *Erwinia chrysanthemi* harpinEch: an elicitor of the hypersensitive response that contributes to soft-rot pathogenesis. *Mol. Plant Microbe Interact*. 8: 484–491.

Bernstein HB, Tucker SP, Kar SR, McPherson SA, McPherson DT, Dubay JW, Lebowitz J, Compans RW, and Hunter E. (1995). Oligomerization of the hydrophobic heptad repeat of gp41. *J. Virol*. 69: 2745-2750.

Boveris A, Cadenas E, and Stoppani AO. (1976). Role of ubiquinone in the mitochondrial generation of hydrogen peroxide. *Biochem. J*. 156: 435-444.

Bradford, MM. (1976). A Rapid and Sensitive Method for the Quantitation of Microgram Quantities of Protein Utilizing the Principle of Protein-Dye Binding. *Anal. Biochem.* 72: 248-254.

Bras M, Queenan B and Susin SA. (2005). Programmed cell death *via* mitochondria: different modes of dying. *Biochemistry* (Mosc). 70: 231-239.

Braun RJ, Zischka H, Madeo F, Eisenberg T, Wissing S, Büttner S, Engelhardt SM, Büringer D, and Ueffing M. (2006). Crucial Mitochondrial impairment upon CDC48 mutation in apoptotic yeast. *J. Biol. Chem.* 281: 25757–25767

Brennan RJ, Swoboda BE, and Schiestl RH. (1994). Oxidative mutagens induce intrachromosomal recombination in yeast. *Mutat. Res*. 308: 159-167.

Bretz JR, Mock NM, Charity JC, Zeyad S, Baker CJ and Hutcheson SW. (2003). A translocated preotin tyrosine phosphatase of *Pseudomonas syringae* pv. *tomato* DC3000 modulates plant defense response to infection. *Mol. Microbiol*. 49: 389-400.

Budinger GR, Duranteau J, Chandel NS, and Schumaker PT. (1998). Hibernation during hypoxia in Cardiomyocytes. Role of mitochondria as the O_2 sensor. *J. Biol. Chem*. 273: 3320-3326.

Buell CR, Joardar V, Lindeberg M Selengut J, Paulsen IT, Gwinn ML, Dodson RJ, Deboy RT, Durkin AS, Kolonay JR, Madupu R, Daugherty S, Brinkac L, Beanan MJ, Haft DH, Nelson WC, Davidsen T, Zafar N, Zhou L, Liu J, Yuan Q, Khouri H, Fedorova N, Tran B, Russell D, Berry K, Utterback T, Van Aken SE, Feldblyum TV, D'Ascenzo M, Deng WL, Ramos AR, Alfano JR, Cartinhour S, Chatterjee AK, Delaney TP, Lazarowitz SG, Martin GB, Schneider DJ, Tang X, Bender CL, White O, Fraser CM and Collmer A. (2003). The complete sequence of the *Arabidopsis* and tomato pathogen *Pseudomonas syringae* pv. *tomato* DC3000. *Proc. Natl. Acad. Sci. USA*. 100: 10181-10186.

Bunn H, Gu J, Huang L, and Park JW. (1998). Erythropoietin: a model system for studying oxygen-dependent gene regulation. *J. Exp. Biol*. 201: 1197-1201.

Bunn HF and Poyton RO. (1996). Oxygen sensing and molecular adaptation to hypoxia. *Physiol. Rev*. 76: 839-885.

Burke PV, Kwast KE, Everts F, and Poyton RO. (1998). A fermentor system for regulating oxygen at low concentrations in cultures of *Saccharomyces cerevisiae J. Appl. Environ. Microbiol*. 64: 1040-1044.

Burke PV, Raitt DC, Allen LA, Kellogg EA and Poyton RO. (1977). Effects of oxygen concentration on the expression of cytochrome c and cytochrome c oxidase genes in yeast. *J. Biol.Chem*. 272: 14705-14712.

Bursch W, Ellinger A, Gerner C, Frohwein U, and Schulte-Hermann R. (2000). Programmed Cell Death (PCD). Apoptosis, autophagic PCD, or others? *Ann. NY Acad. Sci.* 926: 1-12.

Buttner S, Eisenberg T, Carmona-Gutierrez D, Ruli D, Knauer H, Ruckenstuhl C, Sigrist C, Wissing S, Kollroser M, Frohlich K-U, Sigrist S, Madeo F. (2007). Endonuclease G regulates budding yeast life and death. *Mol. Cell*. 25: 233-246.

Cao H, Baldini RL, and Rahme LG. (2001). Common mechanisms for pathogens of plants and animals. *Ann. Rev. Phytopathol*. 39: 259-284.

Carr CM, and Kim PS (1993). A spring-loaded mechanism for the conformational change of influenza hemagglutinin. *Cell*. 73: 823-832.

Chandel NS, Budinger GR, Choe SH, and Schumacker PT. (1997). Cellular Respiration during hypoxia. Role of cytochrome oxidase as the oxygen sensor in hepatocytes. *J. Biol. Chem*. 272: 18808-18816.

Chandel NS, Budinger GS, and Schumacker PT. (1996). Molecular Oxygen Modulates Cytochrome *c* Oxidase Function. *J. Biol. Chem*. 271: 18672-18677.

Chandra D, Bratton SB, Person MD, Tian Y, Martin AG, Ayres M, Fearnhead HO, Gandhi V, and Tang DG. (2006) Intracellular nucleotides act as critical prosurvival factors by binding to cytochrome C and inhibiting apoptosome. *Cell*. 125: 1333-1346.

Chao DT, and Korsmeyer S. J. (1998). Bcl-2 family: regulators of cell death. *Annu. Rev. Immunol*. 16: 395-419.

Chattopadhyay A, Chiang CW, and Yang E. (2001). BAD/Bcl-X_L heterodimerization leads to bypass of G0/G1 arrest. *Oncogene.* 20: 4507-4518.

Chen CH, Lin HJ, and Feng TY. (1998). An amphipathic protein from sweet pepper can dissociate harpin$_{Pss}$multimeric forms and intensify the harpin$_{Pss}$-mediated hypersensitive response. *Physiol. Mol. Plant Pathol*. 52: 139-149.

Cheng EH, Wei MC, Weiler S, Flavell RA, Mak TW, Lindsten T, and Korsmeyer SJ. (2001). Bcl-2, Bcl-X_L sequester BH3 domain-only molecules preventing Bax and Bak mediated mitochondrial apoptosis. *Mol. Cell.* 8: 705-711.

Cheung WL, Turner FB, Krishnamoorthy T, Wolner B, Ahn S-H, Foley M, Dorsey JA, Peterson CL, Berger SL, Allis CD. (2005). Phosphorylation of histone H4 serine 1 during

DNA damage requires casein kinase II in *Saccharomyces cerevisiae*. *Curr. Biol* 15: 656–660.

Chipuk JE and Green DR. (2004). Cytoplasmic p53: Bax and forward. *Cell Cycle*. 3: 429-431.

Clantin B, Tricot C, Lonhienne T, Stalon V, and Villeret V. (2001). Probing the role of oligomerization in the high thermal stability of Pyrococcus furiosus ornithine carbamoyltransferase by site-specific mutants. *Eur. J. Biochem*. 268: 3937-3942.

Clarke PG. (1990). Developmental cell death: morphological diversity and multiple mechanisms. *Anat. Embryol.* 181:195-213.

Coffeen WC and Wolpert TJ. (2004). Purification and characterization of serine proteases that exhibit caspase-like activity and are associated with programmed cell death in *Avena sativa*. *Plant Cell* 16: 857-873

Collmer A, Badel JL, Charkowski AO, Deng W-L, Fouts DE, Ramos AR, Rehm AH, Anderson DM, Schneewind O, van Dijk K, and Alfano JR. (2000). *Pseudomonas syringae* Hrp type III secretion system and effector proteins. *Proc. Natl Acad. Sci. USA.* 97: 8770-8777.

Collmer A, Lindeberg M, Petnicki-Ocwieja T, Schneider D and Alfano JR. (2002). Genomic mining type III secretion system effectors in *Pseudomonas syringae* yields new picks for all TTSS prospectors. *Trends Microbiol*. 10: 462-470.

Conway JF, and Parry DAD. (1990). Structural features in the heptad substructure and longer range repeats of two-stranded α-fibrous proteins. *Int. J. Biol. Macromol*. 12: 328-334.

Cornelis G and van Gijsegem F. (2000). Assembly and function of type III secretion systems. *Annu Rev. Microbiol.* 54: 734-774.

Cornelis GR, Boland A, Boyd AP, Geuijen C, Iriarte M, Neyt C, Sory MP and Stainier I. (1998). The virulence plasmid of *Yersinia,* an antihost genome. *Microbiol Mol. Biol. Rev.* 62: 1315-1352.

Cornelis GR and Wolf-Watz H. (1997). The *Yersinia* Yop virulon: a bacterial system for subverting Eukaryotic cells. *Mol. Microbiol.* 23: 861-867.

Dangl JL and Jones JD. (2001). Plant pathogens and integrated defense responses to infection. *Nature*. 411: 826-833.

Dangl JL, Dietrich RA, and Richberg MH. 1996. Death don't have no mercy. *Plant Cell* 8: 1793-801.

Danial NN and Korsmeyer SJ. (2004). Cell death: critical control points. *Cell*. 116: 205-219.

Danon A, Rotari VI, Gordon A, Mailhac N and Gallois P. (2004). Ultraviolet-C overexposure induces programmed cell death in Arabidopsis, which is mediated by caspase-like activities and which can be suppressed by caspase inhibitors, p35 and defender against apoptotic death. *J. Biol. Chem*. 279: 779-787.

Danon A and Gallois P. (1998). UV-C radiation induces apoptotic-like changes in *Arabidopsis thaliana*. *FEBS Lett*. 437: 131-136.

Daum G, Bohni PC, and Schatz G. (1982). Import of proteins into mitochondria. *J. Biol. Chem*. 257, 13028-13033.

Degterev A, Boyce M, and Yuan J. (2003). A decade of caspases. *Oncogene*. 22: 8543-8567.

Del Pozo O, and Lam E. (2003). Expression of the baculovirus p35 protein in tobacco affects cell death progression and compromises N gene mediated disease resistance response to TMV. *Mol. Plant. Microbe. Inter*. 16: 485-494.

Desagher S, Osen-Sand A, Nichols A, Eskes R, Montessuit S, Lauper S, Maundrell, K, Antonsson B, Martinou JC. (1999). Bid-induced conformational change of Bax is responsible for mitochondrial cytochrome c release during apoptosis. *J. Cell Biol.* 144: 891-901.

Desikan R, Hancock JT, Coffey M.J, Neill SJ. (1996). Generation of active oxygen in elicited cells of *Arabidopsis thaliana* is mediated by a NADPH oxidase-like enzyme. *FEBS Letters*. 382: 213-217.

Djavaheri-Mergny M, Wietzerbin J, Besancon F. (2003). 2-Methoxyestradiol induces apoptosis in Ewing sarcoma cells through mitochondrial hydrogen peroxide production. *Oncogene*. 22: 2558–67.

Dodds PN, Lawrence GJ, Catanzariti A-M, Teh T, Wang C-I.A, Ayliffe MA, Kobe B, Ellis JG. (2006). Direct protein interaction underlies gene-for-gene specificity and coevolution of the flax resistance genes and flax rust avirulence genes. *Proc. Natl Acad. Sci*. 103: 8888-8893.

Dong H, Delaney TP, Bauer DW, and Beer SV. (1999). Harpin induces disease resistance in Arabidopsis through the systemic acquired resistance pathway mediated by salicylic acid and the *NIM1* gene. *Plant J*. 20: 207-215.

Dragan AI, and Privalov PL. (2002). Unfolding of a Leucine zipper is not a Simple Two-state Transition. *J. Mol. Biol.* 321: 891-908.

Duranteau J, Chandel NS, Kulisz A, Shao Z, and Schumacker PT. (1998). Intracellular signaling by reactive oxygen species during hypoxia in cardiomyocytes. *J. Biol. Chem.* 273: 11619-11624.

Enoch T, Gould KL, Nurse P. (1991). Mitotic checkpoint control in fission yeast, Cold Spring Harbor Symp. *Quant. Biol*. 56: 408–416.

Eskes R, Desagher S, Antonsson B, and Martinou JC. (2000). Bid induces the oligomerization and insertion of Bax into the outer mitochondrial membrane. *Mol. Cell Biol*. 20: 929-935.

Evan G, Wyllie A, Gilbert C, Littlewood TLH, Brooks M, Waters C, Penn L, Hancock D. (1992). Induction of apoptosis in fibroblasts by c-myc protein. *Cell.* 63: 119–128.

Fabrizio P, Battistella L, Vardavas R, Gattazzo C, Liou L-L. (2004). Superoxide is a mediator of an altruistic aging program in *Saccharomyces cerevisiae*. *J. Cell Biol.* 166: 1055–1067.

Fahrenkrog B, Sauder U, Aebi U. (2004). The S. cerevisiae HtrAlike protein Nma111p is a nuclear serine protease that mediates yeast apoptosis. *J. Cell Sci.* 117:115–126

Ferri KF and Kroemer G. (2001). Organelle-specific initiation of cell death pathways. *Nat. Cell Biol*. 3: 255-63.

Flattery-O'Brien JA, and Dawes IW. (1998). Hydrogen peroxide causes RAD9-dependent cell cycle arrest in G2 in *Saccharomyces cerevisiae* where as menadione causes G1 arrest independent of RAD9 function. *J. Biol Chem.* 273: 8564-8571.

Fleury C, Pampin M, Tarze A, and Mignotte B. (2002). Yeast as a model to study apoptosis? *Biosci. Rep*. 22: 59-79.

Formigli L, Papucci L, Tani A, Schiavone N, Tempestini A, Orlandini GE, Capaccioli S and Orlandini SZ. (2000). Aponecrosis: morphological and biochemical exploration of a syncretic process of cell death sharing apoptosis and necrosis. *J. Cell Phys*. 182: 41-49.

Fraser A, and James C. 1998. Fermenting debate: do yeast undergo apoptosis? *Trends in Cell Biol.* 8: 219-221.

Frohlich KU and Madeo F. (2000). Apoptosis in yeast: a monocellular organism exhibits altruistic behaviour. *FEBS Letters*. 473: 6-9.

Galan JE and Collmer A. (1999). Type III secretion machines: bacterial devices for protein delivery into host cells. *Science.* 284: 1322-1328.

Garmier M, Dutilleul C, Mathieu C, Chetrit P, Boccara M, and Paepe RD. (2002). Changes in antioxidant expression and harpin-induced hypersensitive response in a *Nicotiana sylvestris* mitochondrial mutant. *Plant Physiol.Biochem*. 40: 561-566.

Gaussand G, (2007). Programmed cell death in plants and caspase-like activities. PhD thesis, University of Leiden.

Gething, M. J. and Sambrook, J. (1992). Protein folding in the cell. *Nature*. 355: 35-45.

Ghosh JK, Ovadia, M. & Shai, Y. (1997). A leucine zipper motif in the ectodomain of Sendai virus fusion protein assembles in solution and in membranes and specifically binds biologically-active peptides and the virus. *Biochemistry*. 36: 15451-15462.

Goldstein JC, Waterhouse N J, Juin P, Evan G I, and Green DR. (2000). The coordinate release of cytochrome c during apoptosis is rapid, complete and kinetically invariant. *Nat. Cell Biol*. 2: 156-162.

Gonzalez Jr, L, Plecs JJ. and Alber T. (1996). An engineered allosteric switch in leucine-zipper oligomerization. *Nat. Struct. Biol*. 3: 510-515.

Gozuacik D and Kimchi A. (2004). Autophagy as a cell death and tumor suppressor mechanism. *Oncogene*. 23: 2891-2906.

Grant CM, Perrone G, and Dawes IW. (1998). Glutathione and catalase provide overlapping defenses for protection against hydrogen peroxide in the yeast *Saccharomyces cerevisiae*. *Biochem. Biophys. Res. Commun*. 253: 893-898.

Grant M and Mansfield J. (1999). Early events in host-pathogen interactions. *Curr. Opin. Plant Biol*. 2: 312-319

Green DR, and Reed JC. (1998). Mitochondria and apoptosis. *Science*. 281: 1309-1312.

Green DR, Kroemer G. (2004). The pathophysiology of mitochondrial cell death. *Science*. 305: 626-629.

Greenberg JT, Guo AA, Klessig DF, Ausubel FM. (1994). Programmed cell death in plants: a pathogen-triggered response activated with multiple defense functions. *Cell*. 77: 551-563.

Greenhalf W, Stephan C, and Chaudhuri B. (1996). Role of mitochondria and C-terminal membrane anchor of Bcl-2 in *bax*-induced growth arrest and mortality in *Saccharomyces cerevisiae*. *FEBS Letters*. 380: 169-175

Grushcow JM, Holzen TM, Park KJ, Weinert T, Lichten M, Bishop DK. (1999). *Saccharomyces cerevisiae* checkpoint genes *MEC1*, *RAD17* and *RAD24* are required for normal meiotic recombination partner choice. *Genetics* 153: 607–620.

Guaragnella N, Pereira C, Sousa MJ, Antonacci L, Passarella S, Corte-Real M, Marra E, Giannattasio S. (2006). YCA1 participates in the acetic acid induced yeast programmed cell death also in a manner unrelated to its caspase-like activity. *FEBS.* 580: 6880-6884.

Gudz TI, Tserng KY, and Hopel CL. (1997). Direct inhibition of mitochondrial respiratory chain complex III by cell-permeable ceramide. *J. Biol.Chem*. 272: 24154-24158.

Guttman DS, Vinatzer BA, Sarkar SF, Ranall MV, Kettler G, and Greenberg JT. (2002). A functional screen for the type III (Hrp) secretome of the plant pathogen *Pseudomonas syringae*. *Science.* 295: 1722-1726.

Ha KS, Kim KM, Kwon YG, Bai SK, Nam WD, Yoo YM, Kim PK, Chung HT. (2003). Nitric oxide prevents 6-hydroxydopamine-induced apoptosis in PC12 cells through cGMP-dependent PI3 kinase/Akt activation. *FASEB J*. 17: 1036–47.

Hatsugai N, Kuroyanagi M, Yamada K, Meshi T, Tsuda S, Kondo M, Nishimura M and Hara-Nishimura I. (2004). A plant vacuolar protease, VPE, mediates virus-induced hypersensitive cell death. *Science*. 305: 855-858.

He S-Y. (1998). Type III protein secretion systems in plant and animal pathogenic bacteria. *Ann. Rev. Phytopathol.* 36: 363-392.

He Sh.Y. (1996). Elicitation of hypersensitive response by bacteria. *Plant Physiol*. 112: 865-869.

He S-Y, Huang H-C, and Collmer A. (1993). *Pseudomonas syringae* pv. *syringae* harpin$_{pss}$ a protein that is secreted via the Hrp-pathway and elicits the hypersensitive response in plants. *Cell.* 73: 1255-1266

Hengartner MO. (2000). The biochemistry of apoptosis. *Nature*. 407: 770-776.

Herker E, Jungwirth H, Lehmann KA, Maldener C, Frohlich K-U. (2004). Chronological aging leads to apoptosis in yeast. *J. Cell Biol.* 164: 501–507

Higuchi M, Proske RJ, and Yeh ET. (1998). Inhibition of mitochondrial respiratory chain complex I by TNF results in cytochrome c release, membrane permeability transition and apoptosis. *Oncogene*. 17: 2515-2524.

Hirasawa K, Amano T, and Shioi Y. (2005). Effects of scavengers for active oxygen species on cell death by cryptogein. *Phytochemistry*. 66: 463-468.

Hissin PJ, and Hilf R. (1976). A fluorometric method for determination of oxidized and reduced glutathione in tissues. *Anal. Biochem*. 74: 214-226.

Hochachka PW, Buck LT, Doll CJ, Land SC. (1996). Unifying theory of hypoxia tolerance: Molecular/metabolic defense and rescue mechanisms for surviving oxygen lack. *Proc. Natl. Acad. Sci*. USA 93: 9493-9498.

Hoeberichts FA and Woltering EJ. (2003). Multiple mediators of plant programmed cell death: interplay of conserved cell death mechanisms and plant-specific regulators. *BioEssay*. 25: 47-57.

Hostanska K, Vuong V, Rocha S, Soengas MS, Glanzmann C, Saller R, Bodis S, Pruschy M. (2003). Recombinant mistletoe lectin induces p53-independent apoptosis in tumor cells and cooperates with ionizing radiation. *Br. J. Cancer*. 88: 1785–1792.

Hoyos ME, Stanley CM, He S-Y, Pike S, Pu XA, and Novacky A. (1996). The interaction of $harpin_{pss}$ with plant cell walls. *Mol. Plant Microbe Inter*. 9: 608-616

Hsu YT, and Youle RJ. (1998) Bax in murine thymus is a soluble monomeric protein that displays differential detergent- induced conformations. *J. Biol. Chem*. 273: 10777-10783.

Hueck CJ. (1998). Type III protein secretion systems in bacterial pathogens of animals and plants. *Microbiol. Mol. Biol. Rev*. 62: 379-433.

Ink B, Zornig M, Baum B, Hajibagheri N, James C, Chittenden T, Evan G. (1997). Human bak induces cell death in *Shizosaccharomyces pombe* with morphological changes similar to those with apoptosis in mammalian cells. *Mol. Cell Biol.* 17: 2468-2474.

Jakubowski W, Bilinski T, Bartosz G. (2000). Oxidative stress during aging of stationary cultures of the yeast *Saccharomyces cerevisiae*. *Free Radic. Biol. Med.* 28: 659-664.

Jamir Y, Guo M, Oh H-S, Petnicki-Ocwieja T, Chen S, Tang X, Dickman MB, Collmer A, and Alfano JR. (2004). Identification of *Pseudomonas syringae* type III effectors that can suppress programmed cell death in plants and yeast. *Plant J.* 37: 554-565.

Jin C and Reed JC. (2002). Yeast and apoptosis. *Nat. Rev, Mol. Cell Biol*. 3: 453-459.

Jin Z and El-Deiry WS. (2005). Overview of cell death signaling pathways. *Cancer Biol. Ther.* 4: 139-163.

Karbowski M, Arnoult D, Chen H, Chan DC, Smith CL, and Youle RJ. (2004). Quantitation of mitochondrial dynamics by photlabelling of individual organelles shows

that mitochondrial fusion is blocked during the Bax activation phase of apoptosis. *J. Cell Biol.* 164: 493-499.

Kerr JF, Wyllie AH and Currie AR. (1972). Apoptosis: a basic biological phenomenon with wide-ranging implications in tissue kinetics. *Br. J. Cancer*. 26: 239-257

Khan MA, Chock PB, Stadtman ER. (2005). Knockout of caspase-like gene, *YCA1*,abrogates apoptosis and elevates oxidized proteins in *Saccharomyces cerevisiae*. *Proc. Natl. Acad. Sci. USA.* 102: 17326-17331.

Khodairy FA, Fotou F, Sheldrick KS, Griffiths DJF, Lehmann AR, Carr AM. (1994). Identification and characterization of new elements involved in checkpoint controls in fission yeast. *Mol. Biol.Cell*. 5: 147–160.

Kim JF, and Beer SV. (1998). HrpW of Erwinia amylovora, a new Harpin that contains a domain homologous to Pectate Lyases of a distinct class. *J. Bacteriol*. 180: 5203-5210.

Kim JS, He L, and Lemasters JJ. (2003). Mitochondrial permeability transition: a common pathway to necrosis and apoptosis. *Biochem. Biophys. Res. Commun*. 304: 463-470.

Kim R (2005). Recent advances in understanding the cell death pathways activated by anticancer therapy. *Cancer*. 103: 1551-1560.

Kim JG, Park BK, Yoo CH, Jeon E, Oh J, & Hwang I. (2003). Characterization of the *Xanthomonas axonopodis* pv. *Glycines* Hrp pathogenicity island. *J. Bacteriol*, 185: 3155–3166.

King KL, and Cidlowski JA. (1998). Cell cycle regulation and apoptosis. *Ann. Rev Physiol*. 60: 601–17.

Klunk, WE, Jacob, RF. and Mason, RP. (1999). Quantifying amyloid by Congo red spectral shift assay. *Methods Enzymol*. 309: 285-305.

Knudson CM, Johnson GM, Lin Y, and Korsmeyer SJ. (2001). Bax accelerates tumorigenesis in P^{53} deficient mice. *Cancer Res*. 61: 659-665.

Kohlhoff, M., Dahm, A. & Hensel, R. (1996). Tetrameric triosephosphate isomerase from hyperthermophilic Archaea. *FEBS Lett*. 383: 245-250.

Komatsu K, Hopkins KM, Lieberman HB, Wang HG. (2000). *Schizosaccharomyces pombe* Rad9 contains a BH3-like region and interacts with the anti-apoptotic protein Bcl-2. *FEBS Lett*. 481: 122-126.

Krause M, and Durner J. (2004). Harpin inactivates mitochondria in *Arabidopsis* suspension cells. *Mol. Plant Microbe Inter.* 17: 131-139.

Kroemer G and Martin SJ. (2005). Caspase-independent cell death. *Nat Med*. 11: 725-730.

Kuriyama H and Fukuda H. (2002). Developmental programmed cell death in plants. *Curr. Opin. Plant Biol*. 5: 568-573.

Kwast KE, Burke PV and Poyton RO. (1998). Oxygen sensing and the transcriptional regulation of oxygen-responsive genes in yeast. *J. Exp. Biol*. 201: 1177-1195.

Lam E, del Pozo O and Pontier D. (1999). Baxing in the hypersensitive response. *Trends Plant Sci.* 4: 419-421.

Lam E., Kato N., Lawton M. (2001). Programmed cell death, mitochondria and the plant hypersensitive response. *Nature*. 411A: 848-853.

Landschulz WH, Johnson PF, and McKnight, SL. (1988). The leucine zipper: a hypothetical structure common to a new class of DNA-binding proteins. *Science*. 240: 1759-1764.

Laun P, Pichova A, Madeo F, Fuchs J, Ellinger A, Kohlwein S, Dawes I, Frohlich KU. (2001). Aged mother cells of *Saccharomyces cerevisiae* show markers of oxidative stress and apoptosis. *Mol. Microbiol*. 39: 1166-1173.

Lawen A. (2003). Apoptosis- an introduction. *Bioessays*. 25: 888-896.

Lee J, Klusener B, Tsiamis G, Stevens C, Neyt C, Tampakaki AP, Panopoulos NJ, Noller J, Weiler EW, Cornelis GR, Mansfield JW, Nurnberger T. (2001). $HrpZ_{Psph}$ from the plant pathogen *Pseudomonas syringae* pv. *phaseolicola* binds to lipid bilayers and forms an ion-conducting pore *in vitro*. *Proc. Natl. Acad. Sci*. USA. 98: 289-294.

Lee REC, Puente LG, Kaern M, and Megeney LA. (2008). A non-death role of the yeast metacaspase: Yca1p alters cell cycle dynamics. *PLoS ONE*. 3: 1-8.

Leist M, Single B, Castoldi AF, Kuhnle S, and Nicotera P. (1997). Intracellular adenosine triphosphate (ATP) concentration: a switch in the decision between apoptosis and necrosis. *J. Exp. Med*. 185: 1481-1486.

Leist M and Jaattela M. (2001). Four deaths and a funeral: from caspases to alternative mechanisms. *Nature Rev. Mol. Cell Biol*. 2: 589-598.

Levine B and Klionsky DJ. (2004). Development by self-digestion: molecular mechanisms and biological functions of autophagy. *Dev. Cell*. 6: 463-477.

Li J, Brieher WM, Scimone ML, Kang SJ, Zhu H, Yin H, Andrian UHV, Mitchison T, and Yuan J. (2007). Caspase-11 regulates cell migration by promoting Aip1-Cofilin-mediated actin depolymerization. *Nat Cell Biol.* 9: 276-286

Li P, Nijhawan D, Budihardjo I, Srinivasula SM, Ahmad M, Alnemri ES and Wang X. (1997). Cytochrome c and dATP-dependent formation of Apaf-1/caspase-9 complex initiates an apoptotic protease cascade. *Cell*. 91: 479-489.

Lindgren PB (1997). The role of *hrp* genes during plant-bacterial interactions. *Ann. Rev. Phytopathol* 35: 129-152.

Lindsten T, Ross A. J, King A, Zong W, Rathmell J. C, Shiels H. A. et al. (2000). The combined functions of proapoptotic Bcl-2 family members Bak and Bax are essential for normal development of multiple tissues. *Mol. Cell.* 6: 1389-1399.

Liu Y, Schiff M, Czymmek K, Talloczy Z, Levine B and Dinesh-Kumar SP. (2005). Autophagy regulates programmed cell death during the plant innate immune response. *Cell*. 121: 567-577.

Lobley A and Wallace BA. (2001). DICHROWEB: a website for the analysis of protein secondary structure from circular dichroism spectra, *Biophys. J*. 80: 373a. (www.cryst.bbk.ac.uk/cdweb/html)

Lockshin RA and Zakeri Z. (2004). Apoptosis, autophagy, and more. *Int. J. Biochem Cell Biol*. 36: 2405-2419.

Longhese MP, Foiani M, Muzi-Falconi M, Lucchini G, and Plevani P. (1998). DNA damage check point in budding yeast. *EMBO J*. 17: 5525-5528.

Ludovico P, Rodrigues F, Almeida A, Silva MT, Barrientos A, and Corte- Real M. (2002). Cytochrome c Release and Mitochondria involvement in programmed cell death induced by acetic acid in *Saccharomyces cerevisiae*. *Mol. Biol. cell*. 13: 2598-2606.

Ludovico P, Sansonetty F, and Corte-Real M. (2001). Assessment of mitochondrial membrane potential in yeast cell populations by flow cytometry. *Microbiology*. 147: 3335-3343.

Lupas A, Van Dyke M, and Stock J. (1991). Predicting coiled coils from protein sequences. *Science*. 252: 1162-1164.

Madeo F, Frohlich E, and Frohlich KU (1997). A yeast mutant showing diagnostic markers of early and late apoptosis. *J Cell Biol.* 139:729–734.

Madeo F, Frohlich E, Ligr M, Grey M, Sigrist SJ, Wolf DH and Frohlich K-U. (1999). Oxygen stress: a regulator of apoptosis in yeast. *J. Cell Biol*. 145: 757-767.

Madeo F, Herker E, Maldener C, Wissing S, Lachelt S, Herlan M, Lauber FK, Sigrist SJ, Wesselborg S, Frohlich K-U. (2002). A caspase-related protease regulates apoptosis in yeast. *Mol Cell.* 9: 911–917.

Makino T, Morii H, Shimizu T, Arisaka F, Kato Y, Nagata K, and Tanokura M. (2007). Reversible and irreversible coiled coils in the stalk domain of ncd motor protein. *Biochemistry*. 46: 9523-9532.

Manon S, Chaudhuri B, and Guerin M. (1997). Release of cytochrome c and decrease of cytochrome c oxidase in Bax-expressing yeast cells and prevention of these effects by coexpression of Bcl-x_L. *FEBS Lett*. 415: 29-32.

Martin SJ, Reutelingsperger CPM, McGahon AJ, Rader JA, Vanschie RCAA, LaFace DM, Green DR. (1995). Early redistribution of plasma membrane phosphatidylserine is a general feature of apoptosis regardless of the initiating stimulus: inhibition by overexpression of Bcl-2 and Abl. *J. Exp. Med*. 182: 1545-1556.

Meier P, Finch A, and Evan G. (2000). Apoptosis in development. *Nature*. 407: 796-801.

Michel B, Proudfoot AE, Wallace CJ, and Bosshard HR. (1989). The cytochrome c oxidase-cytochrome c complex: spectroscopic analysis of conformational changes in the protein-protein interaction domain. *Biochemistry*. 28: 456-462.

Momoi T. (2004). Caspases involved in ER stress-mediated cell death. *J. Chem Neuroanat*. 28: 101-105.

Morrison C, Sonoda E, Takao N, Shinohara A, Yamamoto K, Takeda S. (2000). The controlling role of ATM in homologous recombinational repair of DNA damage, *EMBO J.* 19: 463–471.

Mukherjee A, Cui Y, Liu Y, and Chatterjee AK. (1997). Molecular characterization and expression of the *Erwinia carotovora hrpNEcc* gene, which encodes an elicitor of the hypersensitive reaction. *Mol Plant Microbe Interact*. 10: 462–471.

Muller F. L Liu Y, Van R. H. (2004). Complex III releases superoxide to both sides of the inner mitochondrial membrane. *J Biol Chem*. 279: 49064-49073.

Munkvold KR, Martin ME, Bronstein PA, Collmer A. (2008). A survey of the *Pseudomonas syringae* pv. *tomato* DC3000 type III secretion system effector repertoire reveals several effectors that are deleterious when expressed in *Saccharomyces cerevisiae*. *Mol. Plant Microbe Interact*. 21: 490-502.

Murray A, and Hunt T. (1993). *The Cell Cycle*. New York: Oxford Univ. Press. 251 pp.

Nakagawa T, Shimizu H, Link K, Koide A, Koide S, and Tamura A. (2002). Calorimetric dissection of thermal unfolding of OspA, a predominantly β-sheet protein containing a single-layer β -sheet. *J. Mol. Biol*. 323: 751-762.

Nechushtan A, Smith CL, Hsu YT, and Youle RJ. (1999). Conformation of the Bax c-terminus regulates subcellular location and cell death. *EMBO J*. 18: 2330-2341.

Nicotera P, Leist M, and Ferrando-May E. (1998). Intracellular ATP, a switch in the decision between apoptosis and necrosis. *Toxicol Lett*. 102: 139-142

Oh J, Kim J, Jean E, Yoo C, Moon JS, Rhee S, and Hwang I. (2007). Amyloidogenesis of Type III-dependent Harpins from Plant Pathogenic Bacteria. *J. Biol. Chem.* 282: 13601-13609.

O'Shea EK, Rutkowski R, and Kim PS. (1989). Evidence that the leucine zipper is a coiled coil. *Science*. 243: 538-542.

Ott M, Robertson JD, Gogvadze V, Zhivotovsky B, and Orrenius S. (2002). Cytochrome c release from mitochondria proceeds by a two step process. *Proc. Natl. Acad. Sci.* USA 99: 1259-1263.

Pavlov EV, Priault M, Pietkiewicz D, Cheng EHY, Antonsson B, Manon S, Korsmeyer SJ, Mannella CA, Kinnally KW. (2001). A novel high conductance channel of mitochondria linked to apoptosis in mammalian cells and Bax expression in yeast. *J. Cell. Biol*. 155: 725-731.

Pennell RI and Lamb C. (1997). Programmed cell death in plants. *Plant Cell* 9: 1157-1168.

Pereira C, Camougrand N, Manon S, Sousa MJ, and Corte-Real M. (2007). ADP/ATP carrier is required for mitochondrial outer membrane permeabilization and cytochrome *c* release in yeast apoptosis. *Mol Microbiol*. 66: 571-582.

Perfettini JL, Roumier T, and Kroemer G. (2005). Mitochondrial fusion and fission in the control of apoptosis. *Trends Cell Biol.* 15: 179-183.

Pike, SM, Adam AL, Pu X.-A, Hoyos ME, Laby R, Beer SV, and Novacky A. (1998). Effects *of Erwinia amylovora* harpin on tobacco leaf cell membranes are related to leaf necrosis and electrolyte leakage and distinct from perturbations caused by inoculated *E. amylovora*. *Physiol. Mol. Plant Pathol.* 53: 39-60.

Plomp PJ, Gordon PB, Meijer AJ, Hoyvik H and Seglen PO. (1989) Energy dependence of different steps in the autophagic-lysosomal pathway. *J. Biol. Chem*. 264: 6699-6704.

Podile AR, Lin H-J, Stainforth V, Sripriya P, Chen LFO, and Feng T-y. (2001). Conditional expression of harpin$_{pss}$ causes yeast cell death that shares features of cell death pathway with hapin$_{pss}$-mediated plant hypersensitive response (HR). *Physiol. Mol. Plant Pathol*. 58: 267-276.

Popham P, Pike S, and Novacky A. (1995). The effect of harpin from *Erwinia amylovora* on the plasmalemma of suspension cultured tobacco cells. *Physiol. Mol. Plant Pathol.* 47: 39-50.

Poyton RO and McEwen JE. (1996). Cross talk between nuclear and mitochondrial genomes. *Annu Rev. Biochem*. 65: 563-607.

Pullman M. E., Penefsky H. S., Datta A., and Racker E. (1960). Partial resolution of enzymes catalyzing oxidative phosphorylation. *J. Biol. Chem*. 235: 3322-3329.

Racape J, Belbahri L, Engelhardt S, Lacombe, B, Lee J, Lochman J, Marais A, Nicole, M, Nurnberger, T, Parlange F, Puverel S, and Keller H. (2005). Ca2+-dependent lipid binding and membrane integration of PopA, a harpin-like elicitor of the hypersensitive response in tobacco. *Mol. Microbiol.* 58: 1406–1420.

Rajagopalan S, and Balasubrmanian MK. (1999). *S. pombe* Pbh1p: an inhibitor of apoptosis domain containing protein is essential for chromosome segregation. *FEBS Lett*. 460: 187-190.

Ramstein J, Hervouet N, Coste F, Zelwer C, Oberto J, and Castaing B. (2003). Evidence of a thermal unfolding dimeric intermediate for the *Escherichia coli* histone-like HU proteins: thermodynamics and structure. *J. Mol. Biol.* 331: 101-121.

Ratcliffe P, Rourke J, and Maxwell P. (1998). Oxygen sensing, hypoxia-inducible factor-1 and the regulation of mammalian gene expression. *J. Exp. Biol*. 201: 1153-1162.

Reitter JN, Sergel T, and Morrison TG. (1995). Mutational analysis of the leucine zipper motif in the newcastle disease virus fusion Protein. *J. Virol.*, 69, 5995–6004.

Rep M and Grivell LA. (1996). The role of protein degradation in mitochondrial function and biogenesis. *Curr. Genet*. 30: 367-380.

Riedl SJ and Shi Y. (2004). Molecular mechanisms of caspase regulation during apoptosis. *Nat. Rev. Mol. Cell Biol*. 5: 897-907.

Roucou X, Prescott M, Decenish RJ, Nagley P. (2000). A cytchrome c-GFP fusion is not released from mitochondria into the cytoplasm upon expression of Bax in yeast cells. *EMBO J*. 13**:** 964-972.

Rumsey WL, Schlosser C, Juutinen EM, Robiolio M and Wilson DF. (1990). Cellular energetics and the oxygen dependence of respiration in cardiac myocytes isolated from adult rat. *J. Biol. Chem*. 265: 15392-15399.

Sambrook J, Frotsch CF, and Maniatis T. Molecular cloning. Plain view: Coldspring Harbour. (1989).

Scaife JF. (1996). The effect of lethal doses of x-irradiation on the enzymatic activity of mitochondrial cytochrome c. *Can. J. Biochem*. 44: 433-448.

Scheel D. (1998). Resistance response physiology and signal transduction. *Curr. Opin. Plant Biol*. 1: 305–10.

Semenza GL, Roth PH, Fang HM, and Wang GL. (1994). Transcriptional regulation of genes encoding glycolytic enzymes by hypoxia-inducible factor 1. *J. Biol Chem*. 269: 23757-23763.

Severin FF, and Hyman AA (2002). Pheromone induces programmed cell death in *Saccharomyces cerevisiae*. *Curr. Biol.* 12: R233–R235.

Shi L, Nishioka W. K, Th'ng J, Bradbury, E. M, Litchfield D. W, and Greenberg A. H. (1994). Premature 34dc2 activation required for apoptosis. *Science.* 263: 1143-1145.

Shirogane T, Fukada T, Muller JM, Shima DT, Hibi M, Hirano T. (1999). Synergistic roles for Pim-1 and c-Myc in STAT3-mediated cell cycle progression and anti apoptosis. *Immunity* 11: 709–719.

Silva RD, Sotoca R, Johansson B, Ludovico P, Sansonetty F, Silva MT, Peinado JM, Corte-Real M. (2005). Hyperosmotic stress induces metacaspase- and mitochondria-dependent apoptosis in *Saccharomyces cerevisiae*. *Mol. Microbiol*. 58: 824-834.

Skulachev VP. (2006). Bioenergetic aspects of apoptosis, necrosis and mitoptosis. *Apoptosis*. 11: 473–485

Sottocasa, GL, Kuylenstierna B, Ernster L, and Bergstrand A. (1967). An electron-transport system associated with the outer membrane of liver mitochondria. *J. Cell Biol*. 32: 415–438.

Soylu S. (2006). Accumulation of cell wall bound phenolic compounds and phytoalexin in *Arabidopsis thaliana* leaves following inoculation with pathovars of *Pseudomonas syringae*. *Plant sci*. 170: 942-952.

Sripriya P, Vedantam LV, Podile AR. (2009). Involvement of mitochondria and metacaspase elevation in harpin$_{Pss}$-induced cell death of *Saccharomyces cerevisiae*. *J. Cell. Biochem*. DOI -10.1002/jcb.22217.

Steller H. (1995). Mechanisms and genes of cellular suicide. *Science*. 267: 1445-1449.

Strobel NE, Ji C, Gopalan S, Kuc JA, He SY. (1996). Induction of systemic acquired resistance in cucumber by *Pseudomonas syringae* pv. *syringae* 61 HrpZ-Pss protein. *Plant J.* 9: 431–439.

Tibbetts MD, Zheng L, and Lenardo MJ. (2003). The death effector domain protein family: regulators of cellular homeostasis. *Nat. Immunol*. 4: 404–409.

Turrens JF, and Boveris A. (1980). Generation of superoxide anion by the NADH dehydrogenase of bovine heart mitochondria. *Biochem J*. 191: 421-427.

Turrens JF, Alexandre A, Lehninger AL. (1985). Ubisemiquinone is the electron donor for superoxide formation by complex III of heart mitochondria. *Arch. Biochem. Biophys*. 237: 408-414.

Uren AG, O'Rourke K, Aravind LA, Pisabarro MT, Seshagiri S, Koonin EV, Dixit VM. (2000). Identification of paracaspases and metacaspases: two ancient families of caspase-like proteins, one of which plays a key role in MALT lymphoma. *Mol. Cell*. 6: 961-967.

Vachova L, and Palkova Z. (2005). Physiological regulation of yeast cell death in multicellular colonies is triggered by ammonia. *J. Cell Biol.* 169: 711–717

Vachova L, and Palkova Z. (2007). Caspases in yeast apoptosis-like death: facts and artefacts. *FEMS Yeast Res*. 7: 12-21.

van Dijk K, Fouts DE, Rehm AH, Hill AR, Collmer A and Alfano JR. (1999). The Avr (effector) proteins HrmA (HopPsyA) and AvrPto are secreted in culture from *Pseudomonas syringae* pathovars via the Hrp (type III) protein secretion system in a temperature and pH sensitive manner. *J. Bacteriol.* 181: 4790-4797.

Vieille C, and Zeikus G J. (2001). Hyperthermophilic enzymes: sources, uses, and molecular mechanisms for thermostability. *Microbiol Mol. Biol. Rev.* 65: 1- 43.

Walter D, Wissing S, Madeo F, Fahrenkrog B (2006). The inhibitor-of-apoptosis protein Bir1p protects against apoptosis in S. cerevisiae and is a substrate for the yeast homologue of Omi/HtrA2. *J. Cell Sci*. 119: 1843–1851.

Wang H, Jones C, Ciacci-Zanella J, Holt T, Gilchrist DG, Dickman MB. (1996). Fumonisins and *Alternaria alternata lycopersici* toxins: sphinganine analog mycotoxins induce apoptosis in monkey kidney cells. *Proc. Natl. Acad. Sci.* USA. 93: 3461-3465.

Wanke V, Accorsi K, Porro D, Esposito F, Russo T, Vanoni M. (1999). In budding yeast, reactive oxygen species induce both RAS-dependent and RAS-independent cell cycle specific arrest. *Mol. Microbiol*. 32: 753-764.

Watt R, and Piper PW. (1997). *UB14*, the polyubiquitin gene of *Saccharomyces cerevisiae*, is a heat shock gene that is also subject to catabolite derepression control. *Mol. Gen. Genet*. 253: 439-447.

Wattiau P, Woestyn S and Cornelis GR. (1996). Customized secretion chaperones in pathogenic bacteria. *Mol. Microbiol.* 20: 255-262.

Wei MC, Lindsten T, Mootha VK, Weiler S, Gross A, Ashiya M, Thompson CB, Korsmeyer SJ. (2000). tBid, a member targeted death ligand, oligomerizes Bak to release cytochrome c. *Genes Dev*. 14, 2060-2071.

Wei MC, Zong WX, Cheng EH, Lindsten T, Panoutsakopoulou V, Ross AJ, Roth KA, Korsmeyer SJ. (2001). Proapoptotic Bax and Bak: a requisite gateway to mitochondrial dysfunction and death. *Science.* 292: 727-730.

Wei Z, Laby RJ, Zumoff CH, Bauer DW, He SY, Collmer A, & Beer SV. (1992). Harpin, elicitor of the hypersensitive response produced by the plant pathogen *Erwinia amylovora*. *Science*. 257: 85-88.

Wilkins DK, Grimshaw SB, Receveur V, Dobson CM, Jones JA, and Smith LJ. (1999). Hydrodynamic radii of native and denatured proteins measured by pulse field gradient NMR techniques. *Biochemistry*. 38: 16424-16431.

Wilson DF, Rumsey WL, Green TJ, and Vanderkooi JM. (1988). The oxygen dependence of mitochondrial oxidative phosphorylation measured by a new optical method for measuring oxygen concentration. *J. Biol. Chem*. 263: 2712-2718.

Wissing S, Ludovico P, Herker E, Buttner S, Engelhardt SM, Decker T. (2004). An AIF orthologue regulates apoptosis in yeast. *J. Cell Biol*. 166: 969–974.

Wright KM, Duncan GH, Pradel KS, Carr F, Wood S, Oparka KJ, and Santa Cruz S. (2000). Analysis of the *N* gene hypersensitive response induced by a fluorescently tagged tobacco mosaic virus. *Plant Physiol.* 123: 1375–1386.

Wyllie A. (1998) Apoptosis. An endonuclease at last. *Nature*. 391: 20-21.

Wyllie A.H. (1980) Glucocorticoid-induced thymocyte apoptosis is associated with endogenous endonuclease activation. *Nature.* 284: 555-556.

Xie Z, and Chen Z. (1999). Salicylic acid induces rapid inhibiton of mitochondrial electron transport and oxidative phosphorylation in tobacco cells. *Plant Physiol*. 120: 217-225.

Xie Z, and Chen Z. (2000). Harpin-induced hypersensitive cell death is associated with altered mitochondrial functions in tobacco cells. *Mol. Plant Microbe Inter*. 13: 183-190.

Yadav, SP, Kundu B, and Ghosh JK. (2003). Identification and characterization of an amphipathic leucine zipper-like motif in *Escherichia coli* toxin hemolysin E. Plausible role in the assembly and membrane destabilization. *J. Biol. Chem*. 278: 51023-51034.

Yao N, Eisfelder BJ, Marvin J and Greenberg JT. (2004). The mitochondrion- an organelle commonly involved in programmed cell death in *Arabidopsis thaliana*. *Plant J*. 40: 596-610.

Yontsh-Rouach, E., Resnitzky, D., Lotem. J.. Sachs. L., Kinichi. A.. and Oren, M. (1991) Wild-type p53 induces apoptosis of myeloid leukaemic cells that is inhibited by interleukin-6. *Nature*. 352: 345-347.

Yoon HJ, and Carbon J. (1999). Participation of Bir1p a member of the inhibitor of apoptosis family in yeast chromosome segregation events. *Proc. Natl. Acad. Sci.* USA. 96: 13208-13213.

Zhang L, Yu L, and Yu CA. (1998). Generation of superoxide anion by succinate-cytochrome c reductase from bovine heart mitochondria. *J. Biol. Chem*. 273: 33972-33976.

Zhu H, Celinski SA, Scholtz JM, and Hu JC. (2001). An engineered leucine zipper a position mutant with an unusual three-state unfolding pathway. *Protein Sci*. 10: 24-33.

Zischka H, Braun RJ, Marantidis EP, Buringer D, Bornhovd C, Hauck SM, Demmer O, Gloeckner CJ, Reichert AS, Madeo F. (2006). Differential analysis of *Saccharomyces cerevisiae* mitochondria by free-flow electrophoresis. *Mol. Cell Proteomics*. 5: 2185–2200.

Zong WX, Lindsten T, Ross AJ, MacGregor GR, and Thompson CB. (2001). BH3-only proteins that bind pro-survival Bcl-2 family members fail to induce apoptosis in the absence of Bax and Bak. *Genes Dev*. 15: 1481-1486.